

AD-A053 420

GENERAL ELECTRIC CO ALBUQUERQUE N MEX TEMPO
PHOTOGRAVEMETRY OF THE PARTICLE TRAJECTORIES ON DIPOLE WEST SHOT--ETC(U)
OCT 77 J M DEWEY, D J MCMILLIN, D TRILL

DNA001-77-C-0305

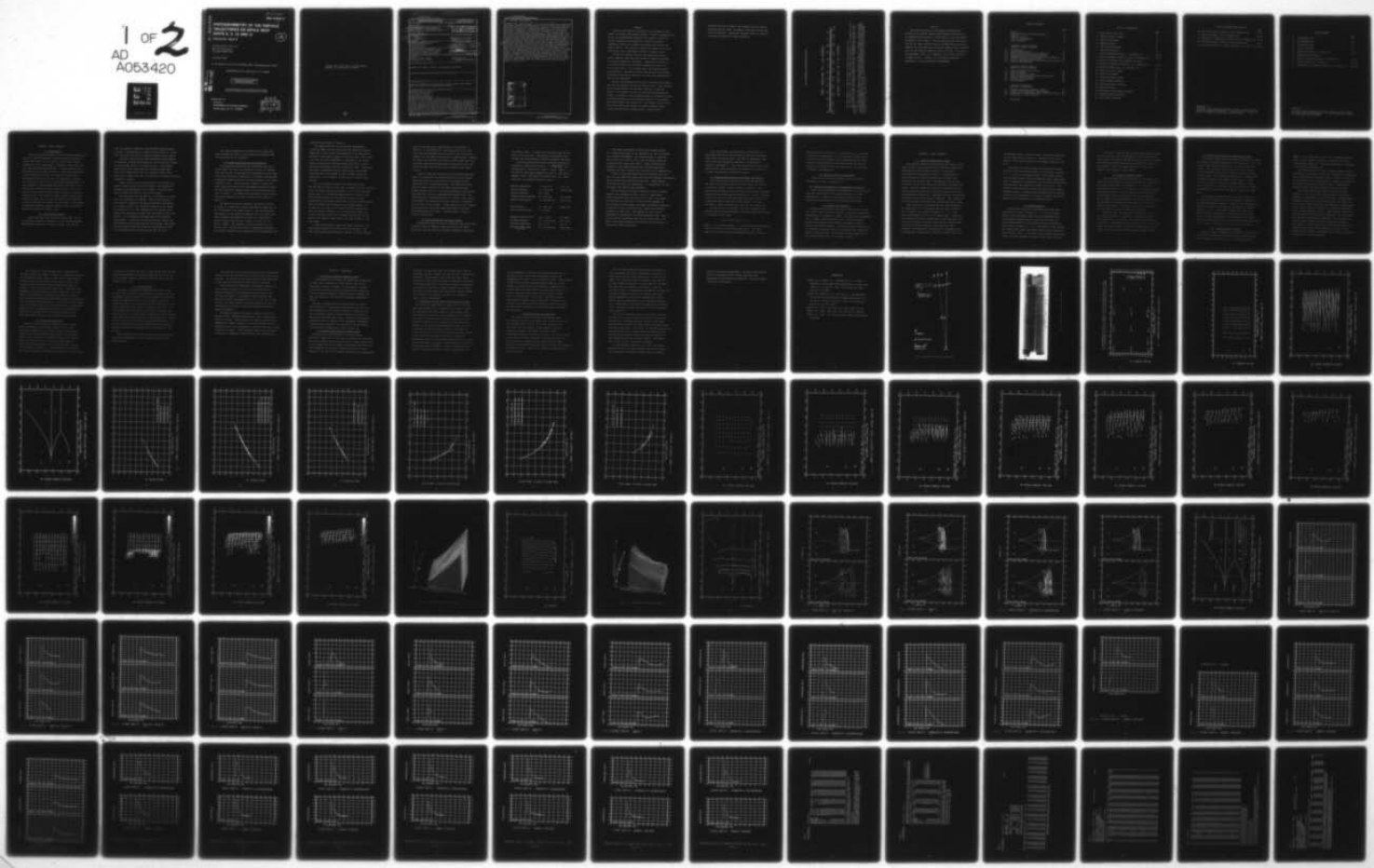
NL

UNCLASSIFIED

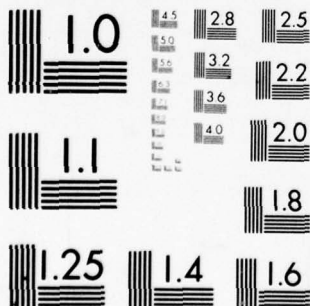
DNA-4326F-2

F/G 18/3

1 OF 2
AD
A053420



05342



MICROCOPY RESOLUTION TEST CHART
NATIONAL BUREAU OF STANDARDS-1963

AD A 053420

AD-E300165

DNA 4326F-2

**PHOTOGRAMMETRY OF THE PARTICLE
TRAJECTORIES ON DIPOLE WEST
SHOTS 8, 9, 10 AND,11**

Volume II – Shot 9

12

University of Victoria
British Columbia
Canada V8W 2Y2

October 1977

Final Report for Period 15 May 1977–30 September 1977

CONTRACT No. DNA 001-77-C-0305

APPROVED FOR PUBLIC RELEASE;
DISTRIBUTION UNLIMITED.

THIS WORK SPONSORED BY THE DEFENSE NUCLEAR AGENCY
UNDER RDT&E RMSS CODE B342077464 N99QAXAA11114 H2590D.

Prepared for
Director
DEFENSE NUCLEAR AGENCY
Washington, D. C. 20305



Destroy this report when it is no longer
needed. Do not return to sender.



(18) DNA, SBIE

(19) 4326F-2, AD-E300165

UNCLASSIFIED

SECURITY CLASSIFICATION OF THIS PAGE (When Data Entered)

REPORT DOCUMENTATION PAGE		READ INSTRUCTIONS BEFORE COMPLETING FORM
1. REPORT NUMBER DNA 4326F-2	2. GOVT ACCESSION NO.	3. RECIPIENT'S CATALOG NUMBER
4. TITLE (and Subtitle) PHOTOGRAMMETRY OF THE PARTICLE TRAJECTORIES OF DIPOLE WEST SHOTS 8, 9, 10, AND 11. Volume II, Shot 9.		5. TYPE OF REPORT & PERIOD COVERED Final Report, for Period 15 May - 30 Sep 77
6. AUTHOR(s) J. M. Dewey D. J. McMillin D. Trill		7. PERFORMING ORGANIZATION NAME AND ADDRESS University of Victoria British Columbia Canada V8W 2Y2
8. CONTRACT OR GRANT NUMBER(s) DNA 001-77-C-0305		9. PROGRAM ELEMENT, PROJECT, TASK AREA & WORK UNIT NUMBERS NWED Subtask N99QAXAA111-14
10. MONITORING AGENCY NAME & ADDRESS (if different from Controlling Office) Director Defense Nuclear Agency Washington, D.C. 20305		11. REPORT DATE October 1977
12. NUMBER OF PAGES 114		13. SECURITY CLASS (of this report) UNCLASSIFIED
14. DISTRIBUTION STATEMENT (of this Report) Approved for public release; distribution unlimited.		15a. DECLASSIFICATION/DOWNGRADING SCHEDULE
16. DISTRIBUTION STATEMENT (of the abstract entered in Block 20, if different from Report)		
17. SUPPLEMENTARY NOTES This work sponsored by the Defense Nuclear Agency under RDT&E RMSS Code B342077464 N99QAXAA11114 H2590D.		
18. KEY WORDS (Continue on reverse side if necessary and identify by block number) Photogrammetric Analysis Particle Trajectories Air Particle Tracers Simultaneous Detonations Multiburst Detonations This volume describes the		
19. ABSTRACT (Continue on reverse side if necessary and identify by block number) Volume 2 of this report describes the photogrammetry and analysis of the particle trajectories in blast waves produced by the simultaneous detonation of two spherical 1080-lb (491-kg) Pentolite charges, (Dipole West Shot 9). One of the charges was positioned at a height of 15 ft (4.6 m) above smooth ground and the second charge 30 ft (9.2 m) above the first. Photogrammetrical measurements were made of the trajectories of air particle flow tracers (smoke puffs), which had been placed in a vertical grid at heights (Lover)		

UNCLASSIFIED

SECURITY CLASSIFICATION OF THIS PAGE(When Data Entered)

20. ABSTRACT (Continued)

ranging from 3 ft (0.92 m) to 58 ft (17.7 m) above the ground and at radial distances ranging from 25 ft (7.6 m) to 85 ft (25.9 m) from the vertical axis through the charges. From the measured particle trajectories, calculations were made of the particle velocities, densities, hydrostatic overpressures, and dynamic pressures throughout the blast wave, at times ranging from 3 ms to 60 ms after detonation of the charges. The shock front times-of-arrival were also determined from the photogrammetrical measurements for the primary shock from each of the two charges; for the Mach stems produced above and below the interaction plane midway between the two charges; and for the Mach stem produced at the ground surface. From the shock front times-of-arrival, calculations were made of the shock velocities, and, in turn, the peak particle velocities, air densities and hydrostatic overpressures immediately behind each shock. Calculations were also made of the variation with time of the particle velocity, density, hydrostatic overpressure and dynamic pressure at several fixed points. Results are presented both graphically and in tables, and are compared to results previously calculated for the same experiment using shock front photogrammetry and refractive image analysis. The analytical procedures used were similar to those used for Dipole West Shot 10, which were described in Volume I (Dewey, et al, 1977).

ACCESSION for		
NTIS	White Section <input checked="" type="checkbox"/>	
DDC	S.R. Section <input type="checkbox"/>	
UNANNOUNCED	<input type="checkbox"/>	
JUSTIFICATION		
BY		
DISTRIBUTION/AVAILABILITY CODES		
Dist.	AVAIL.	SPECIAL
A		

UNCLASSIFIED

SECURITY CLASSIFICATION OF THIS PAGE(When Data Entered)

SUMMARY

Owing to the quantity of material to be presented, this report is divided into several volumes. Volume 1 introduced the series and presented and discussed the results for Shot 10. Volume 2 presents and discusses the results for Shot 9. Subsequent volumes will present and discuss the results for Shots 8 and 11. The method of analysis is common to all four experiments and is described in detail in Volume 1 only.

So that the results from the four experiments may be easily compared, they have been scaled to remove the effects of varying atmospheric conditions. (Results are scaled to a 1 kg charge weight and a standard atmosphere of dry air at 15°C at sea level.) For the most part, only scaled results are presented. Exceptions include some derived pressure-time histories, which may be compared to actual gauge measurements made in the experiment.

Results are presented in SI units, even though the experiments were originally laid out in British units. Only distance and time measurements are affected, however, as velocity density, and pressure results are presented as dimensionless ratios. A distance units conversion scale is included on page 3 to convert between SI units (meters scaled to a 1 kg charge) and British units (feet scaled to a 1 lb charge), plus a time scale factor and scale factors to convert pressure ratios to both British and SI pressure units. Scale factors

which may be used to compute the distance and time values actually observed under the ambient conditions of each shot are also provided. Dimensional pressure units are used for the results presented at gauge locations.

FEET (SCALING TO 1 LB CHARGE)

0	1	2	3	4	5	6	7	8	9	10	11	12
0.0	0.5	1.0	1.5	2.0	2.5	3.0	3.5	4.0	4.5	5.0		

METERS (SCALING TO 1 KG CHARGE)

For feet scaled to a 1000 lb charge, multiply the top scale by 10.

For time scaled to a 1000 lb charge, multiply time scaled to a 1 kg charge by 8.683.

For pressure in kPa, multiply a pressure ratio (in atmospheres) by 101.325. For pressure in psi, multiply the pressure ratio by 14.696. To convert kPa to psi, divide by 6.895.

To obtain distance values actually observed for Shot 9, in meters, multiply scaled values in this report by 8.111. To obtain the observed distance values in feet, multiply the reported scaled values by 26.611. To obtain observed time values, multiply scaled time values by 8.1069. For observed pressures in kPa, multiply by 93.02; for observed pressures in psi, multiply by 13.49.

PREFACE

The authors gratefully acknowledge the opportunity offered by the Defence Research Establishment Suffield and the Defense Nuclear Agency to participate in the experiments described in this report. The analyses described here were carried out under contract with the Canadian General Electric Company, and with additional financial support from a research grant by the National Research Council (A 2952). The advice and assistance of Mr. A.P. Lambert, C.G.E. Project Officer at DRES, and Mr. J. Keefer, of the Ballistic Research Laboratory, is also gratefully acknowledged.

TABLE OF CONTENTS

	page
Summary	1
Unit Conversion and Scaling Factors	3
Preface	4
Table of Contents	5
List of Illustrations	6
List of Tables	8
<hr/>	
<u>CHAPTER 1, SHOT 9 ANALYSIS</u>	
1.1 Introduction	9
1.2 Description of Shot 9	9
1.3 Camera Calibration and Data Reduction	11
1.4 Data Scaling and Trajectory Fitting	13
1.5 Regionalization and Shock Strength Calculations	16
1.6 Particle Velocity Calculations	17
1.7 Density and Hydrostatic Overpressure Calculations	17
1.8 Surface Representation	17
<hr/>	
<u>CHAPTER 2, SHOT 9 RESULTS</u>	
2.1 Times of Shock Front Arrival	18
2.2 Shock Strengths	19
2.3 Particle Velocity Fields	20
2.4 Density and Hydrostatic Overpressure Fields	21
2.5 Times-of-Arrival Surface	21
2.6 Field Surface Contours	23
2.7 Time Histories	24
<hr/>	
<u>CHAPTER 3, DISCUSSION</u>	
3.1 Particle Trajectory Analysis, Shot 9	26
3.2 Primary Shock Strength of Upper Charge	26
3.3 Comparison of Mach Shocks over Different Surfaces	27
3.4 Resolution of Time Histories	28
References	31

LIST OF ILLUSTRATIONS

	page
1. Plan view of test site	32
2. Field of view of camera	33
3. Camera calibration	34
4. Smoke puff grid	35
5. Particle trajectories	36
6. Regions definition	37
7. Shock trajectories (Figs. 7.1 through 7.3)	38-40
8. Shock strengths, method 1 (Figs. 8.1 through 8.3)	41-43
9, 10 and 11 (Deleted: see footnote next page)	
12. Particle velocity fields (Figs. 12.1 through 12.7)	44-50
13. Density fields (Figs. 13.1 through 13.4)	51-54
14. Time-of-arrival surface	55
15. Shock front shapes	56
16. A shock strength surface	57
17. Shock strength contours	58
18. Particle velocity contours	59
19. Density contours	60
20. Hydrostatic overpressure contours	61
21. Dynamic pressure contours	62
22. Time history stations	63

LIST OF ILLUSTRATIONS (cont'd)

	page
23. Particle velocity histories (23.1 through 23.4)	64-67
24. Density histories (24.1 through 24.4)	68-71
25. Hydrostatic overpressure histories (25.1 through 25.4)	72-75
26. Dynamic pressure histories (26.1 through 26.4)	76-79
27. Pressure histories at gauge locations (27.1 thru 27.7)	80-86

Footnote:

To assist in the comparison between volumes, similar figures have been numbered identically. For this reason, figures numbers 9, 10 and 11 are not used in this volume.

LIST OF TABLES

	page
1. Survey data list	87
2. Photogrammetrics	88
3. Film timing data	89
4. Times of arrival	90
5. Shock front data (5.1 through 5.5)	92-96
6. (Deleted: see footnote)	
7. Particle velocity fields (7.1 through 7.6)	97-102
8. Density fields (8.1 through 8.3)	103-105
9. Hydrostatic overpressure fields (9.1 through 9.3)	106-108

Footnote:

To assist in the comparison between volumes, similar tables have been numbered identically. For this reason table number 6 is not used in this volume.

CHAPTER 1, SHOT 9 ANALYSIS

1.1 Introduction

This is the second volume in a series which presents the particle trajectory analysis results from four experiments (Dipole West Shots 8, 9, 10 and 11) carried out to obtain information on the interaction of spherical blast waves with real and ideal reflecting surfaces. A general description of the project can be found in Volume 1. The results presented in this volume are for Shot 9, in which the same charge configuration was used as in Shot 10 (reported in volume 1), but which was carried out over a smoother ground surface. In each experiment, photogrammetrical studies were made of the shock fronts (refractive image analysis, RIA), and of the motions of smoke puff particle tracers (particle trajectory analysis, PTA). The refractive image analysis results were reported by Dewey et al. (1975) and results of the particle trajectory analysis are presented in this report. The method of particle trajectory analysis, common to all four shots is described in detail in Volume 1 only.

1.2 Description of Shot 9

Dipole West Shot 9 was fired on October 22nd, 1973 by the Ballistics Research Laboratories at the Defence Research Establishment Suffield, in Alberta, Canada. Two 1080 lb

(491 kg) spheres of Pentolite were detonated simultaneously, to within 5 microseconds, at nominal charge heights of 15 and 45ft (4.6 and 13.7m) over a relatively smooth ground surface.

Particle trajectory data were gathered by photographing the movement of smoke puffs formed in a vertical plane running out from ground zero at 6.7° south of west. A WF5 camera operating at about 3400 frames per second was positioned 30ft (9.2m) above ground level at a position 600ft (183m) due south of ground zero (GZ), the point on the ground vertically beneath the charges.

Table 1 gives the field survey data for the event, and Figure 1 shows a plan view of the layout. The dashed line represents the approximate line of sight of the WF5 camera. Figure 2 shows the field of view of this camera.

The smoke puff grid was made up of 9 columns of 12 puffs each, hung vertically on strings. The vertical spacing of puffs was 5ft, beginning 3ft above ground level and ending at a height of 58ft. The horizontal spacing of the columns of puffs was 10, 7 or 5ft, depending on the distance from ground zero, beginning at about 25ft and ending at about 85ft from GZ. Of the possible 108 smoke puffs, 106 detonated successfully. A good film record was obtained, except that the detonation zero timing mark was not recorded, which means that the results cannot be related to the detonation pulse to the charges with an accuracy better than ±0.15 ms.

This report describes the analysis of the smoke puff data collected for Shot 9, and presents and discusses some of the results of that analysis.

1.3 Camera calibration and data reduction

The calculated camera position coordinates and orientation angles for Shot 9 are presented in Table 2, together with the positions of photomarkers transformed from one frame of the film just before detonation to an object plane defined as passing through ground zero and being normal to the camera orientation axis. The differences ("shifts") between the object plane positions of the transformed calibration points and their positions computed from the field survey data are given in Table 2. The object plane positions of the calibration points computed in these two ways are also shown in Figure 3.

The camera calibration procedure, described in detail in Volume 1, ensured that selected photomarker images (P1 to P5) transformed to the object plane in a way which matched them exactly to the positions computed using the survey data. These reference photomarkers for Shot 9 are indicated in Figure 3 using large circles: namely, P1 = W1, P2 = W3, and P3 = 300W2. The separation distance between P4 = P3 = 300 WZ and P5 = W2 was also used as a calibration parameter. The probable reasons for the shifts seen for photomarkers VP1A

and VP1B was discussed in Volume 1.

The image positions of two reference photomarkers (VP3B and 300W2) and all smoke puffs were measured frame-by-frame over a time interval corresponding to the approximate duration of the positive phase of the blast waves (film frames 9 to 200), and were transformed to distances in the object plane by matching the reference marker positions to their positions transformed from the calibration frame. These data were again transformed from the object plane to the smoke puff plane which was assumed to pass through "corrected" ground zero; to be vertical, and to run 6.7° south of west from GZ.

The x-y coordinate system in the smoke puff plane was the same for Shot 9 as for Shot 10 except that the corrected value for ground zero was displaced 1.0 ft from the surveyed ground zero, in a direction approximately 46° south of east. The corrected ground zero was defined to have the same elevation as the surveyed ground zero, but was located directly under the midway point between the two charge centers. As for Shot 10, all data in the output plane are plotted with the x coordinate reflected, i.e. with positive values of x to the right hand side, as if the smoke grid had run to the right of the charges rather than to the left as seen in the film images.

A time was assigned to each film frame using the 1 ms timing marks placed on the film during its exposure. The film timing method was described in Volume 1, and the complete

set of film timing data used for Shot 9 is provided in Table 3. In the absence of a zero time pulse on the film, zero time was determined using the static zero calibration distance for the camera plus one-half a frame length. Because the static zero distance is at most a frame length less than the actual zero distance measured from any moving film, the error in frame times can be at most one-half frame (about 0.15 ms).

Figure 4 shows the positions of the 106 detonated smoke puffs at a time prior to the detonation of the two charges. These positions are in the plane of the charges and the smoke puff grid, as described above. The smoke puff plane was not exactly parallel to the camera image and object planes (Figures 2 and 3), and various geometrical corrections were applied to make the transformation between them. The puffs enclosed in parentheses were not visible in the earlier film frames, but were seen later when they were illuminated by the light of the fireball. Charge positions in the figures are plotted as if they were positioned exactly above the corrected ground zero origin. The data shown in Figure 4 have not been scaled.

1.4 Data scaling and trajectory fitting

The position-time histories of individual smoke puffs were extracted from the frame-by-frame positions of the smoke puff grid, and then scaled to standard atmospheric conditions

and charge weight. A change to SI units was made at this point in the analysis. The resulting trajectories were edited, and then smoothed by fitting polynomial functions.

Particle trajectory data were scaled by dividing all distances by Sachs scaling factor $S = \sqrt[3]{(WP_o)/(W_oP)}$ and multiplying all times by the factor $C/(C_oS)$, where C is the ambient sound speed computed for Shot 9. Data used to compute C and S , and define the scaled event, are listed below with the computed values of C and S .

Ambient temperature,	$T = 14.17^{\circ}\text{C}$	(57.5 °F)
Ambient pressure,	$P = 93.02 \text{ kPa}$	(13.491 PSI)
Relative humidity,	$RH = 55.0\%$	
Computed vapour pressure,	$VP = 0.89 \text{ kpa}$	(6.7 mm Hg)
Ambient sound speed,	$C = 340.469 \text{ m/s}$	(1117 ft/s)
Charge weight,	$W = 489.9 \text{ kg}$	(1080 lbs)
Sachs scaling factor,	$S = 8.1111$	
Standard charge weight,	$W_o = 1.0 \text{ kg}$	(2.2 lbs)
Standard pressure,	$P_o = 101.325 \text{ kpa}$	(14.7 PSI)
Standard temperature	$T_o = 15^{\circ}\text{C}$	(59 °F)
Standard sound speed, (dry air)	$C_o = 340.292 \text{ m/s}$	(1116 ft/s)

The results presented in this report therefore apply to a scaled event which is the detonation of two 1 kg charges in a standard atmosphere. The scaled heights of burst for Shot 9 were 0.571 m and 1.707 m, and the charge separation divided by two, scaled, was 0.568 m. These figures may be compared to the scaled charge height and half-separation distances for Shot 10 which were 0.563 and 0.575 m respectively.

Figure 5 shows the scaled particle trajectory data for Shot 9 in the smoke puff plane with positions measured horizontally and vertically from corrected ground zero. Approximately 9350 puff positions are represented. As represented, the raw trajectory data have not been smoothed.

The raw particle trajectory data were edited to remove obvious data processing errors, such as a single point widely displaced from its trajectory for one or two frames. The trajectory of each puff in turn was then smoothed by least squares fitting simple polynomial expressions separately to both the x and y coordinate data, these being discrete functions of frame time. The adequacy of each fit was determined by examining on the same graphical output, plots of both the raw trajectory data and the fitted curve. For Shot 9 this meant examining and adjusting 212 such plots, at least two or three times each.

For a given puff, the first step in fitting the raw trajectory data was to set the time of arrival of the shock front first hitting the puff. The data at subsequent times were fitted with polynomial functions, as described in Volume 1, paragraph 2.5. The first derivatives of the fitted functions were also calculated at a series of times for use in later calculations of particle velocity.

1.5 Regionalization and shock strength calculations

Five regions were defined in the smoke puff plane on the basis of the shock front which first struck the puffs in a particular region. These are shown in Figure 6. The regions were bounded by the triple point trajectories measured using refractive image analysis (Dewey et al., 1975). Regions 1 and 2 are those in which the smoke puffs were first hit by a spherical primary shock front, and regions 3, 4, and 5 are those in which the puffs were first hit by a Mach stem.

In each of the five regions, the shock trajectory data obtained from the first movement of the smoke puffs were fitted to a function of the form

$$r(t) = A + Bt + C \log(1 + t) ,$$

where r is the shock radius, t is the time after detonation, and A , B , and C are the fitted coefficients. The shock velocities were calculated by differentiating this function.

The peak particle velocity, V_s , peak density, D_s , and peak hydrostatic overpressure, P_s , as functions of shock radius in each of the five regions, were calculated from the shock velocity using extensions of the Rankine-Hugoniot equation. Details of the shock radius calculations etc. are described in Volume 1, paragraph 2.6.

1.6 Particle velocity calculations

Particle velocities were computed using the methods described in Volume 1, paragraph 2.7.

1.7 Density and hydrostatic overpressure calculations

Densities and hydrostatic overpressures in the smoke puff plane were calculated by the method described in Volume 1, paragraph 2.8. Results in both cases represent average values over cells defined by four adjacent smoke puffs.

1.8 Surface representation

Surfaces were fitted to the times of shock front arrival and to the fields of particle velocity, density and hydrostatic overpressure at a sequence of times. All data were interpolated onto a common regular Eulerian grid. Fields of dynamic pressure were computed from surface-interpolated particle velocity and density results. Contour plots were generated for all surfaces at selected times, and time histories computed at several fixed locations. The methods used were identical to those described for Shot 10 in Volume 1, Chapter 3.

CHAPTER 2. SHOT 9 RESULTS

2.1 Times of shock front arrival

The measured initial puff positions, the times of first shock arrival, and the peak particle velocities obtained by differentiating the functions fitted to the particle trajectories are presented in Table 4. Puff position is given relative to corrected ground zero as origin with horizontal and vertical axes. Puff position and the time of arrival of the first shock are given both as observed and scaled. Particle velocities listed are derivatives of the fitted puff trajectories at the times of shock arrival, and are expressed in Mach units. Expressed this way, the particle velocities are the same scaled as unscaled. Also listed are the initial radial puff positions (scaled) and region codes.

Shock front data determined from the first movement of the smoke puffs, i.e. calculated from the time-of-arrival data in Table 4, are listed in Tables 5.1 - 5.5. Each table corresponds to one of the 5 regions used. Listed are the observed and fitted unscaled shock trajectory data, the scaled fitted shock trajectory data, and the computed shock velocities and peak parameters associated with shock strength: peak hydrostatic overpressure in atmospheres and in kilopascals, peak particle velocities in Mach units, and

peak density ratios. Given as ratios, these peak parameters are the same scaled as unscaled. Pressure given in kilo-pascals in the tables refers to the unscaled (observed) case only.

The shock front radius versus time data derived using particle trajectory analysis (PTA) are also shown in Figures 7.1 - 7.3 for the two primary fronts, the two Mach stems at the interaction plane, and the ground Mach stem, respectively. They are compared to corresponding data derived from refractive image analysis (RIA) reported by Dewey et al (1975). The refractive image analysis results were obtained using photogrammetry against a striped canvas backdrop and they describe the shock as it travelled in a direction almost diametrically opposite to the direction of the smoke puff grid.

2.2 Shock strengths

Peak particle velocities calculated from shock front velocities are shown in Figure 8.1 - 8.3 for the primary fronts, interaction Mach stems, and the ground Mach stem. This method of determining peak particle velocities has been labelled method 1, and the data plotted correspond to those listed in Tables 5.1 - 5.5. The results in the figures are compared with those previously obtained using refractive image analysis (RIA). In the case of the primary shock fronts, results are also compared to those of Brode (1957) for TNT.

In Volume 1 other methods of determining shock strengths in the various regions were described. It was demonstrated that method 1 was clearly the most accurate, and in the present volume shock strengths calculated using methods 2 and 3 are not reported. For this reason Figures 9, 10 and 11 and Table 6 do not appear in this volume.

2.3 Particle velocity fields

The calculated particle velocities in the plane of the smoke puffs are shown as vectors in Figures 12.1 through 12.7, for various times after the detonation. All times and positions are scaled to a 1 kg charge in a standard atmosphere. The particle velocity vectors represent the derivatives of the smoothed particle trajectories, and their magnitudes may be judged using the standard vector shown on each figure. All velocities are measured in Mach units, relative to the standard sound speed. Puffs not yet struck by a shock wave are represented by small circles (zero velocity).

Numerical data corresponding to Figures 12.1 - 12.7 are listed in Tables 7.1 through 7.6, along with scaled radial positions of the puffs, and region codes as defined in Figure 6. Conversion factors are given at the foot of each table, which may be used to convert the scaled data in the tables and figures back to their original unscaled values.

2.4 Density and hydrostatic overpressure fields

Calculated average relative densities throughout the smoke puff plane are depicted graphically in Figures 13.1 - 13.4, for various times after the detonation. All time values are scaled. Cell positions are scaled and are given relative to the corrected ground zero as origin with horizontal and vertical axes. The calculated densities may be judged using the density shading scale shown on each figure. Density is given as a ratio, relative to ambient density. Cells not yet struck by a shock wave and cells in which the density has dropped to a value less than ambient density are shown blank.

Corresponding numerical data are listed in Tables 8.1 - 8.3 along with radial cell positions computed according to the regions defined previously. Numerical data describing the fields of hydrostatic overpressure are similarly listed in Tables 9.1 - 9.3. The pressure results for a given cell were obtained by multiplying the density results for that cell by a factor determined by the strength of the shock which first traversed the cell and which then remained constant, i.e. by assuming isentropic flow after the first shock.

2.5 Times-of-arrival surface

Figure 14 shows a perspective view of the surface fitted to the original smoke puff positions and the observed times of first shock front arrival, i.e., to the data listed in

Table 4. The grid mesh size is 0.1 by 0.1 meters (scaled), about 2.5 feet square (unscaled), or about $\frac{1}{2}$ that of the original smoke puff grid. The charge positions are indicated on the vertical distance axis.

The times-of-arrival surface is smooth enough to permit contouring, the contours in this case (isochrones) representing shock front shapes at different times, as shown in Figure 15, but the surface is not smooth enough to permit the calculation of gradient vectors which could be used to compute shock velocity vectors and shock strengths over the new grid.

Two attempts were made to obtain contours of shock strength. In the first, the times-of-arrival surface was smoothed by least-squares fitting low-order, one-dimensional polynomial functions to the time-of-arrival data along each grid row and column separately, and computing the derivatives of the fitted functions to obtain the associated components of the surface gradient vectors. Shock velocity vectors were obtained from the time-of-arrival gradients, and from these peak particle velocities were computed. The peak particle velocity (shock strength) surface is shown in Figure 16. The contours of this surface (not shown) did not exhibit any discontinuities across the boundaries of the shock front regions, as they would if surfaces were fitted to the time of arrival in each region separately.

The results of a second method used to compute shock strength contours are shown in Figure 17. These were obtained by interpolating shock radius at each value of peak particle velocity shown, for each shock front region in turn, using the peak particle velocity versus radius curves shown in Figure 8. Arcs of circles with these radii, centered on the appropriate points along the vertical charge axis, were then drawn in the regions to represent shock strength contours. These peak value contours are discontinuous across triple point locii and other region boundaries. As a result, some horizontal lines are crossed twice by the same contour or, in other words, identical shock strengths can be found at two locations the same vertical distance from a reflecting surface, but at different radial distances from the vertical charge axis.

2.6 Field surface contours

Contours of equal particle velocity, density, hydrostatic overpressure, and dynamic pressure in the blast waves were determined for a series of times, using surfaces fitted to the various measured data fields at those times. Sample results are shown in Figures 18 through 21 at scaled times of 2.5 ms and 4.0 ms. The shock fronts shown in these figures are obtained from the time-of-arrival surface (as were those in Figure 15). Field contours such as those shown can be drawn for any scaled time between 0.5 ms and 7.0 ms.

It should be re-stated that all of these results were obtained from the photography of the smoke puffs only and do not rely on the results obtained using the refractive image analysis (Dewey et al., 1975).

2.7 Time histories

By mapping the physical properties of the blast waves at short time intervals it was possible to determine the time histories of these properties at any selected fixed position within the smoke puff grid. This was done at 12 fixed locations, three in the two primary regions and three in each of the three Mach stem regions, as shown in Figure 22. At each distance from the axis of the charges in the Mach stem regions, each of the time history stations is the same distance from either the interaction plane or the ground plane. Particle velocity time histories could be interpolated closest to the ground level because these were measured at puff locations, whereas the density and pressure data were measured at cell centers.

Time histories of particle velocity, density, hydrostatic and dynamic overpressure at these locations are given in Figures 23 to 26.

Also plotted with the time histories are the interpolated values of the time of arrival of the first shock front at the stations. The height of this time-of-arrival line represents a peak value derived from the shock velocity analysis.

Time histories for hydrostatic and dynamic pressure are also plotted in Figure 27.1 to 27.7 for stations at the nominal positions of field-mounted pressure gauges on the "60 foot gun barrel". The gauges on this gun barrel were mounted at nominal elevations of 10, 15, 20, 27, 30, 33, and 40 feet. The time histories at these locations are given in unscaled units in order to facilitate comparisons with the gauge measurements.

The dynamic pressures plotted in figures 26 and 27 are maximum values, computed using both the x and y components of particle velocity. Similar plots were made of the horizontal components of dynamic pressure, but the differences were not significant since the y components of particle velocity at these locations were small. Other locations could have been chosen at which the y components would not have been insignificant.

CHAPTER 3, DISCUSSION

3.1 Particle trajectory analysis, Shot 9

The methods used to analyze the smoke puff trajectories on Shot 9 were identical to those used for Shot 10 and described in detail in Volume 1 of this report. However, the results for Shot 10 clearly indicated the superiority of one of several methods of analyzing shock strength, and only the results of the superior method were reported for Shot 9.

The rate of smoke puff failure was greater for Shot 9 than for Shot 10 (there were no failures for Shot 10), but the incompleteness of the Shot 9 particle trajectory grid did not greatly interfere with the analysis of the blast wave within the smoke puff region. The extra interpolation required for Shot 9, however, will undoubtedly correspond to some slight decrease in the accuracy of the calculated blast parameters compared with those for Shot 10.

3.2 Primary shock strength of upper charge

The refractive image analysis of the shock fronts described by Dewey et al, 1975 did not provide any information about the primary spherical shocks from the upper charges, and it was assumed that these charges had detonated satisfactorily. This assumption has now been validated for Shot 9 by the analysis of the particle trajectory time-of-arrival measurements.

In Figure 7.1 the shock radii are plotted versus time for the upper and lower charges, and the two curves appear to be identical. Unfortunately, the relatively small charge separation in this experiment made it impossible to observe the primary shocks over a sufficient distance to calculate accurately the variation of shock strength with distance. The limited results which were obtained for shock strength versus distance are plotted in Figure 8.1, compared to Brode's (1957) calculations.

3.3 Comparison of Mach shocks over different surfaces

The refractive image analysis (Dewey et al, 1975) has shown what appears to be a significant difference between the strengths of the Mach shocks over the smooth ground and beneath the interaction plane between the two charges. The results of the particle trajectory analysis given in Figures 8.2 and 8.3 do not indicate the same difference. However, in the RIA case measurements were made as close as possible to the reflecting surfaces, 0.5m above the ground plane and 0.2 m below the interaction plane, whereas in the PTA case the results represent an average of measurements made at puff positions which were not so close to those surfaces, at heights ranging between 1.0 and 4.5 m. The results shown in Figures 8.2 and 8.3 therefore merely indicate that the difference in shock strength over the

ground compared with that at the interaction plane may be dependent on the height above the ground at which the measurements are made - not an unexpected result. Determination of Mach shock strength from measurements made at various heights is also made difficult because an assumption must be made about the exact shape of the Mach shock front, in order to correctly assign shock radius values to smoke puffs in the PTA case. At or near a reflecting surface the problem of shape is not so important. Details of the problem in the PTA case and the manner in which the problem was dealt with for Shots 9 and 10 are described in Volume 1 of this report.

3.4 Resolution of time histories

The time histories of density and pressure shown in Figures 24 and 25 do not always show a sharp rise at the time of shock front arrival. This slow rising is not a real effect but one inherent to the method of particle trajectory analysis, which does not permit a high resolution of density in space or in time. The finite spacing of the smoke puffs does not permit the average density of the air within a rectangular cell defined by four smoke puffs to be calculated accurately until the shock has completely traversed the cell. (The time of complete traversal may be 'as much as 5 ms.)

For the same reason the calculated time histories often anticipate the time of shock front arrival or, in other words, because a cell lies partly in front of the shock front during the time of traversal, the value of average density calculated at a point ahead of the shock may rise before the arrival of the shock. Also for the above reason, time histories calculated by the particle trajectory analysis method do not resolve any weaker shocks subsequent to the first, although these shocks may be detected occasionally in the calculated histories as a rounded bump in the normally exponentially decaying curve. Efforts are being made to see if this resolution can be improved.

The lack of resolution close to the shock front does not occur in the case of particle velocity, which can be measured with reasonable accuracy as soon as the shock has traversed the relatively small space represented by an individual smoke puff. This effect of improved resolution is manifested also in the dynamic pressure histories since although this parameter depends on measured density, it also depends on particle velocity squared. The squared term is able to exert the greater influence.

In the subsequent volume of this report hydrostatic overpressure and total head pressure histories determined from the particle trajectory analysis will be compared

directly with gauge measurements. The total head pressure will be calculated from the dynamic pressure using appropriate compressibility corrections. Pressure impulse curves will be included.

References

Dewey, J.M., Classen, D.F., and McMillin, D.J. Photogrammetry of the Shock Front Trajectories on Dipole West Shots 8, 9, 10 and 11. Univ. of Victoria Res. Rept., UVic PF 1-75, 1975.

Dewey, J.M., McMillin, D.J. and Trill, D. Photogrammetry of the Particle Trajectories on Dipole West Shots 8, 9, 10 and 11. Volume 1, Shot 10. Univ. of Victoria Res. Rept. UVic PF 1-77, 1977.

Dewey, J.M. 1971. Proc. Roy. Soc. Lond. A324, 275-299.

Dewey, J.M. 1964. Proc. Roy. Soc. Lond. A279, 366-385.

Brode, H.L. 1957. U.S. Air Force Res. Memo. ASTIA document AD 144302.

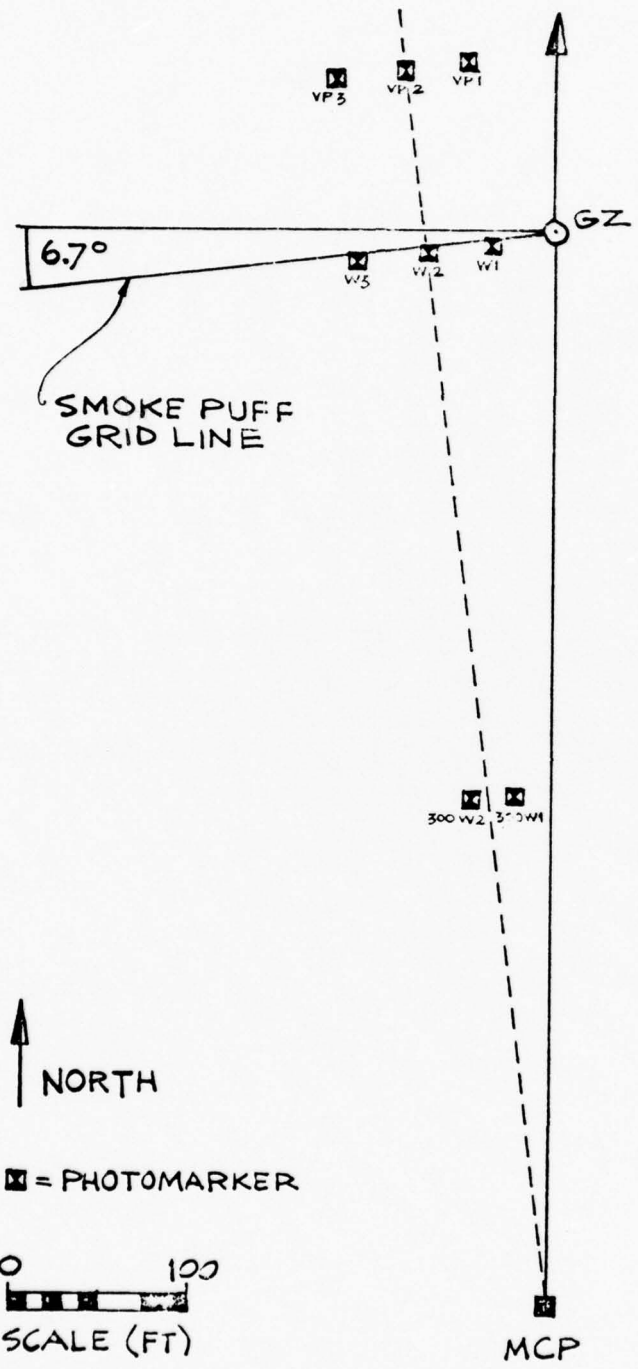


Fig. 1. Plan view of test site, Dipole West/9

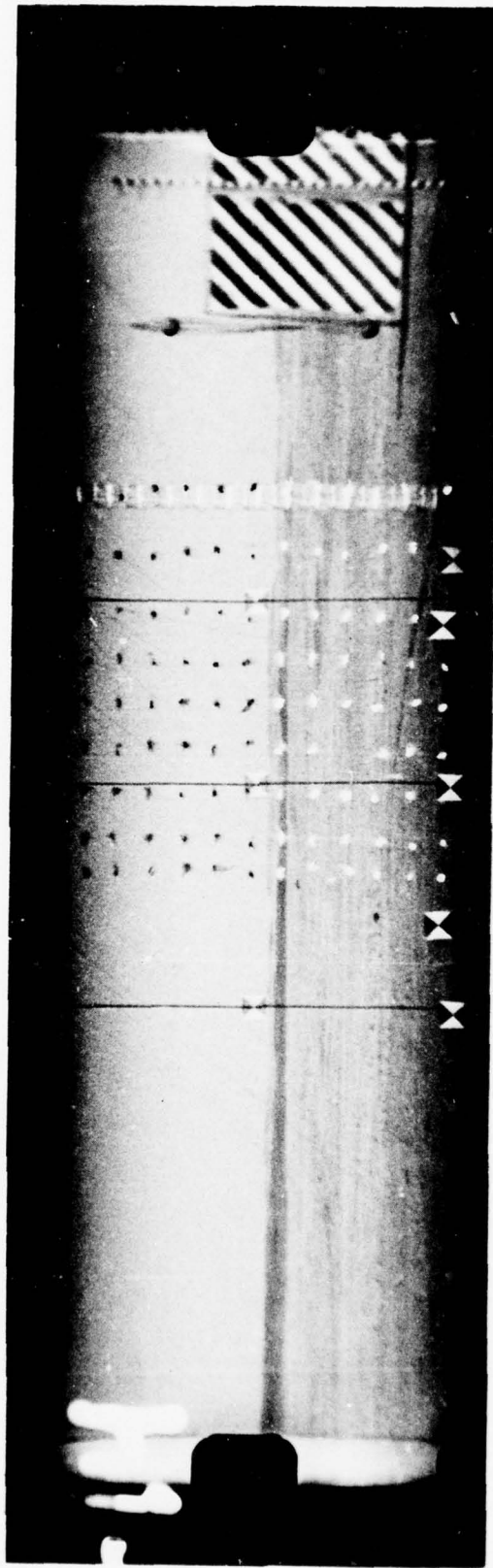


Fig. 2. Field of view of camera, Dipole West/9

□ = PHOTOMARKER POSITION IN OBJECT PLANE CALCULATED FROM SURVEY DATA
 ⊖ = PHOTOMARKER POSITION IN OBJECT PLANE TRANSFORMED FROM FILM IMAGE

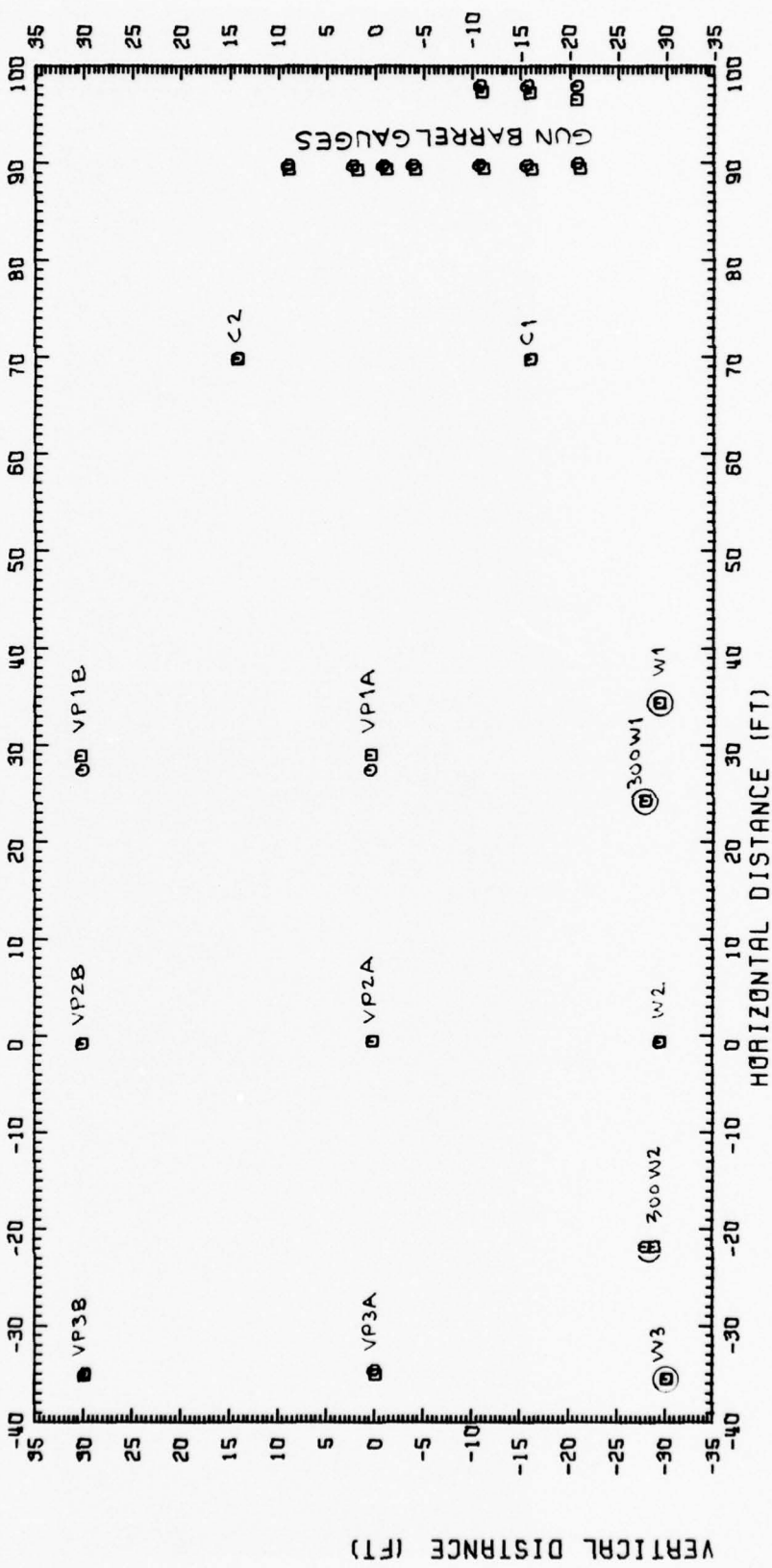


Fig. 3 CAMERA CALIBRATION, DIPOLE WEST/9

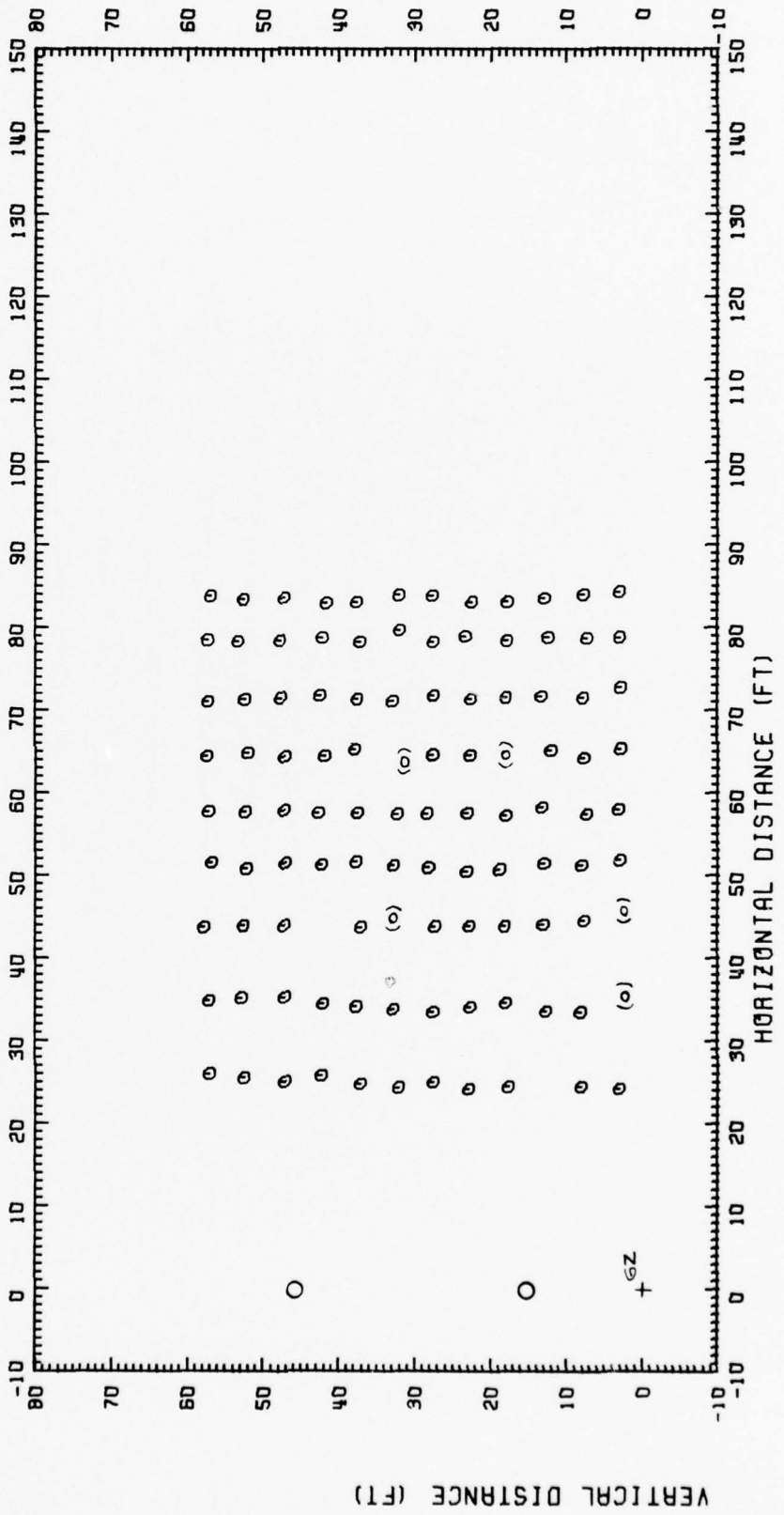


Fig. 4 SMOKE PUFF GRID, DIPOLE WEST/9

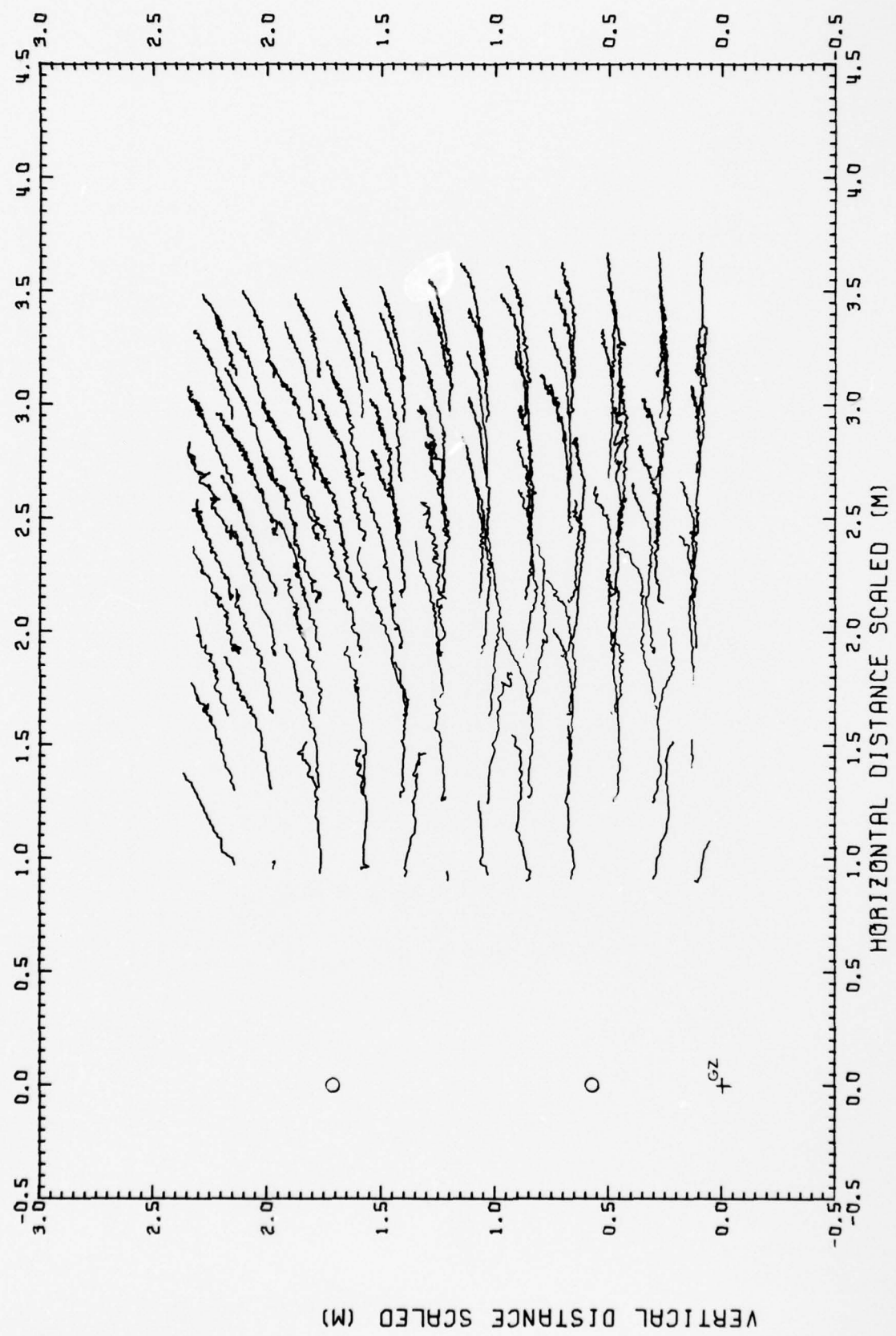


Fig. 5 PARTICLE TRAJECTORIES, DIPOLE WEST/9

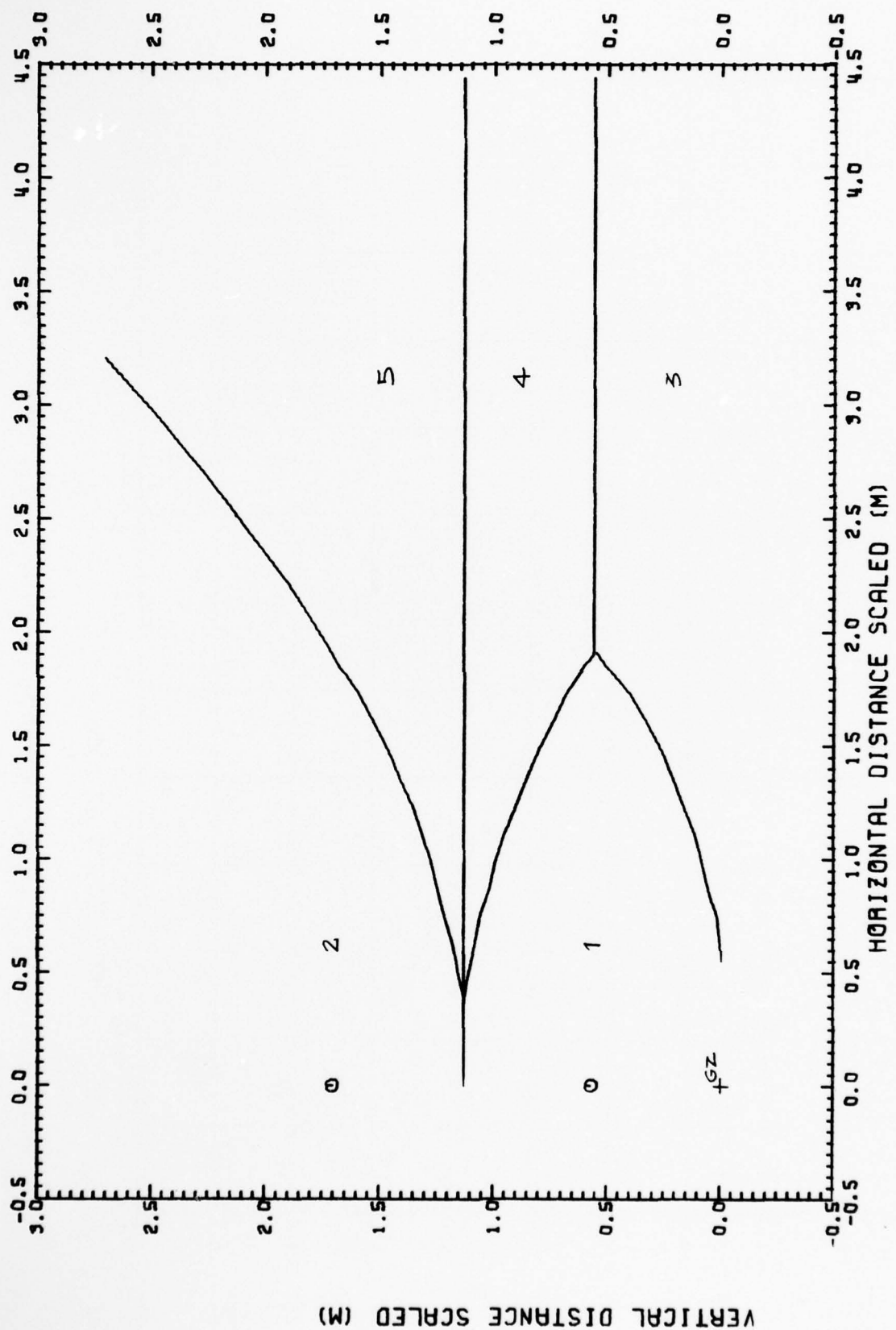


Fig. 6 REGIONS DEFINITION, DIPOLE WEST/9

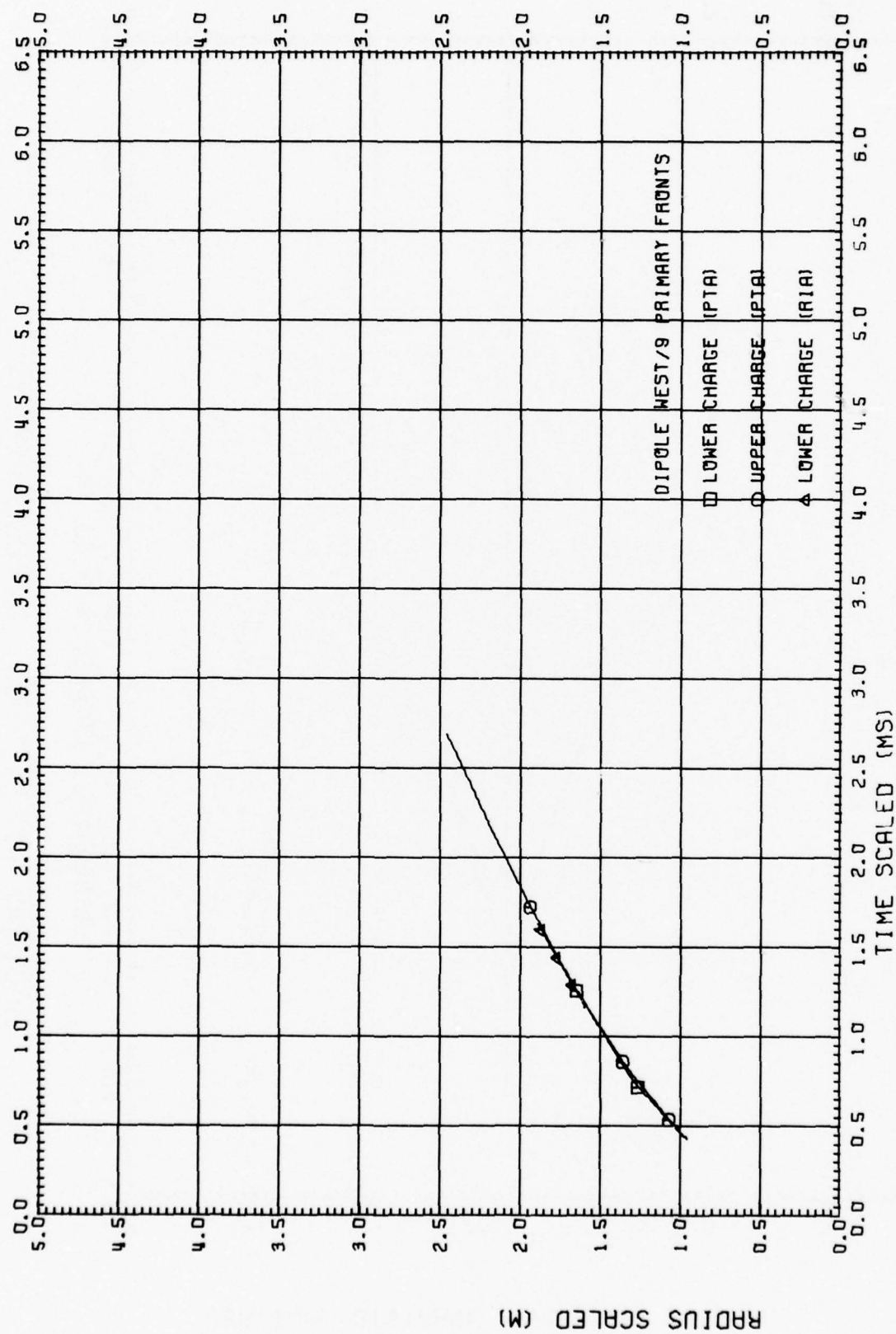


Fig. 7.1 SHOCK TRAJECTORIES, DIPOLE WEST/9

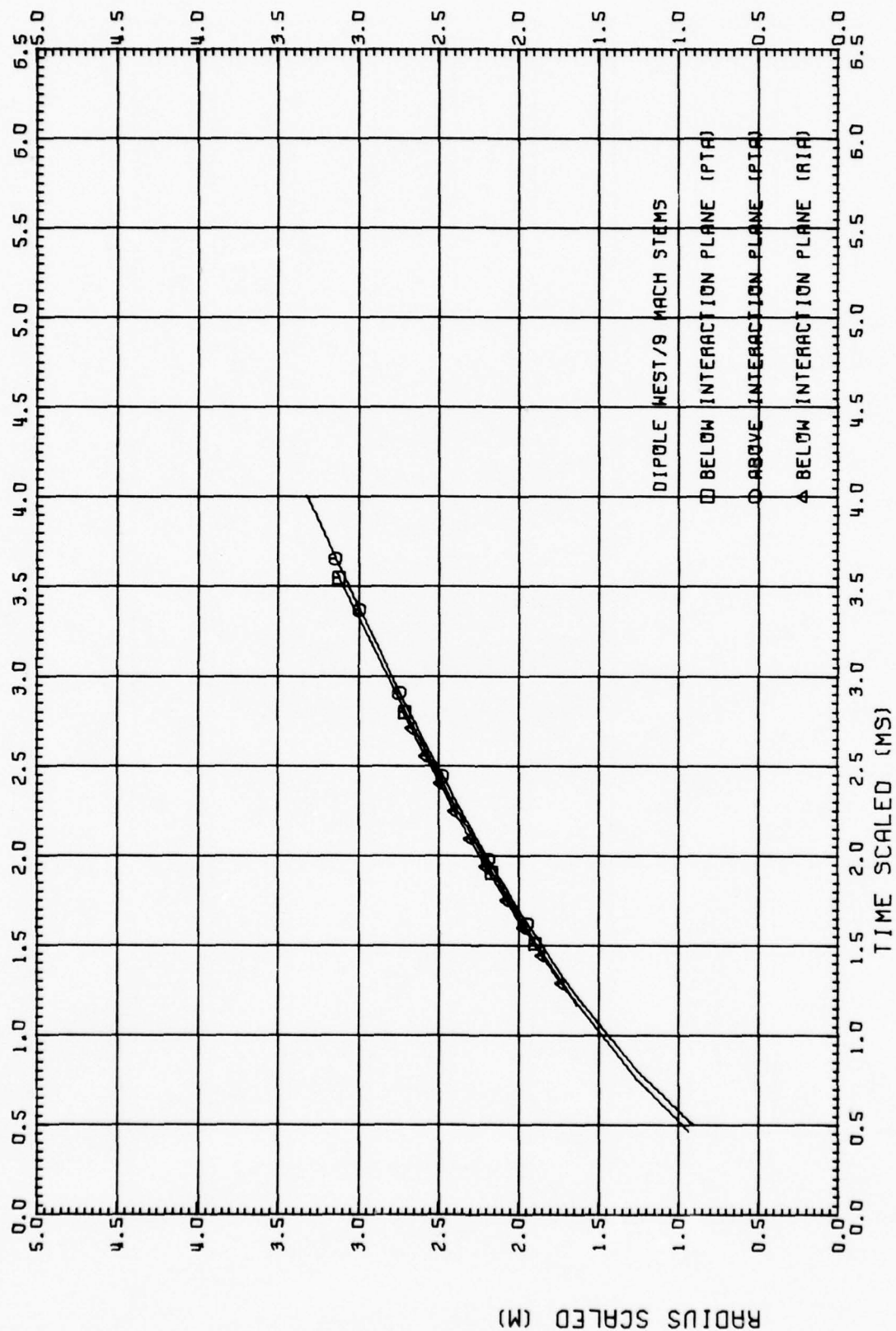


Fig. 7.2 SHOCK TRAJECTORIES, DIPOLE WEST/9

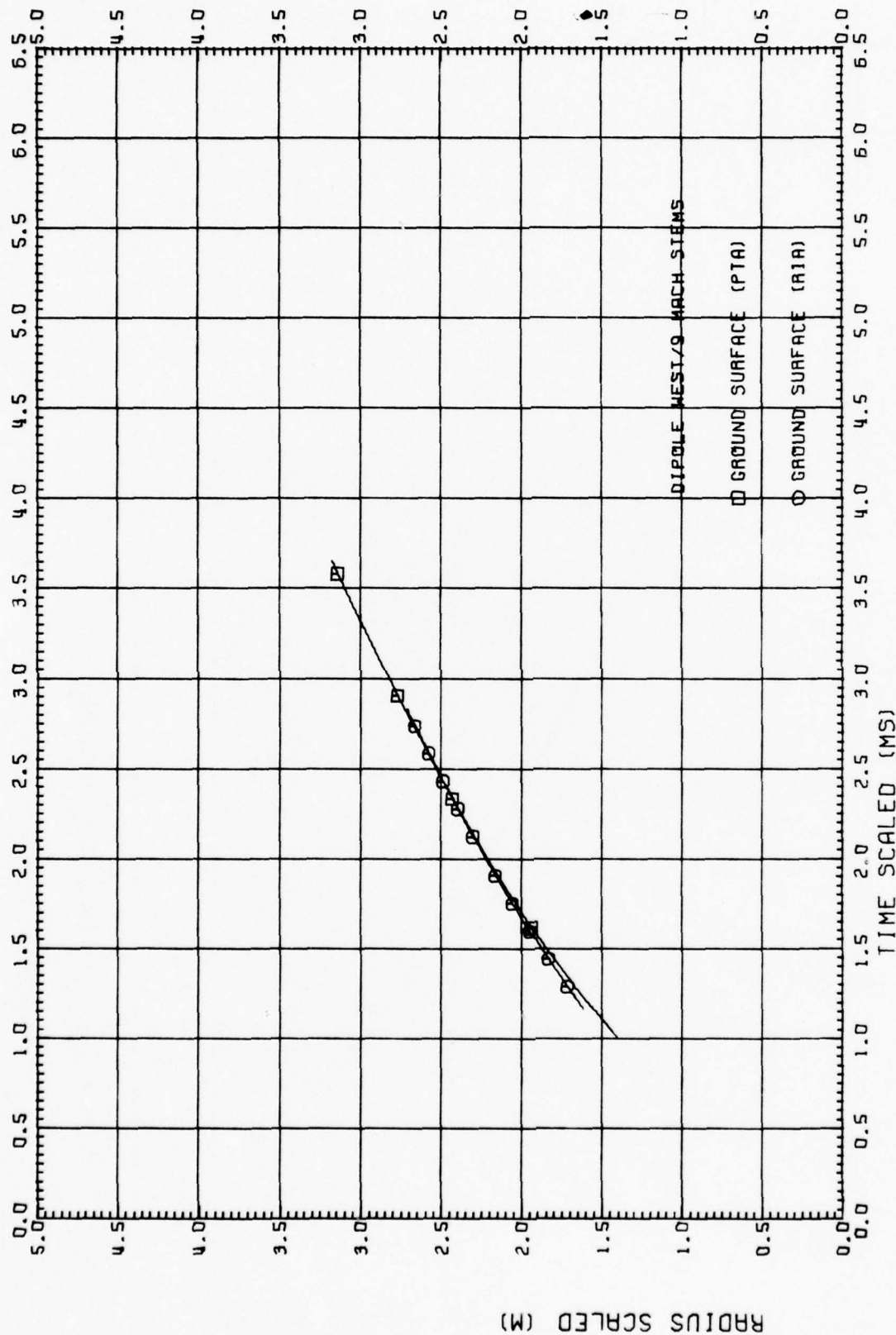


Fig. 7.3 SHOCK TRAJECTORIES, DIPOLE WEST/9

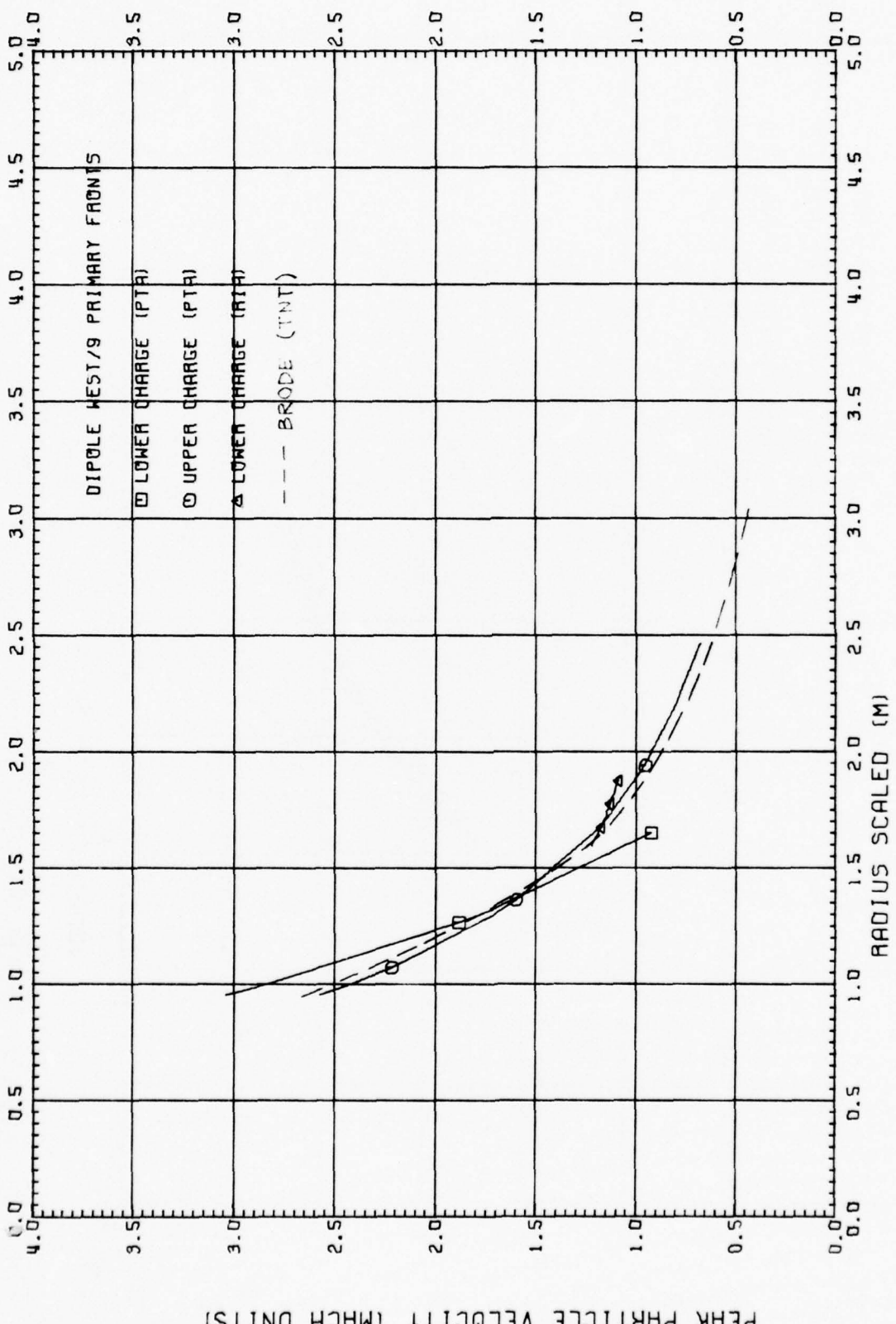


Fig. 8.1 SHOCK STRENGTH, METHOD 1

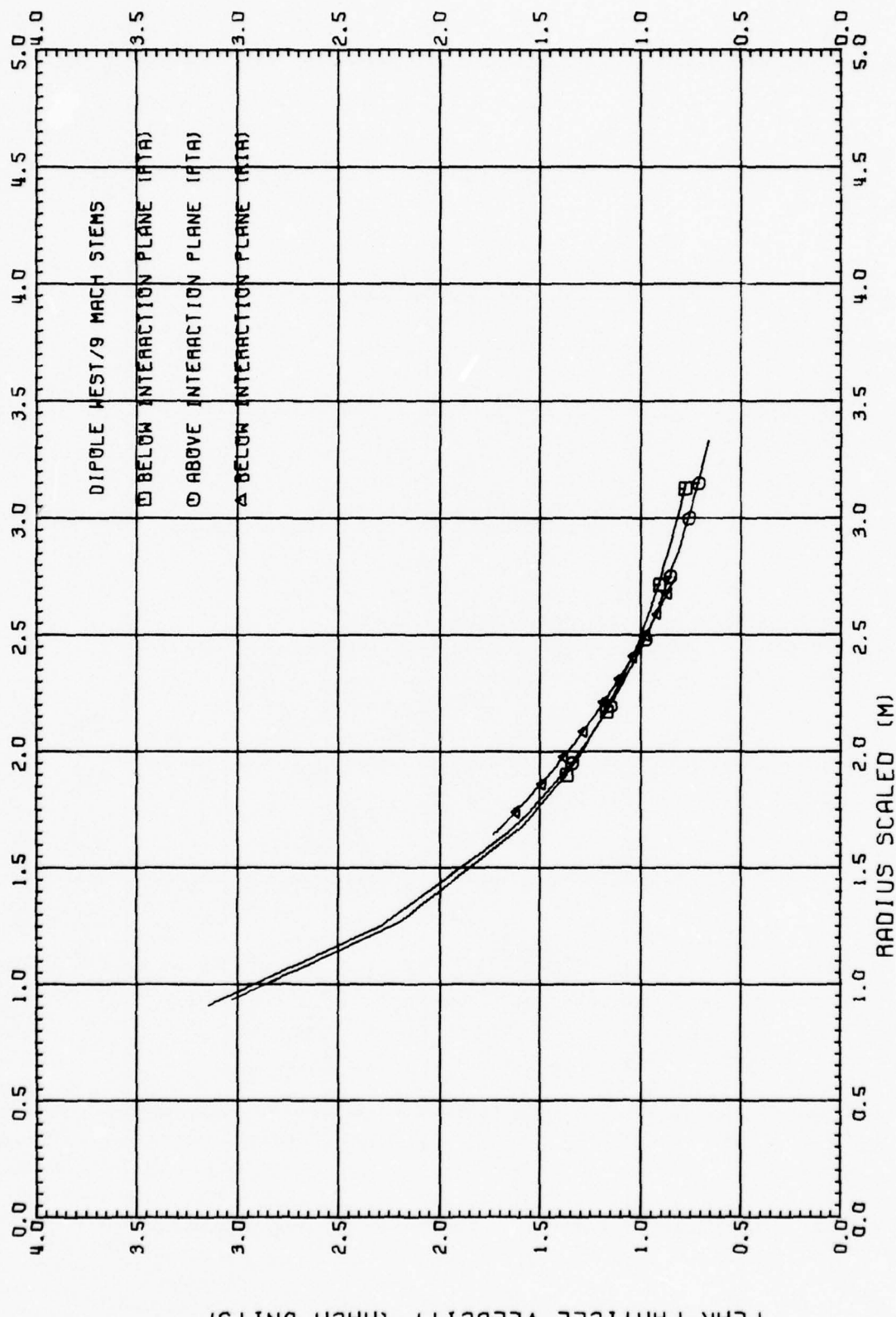


Fig. 8.2 SHOCK STRENGTH, METHOD 1

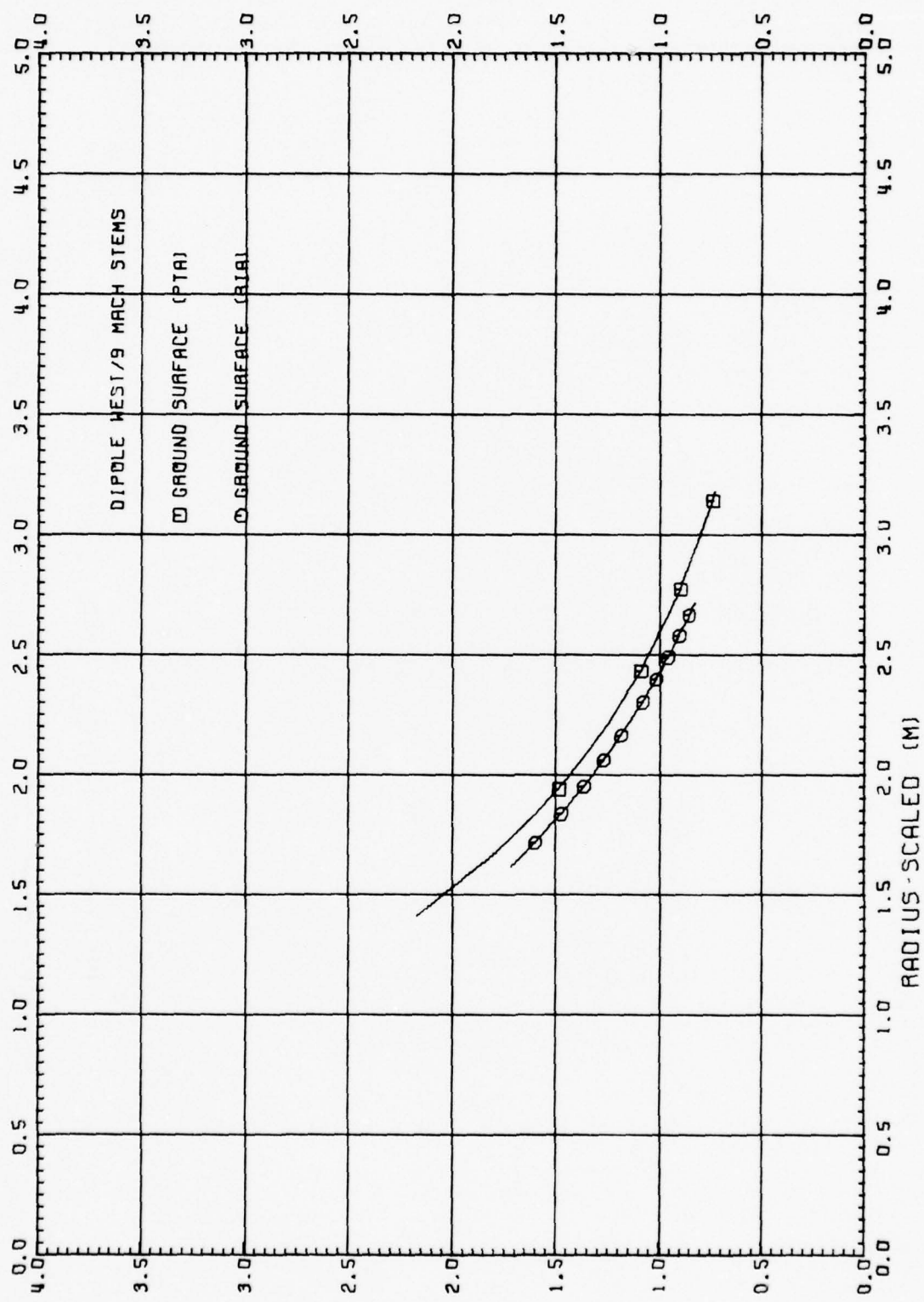


Fig. 8.3 SHOCK STRENGTH, METHOD 1

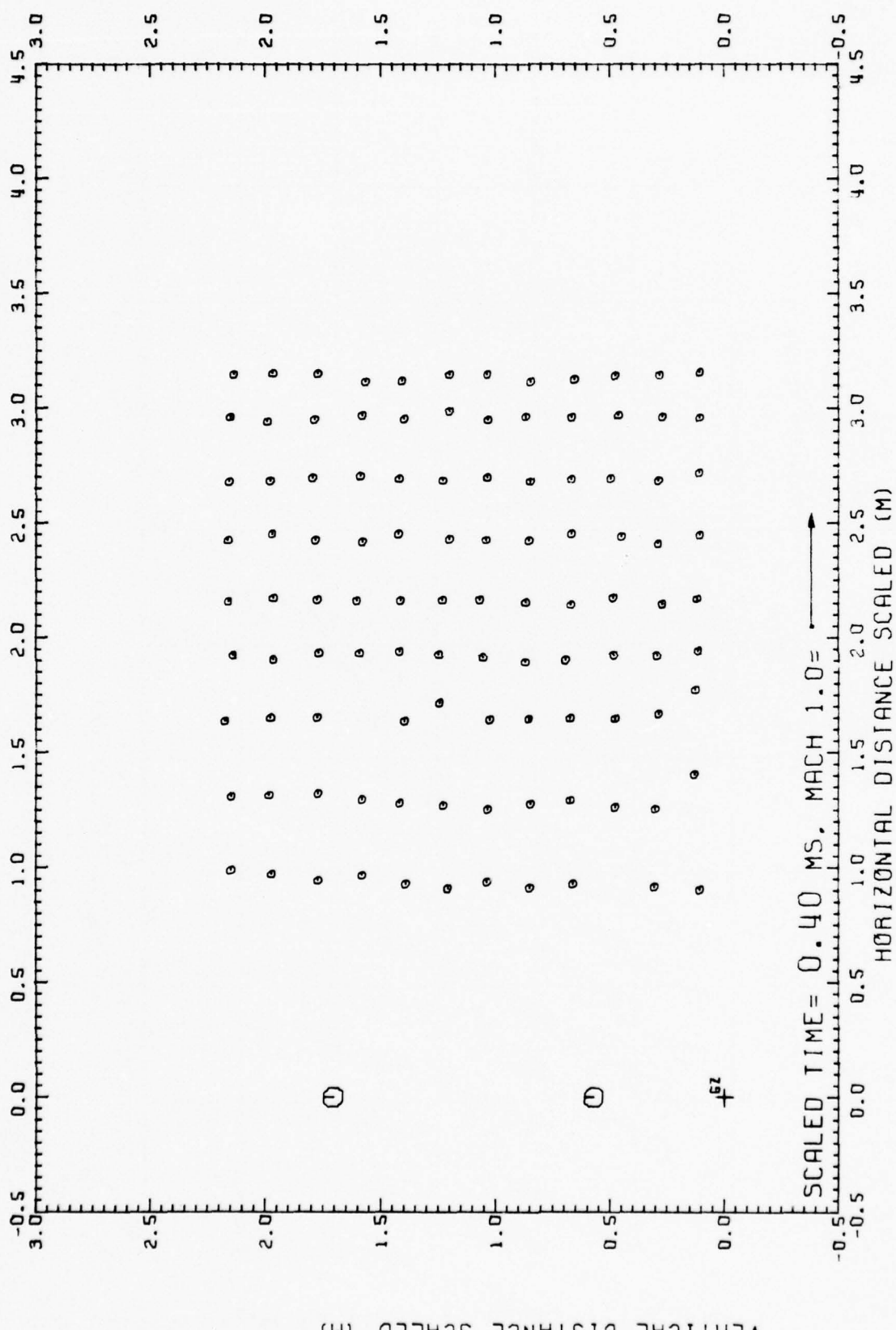


Fig. 12.1 PARTICLE VELOCITY FIELD, DIPOLE WEST/9

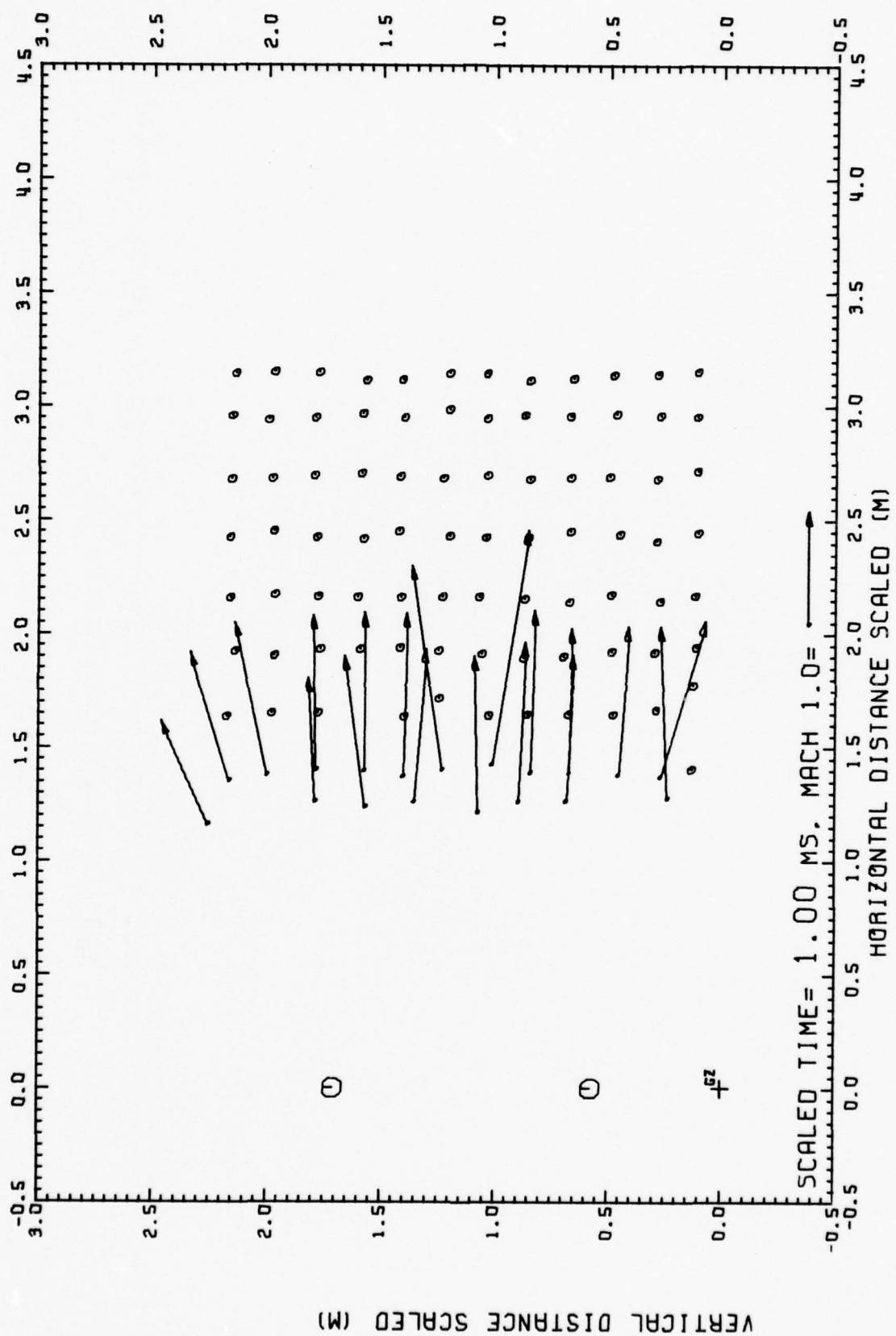
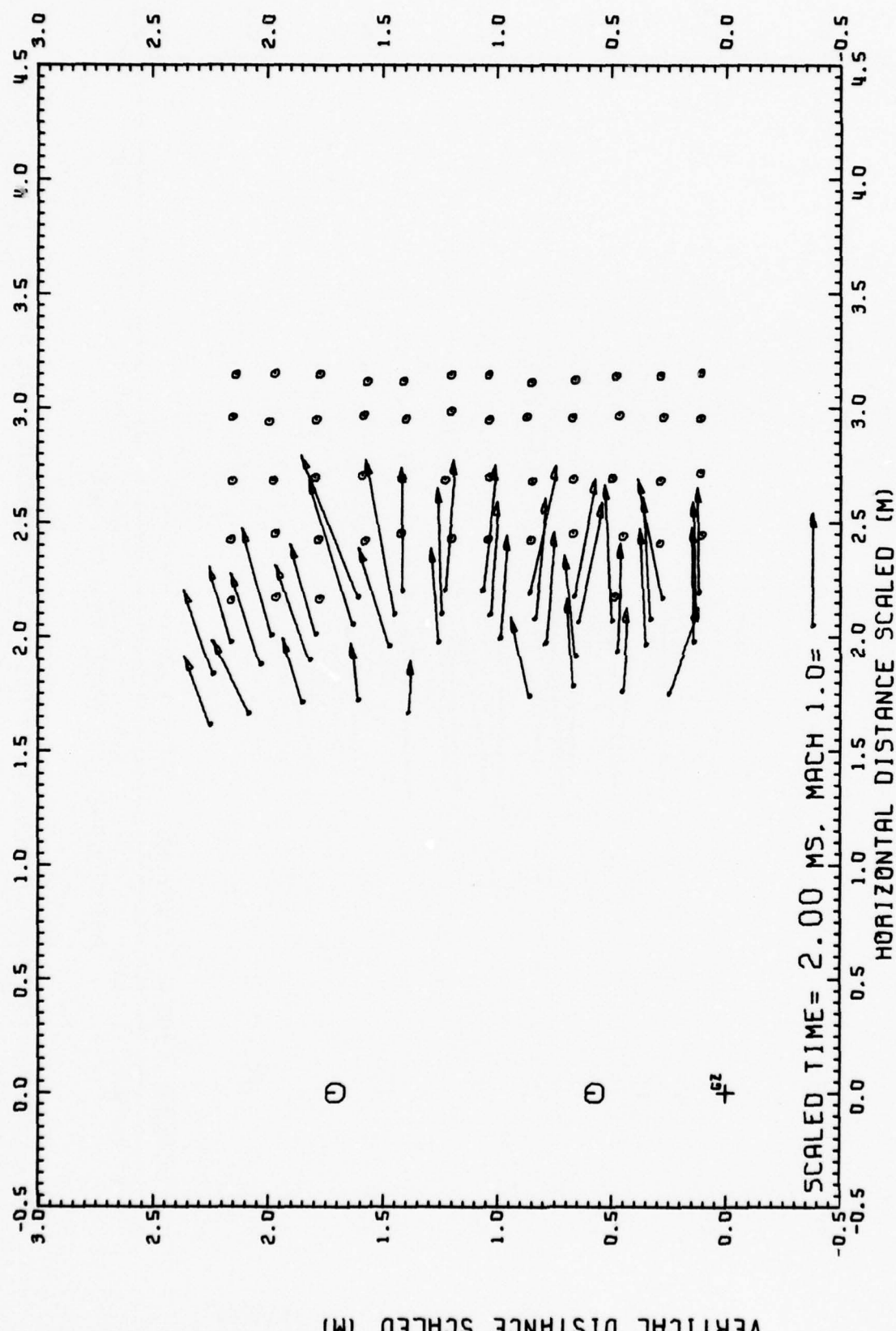


Fig. 12.2 PARTICLE VELOCITY FIELD, DIPOLE WEST/9



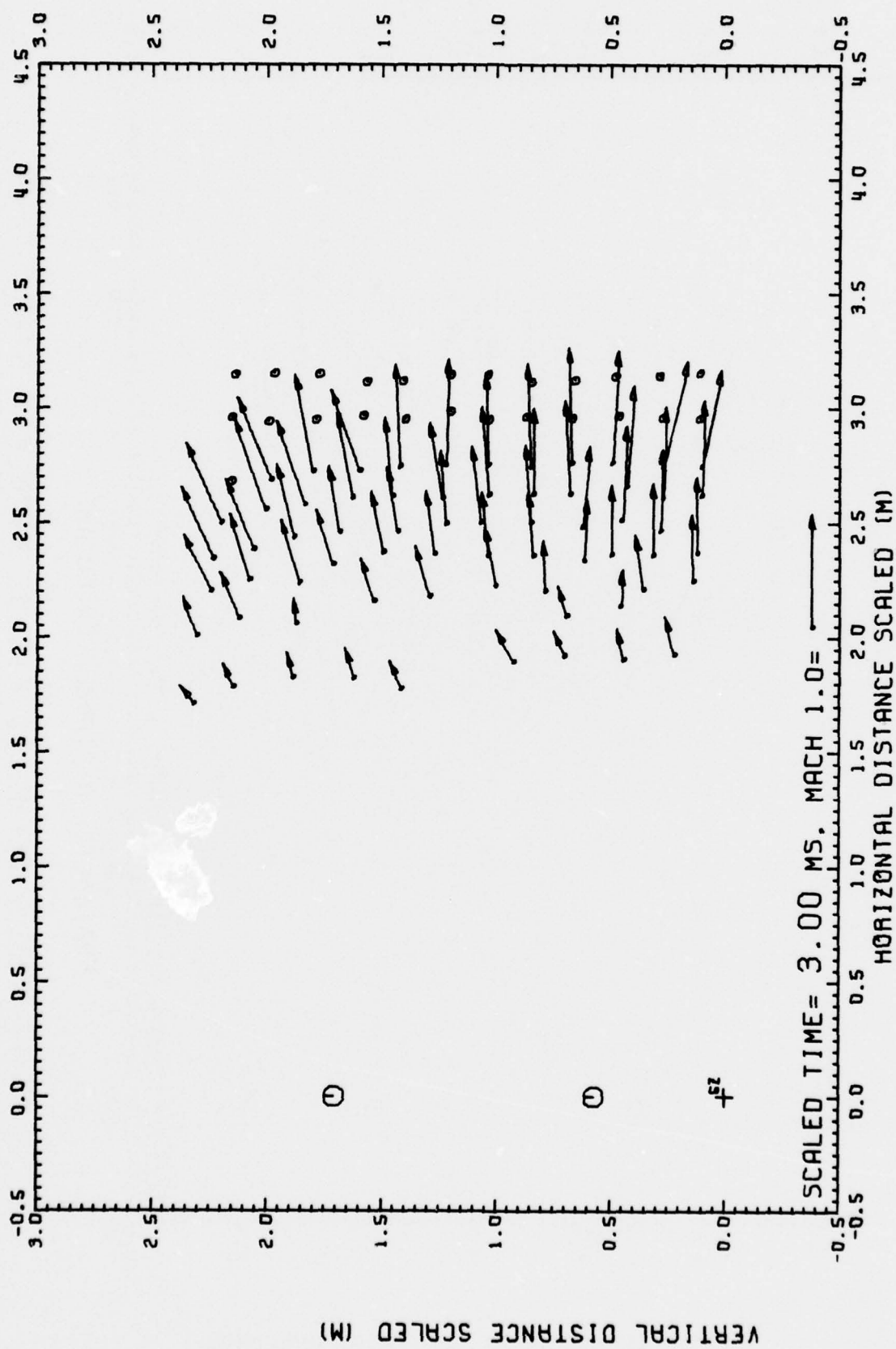


Fig. 12.4 PARTICLE VELOCITY FIELD. DIPOLE WEST/9

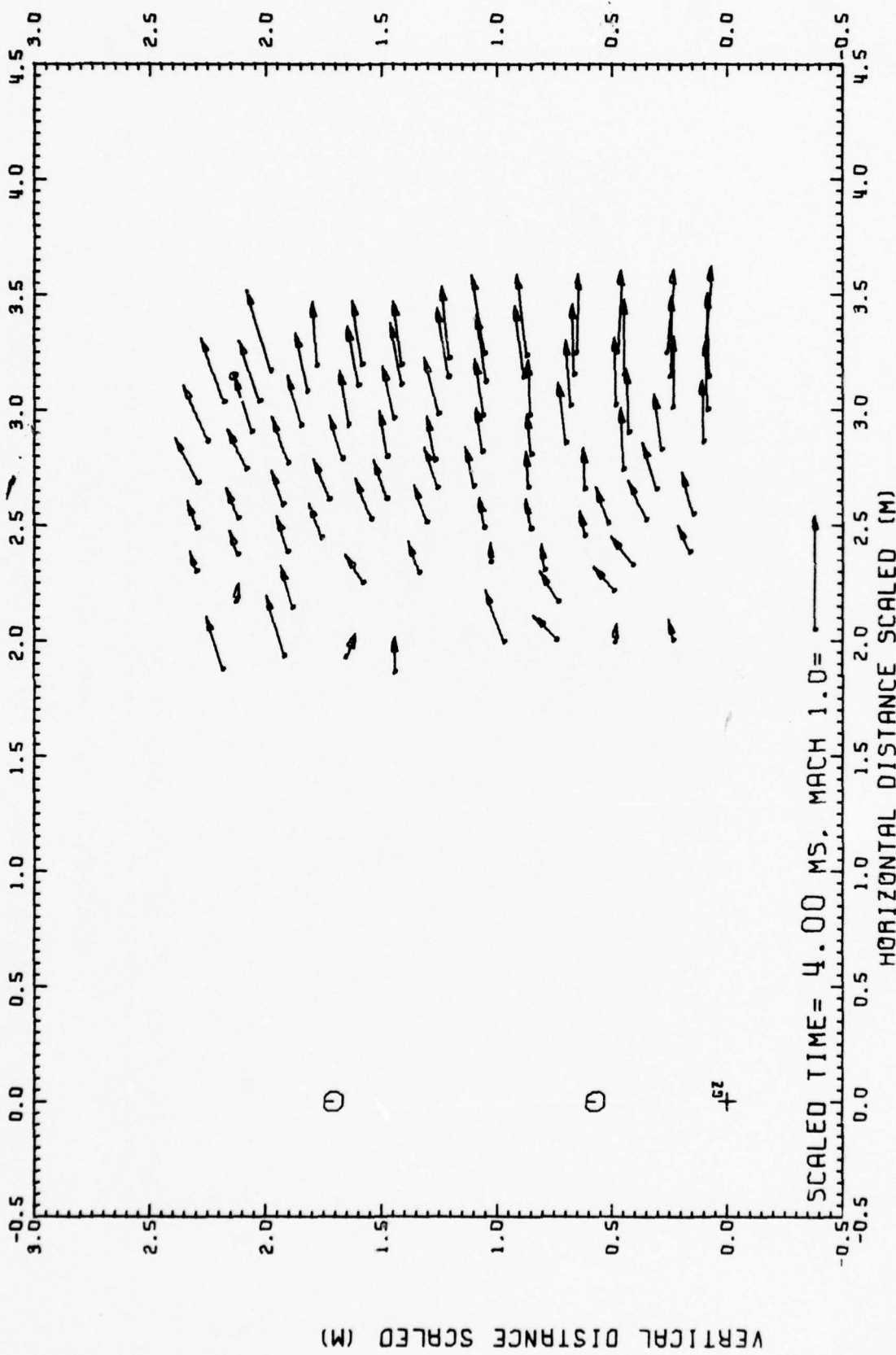


Fig. 12.5 PARTICLE VELOCITY FIELD, DIPOLE WEST/9

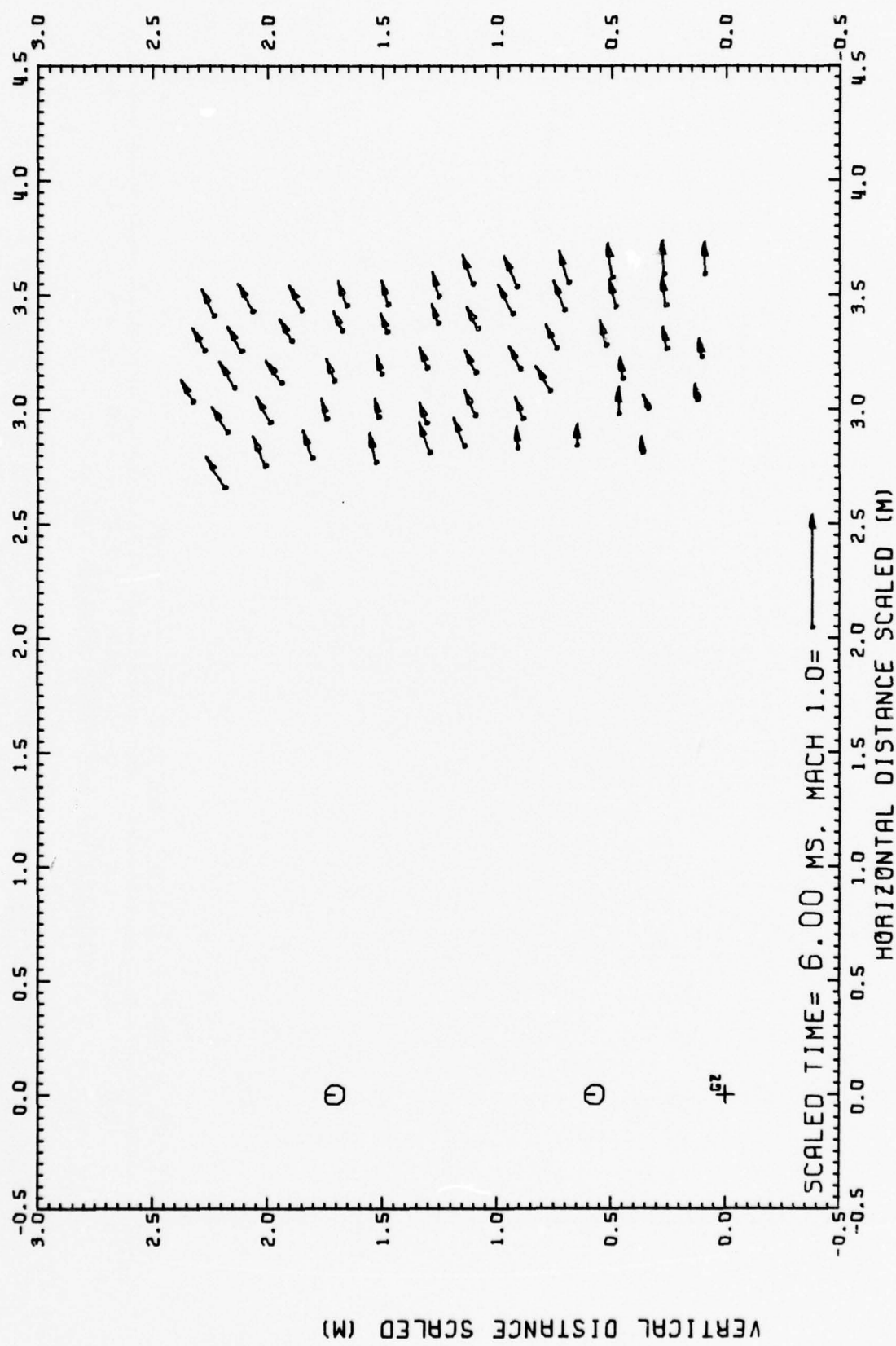


Fig. 12.6 PARTICLE VELOCITY FIELD, DIPOLE WEST / 9

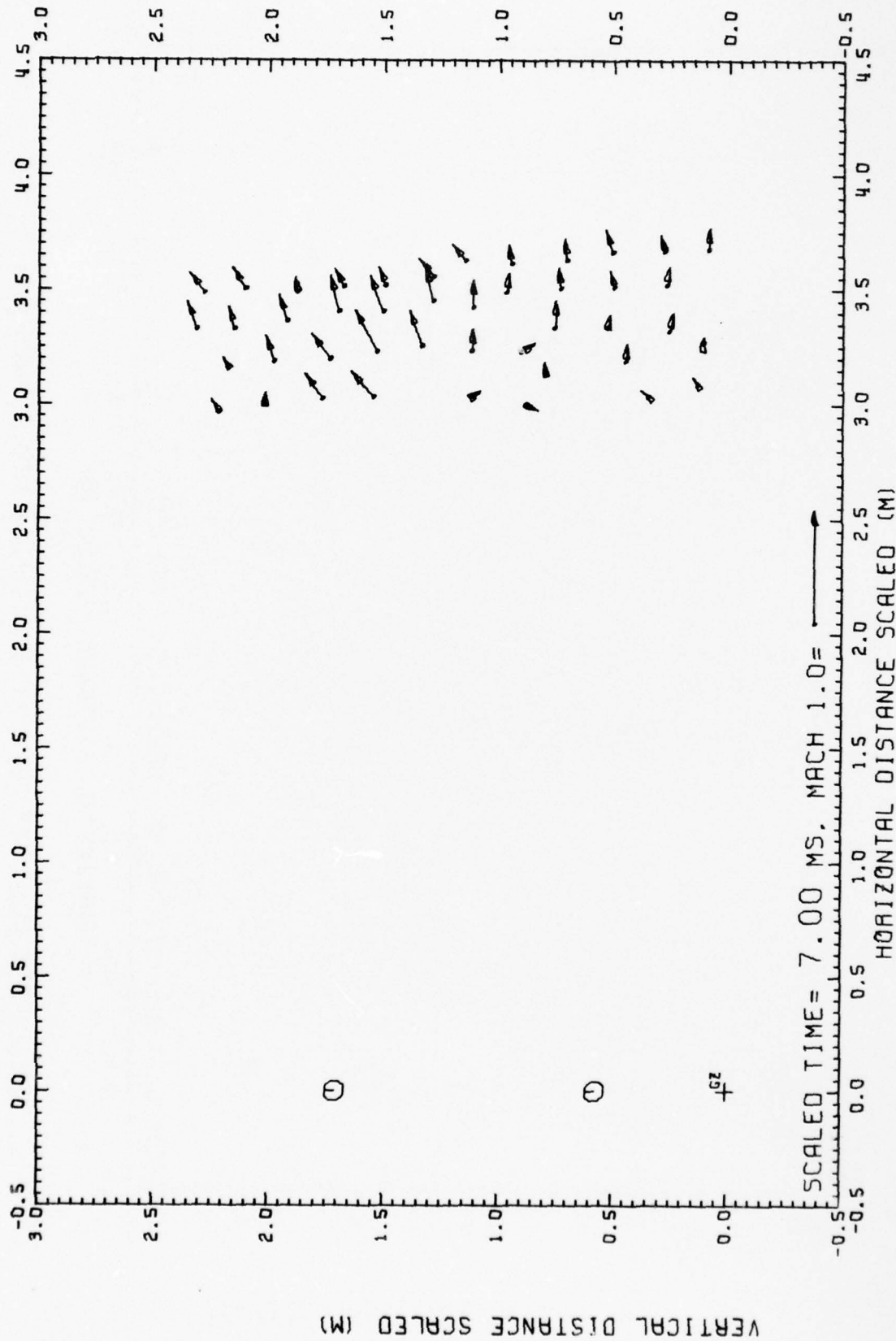


Fig. 12.7 PARTICLE VELOCITY FIELD, DIPOLE WEST/9

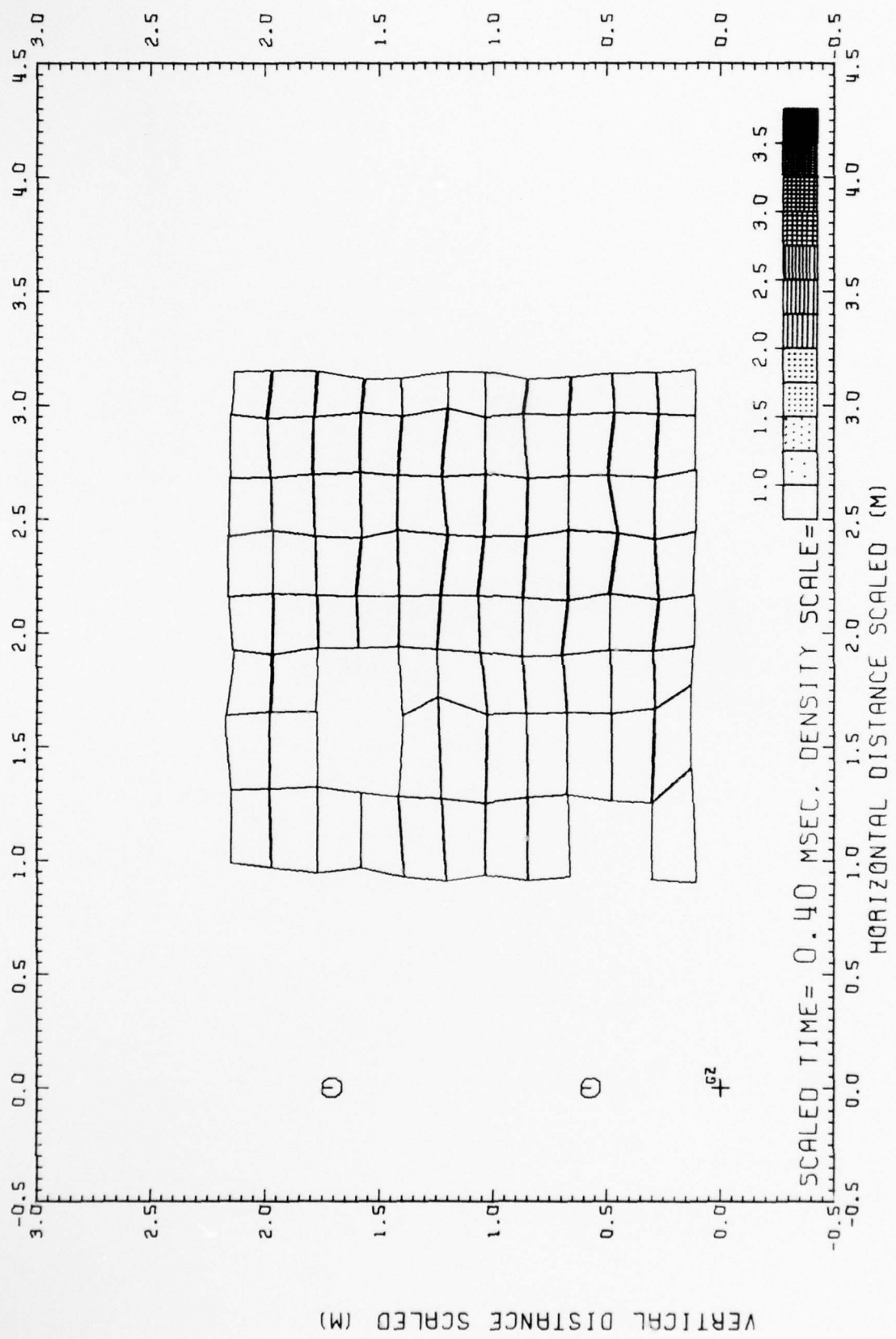


Fig. 13.1 DENSITY FIELD, DIPOLE WEST/9

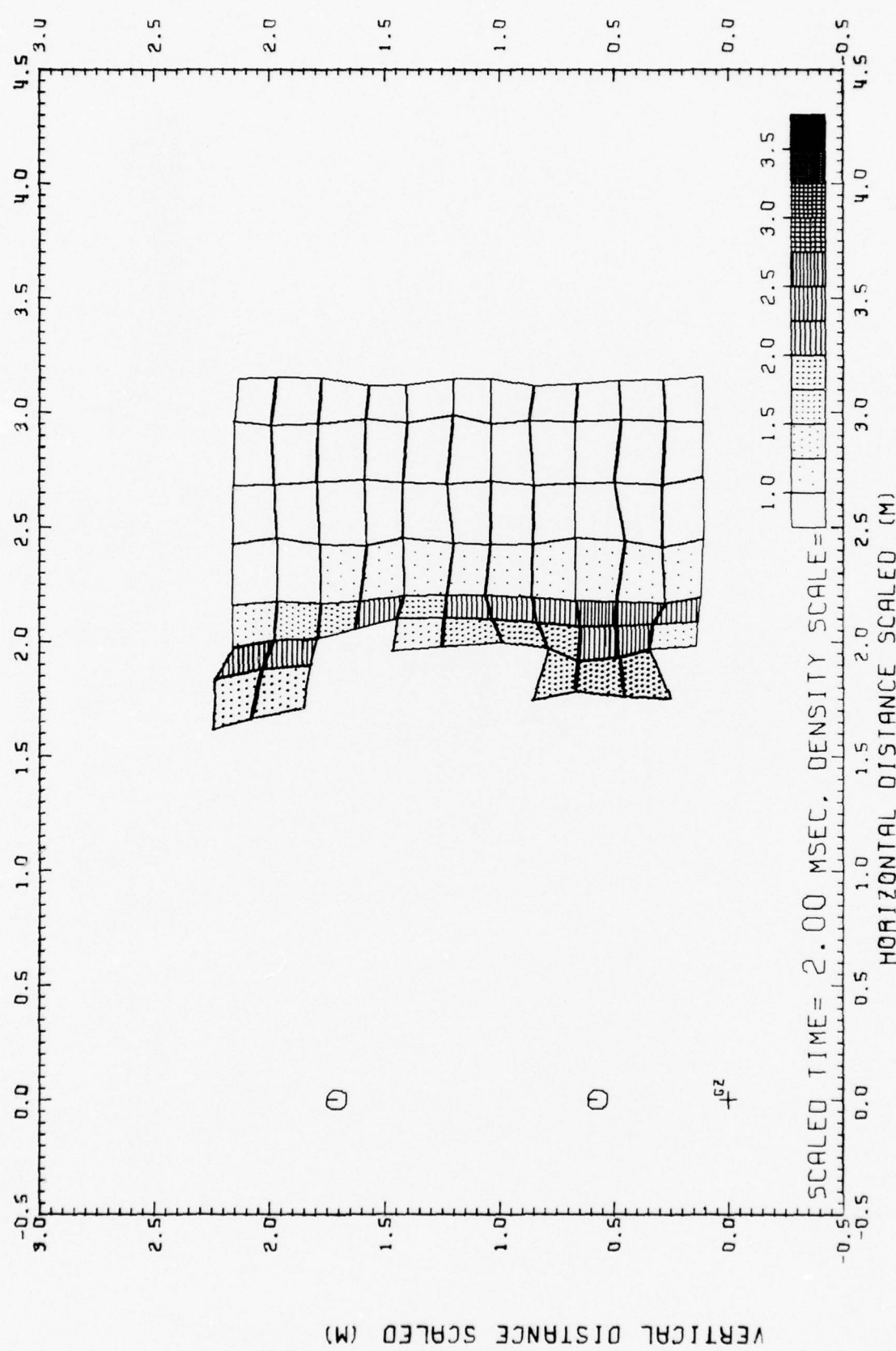


Fig. 13.2 DENSITY FIELD, DIPOLE WEST/9

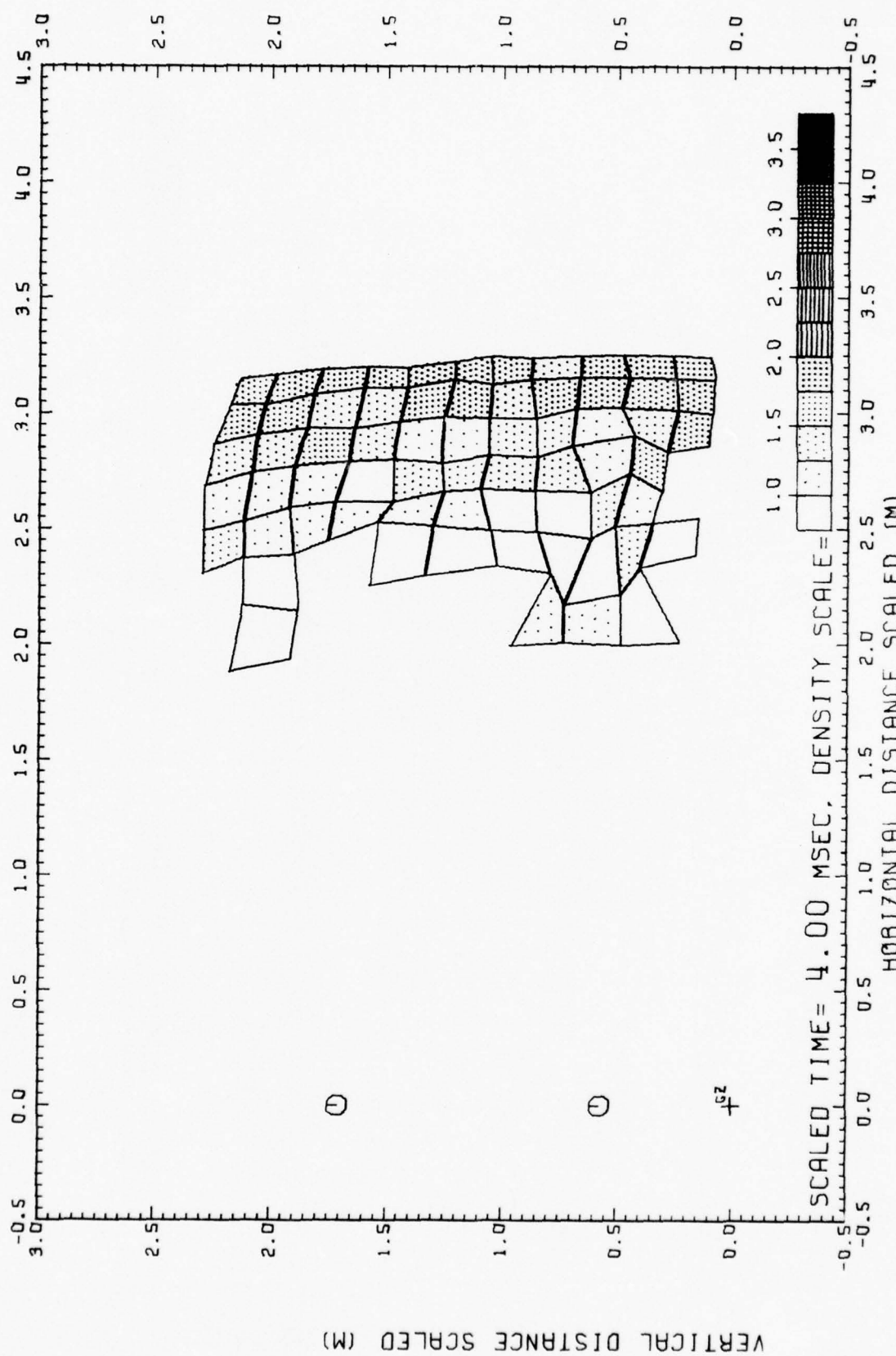


Fig. 13.3 DENSITY FIELD, DIPOLE WEST / 9

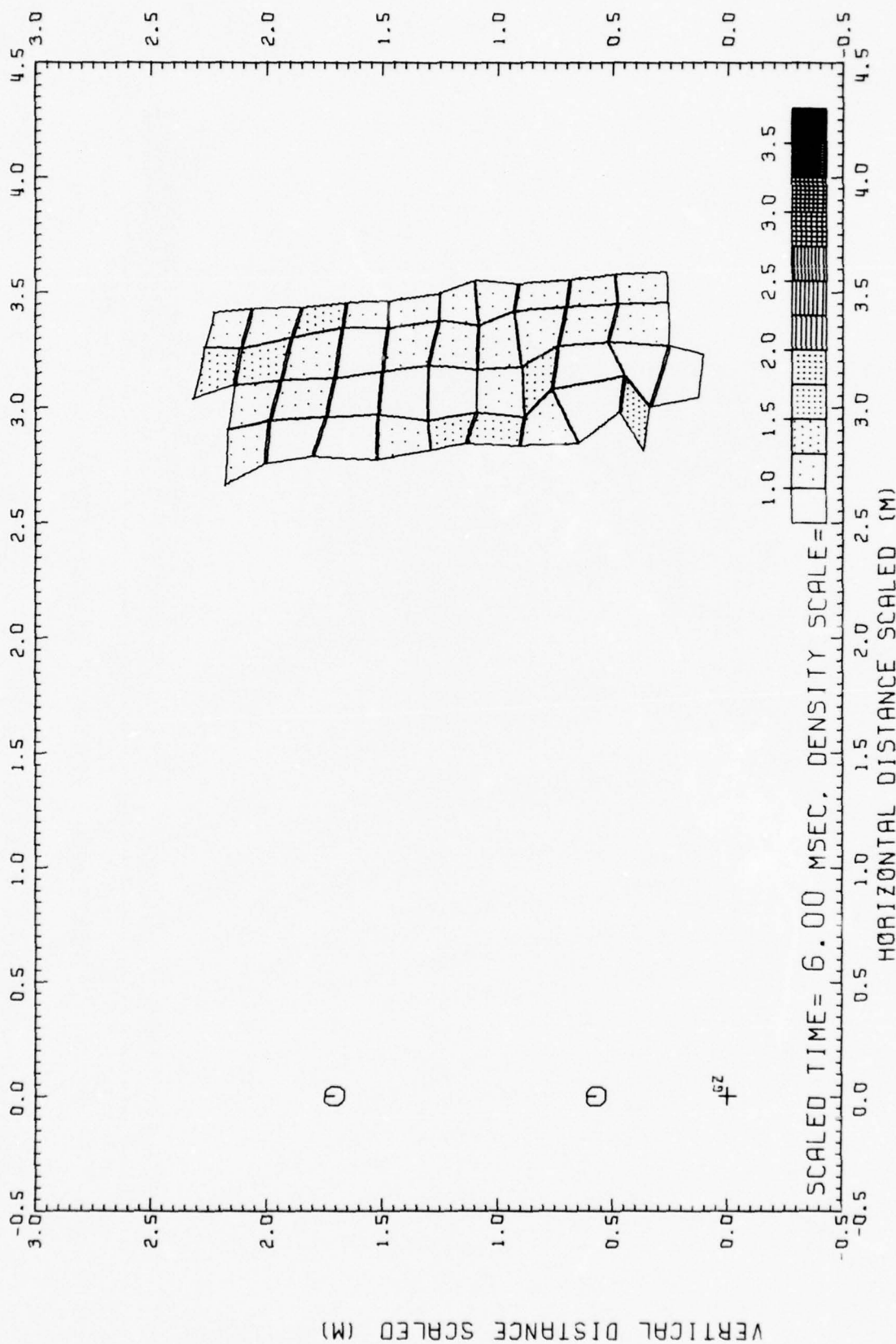


Fig. 13.4 DENSITY FIELD, DIPOLE WEST /9

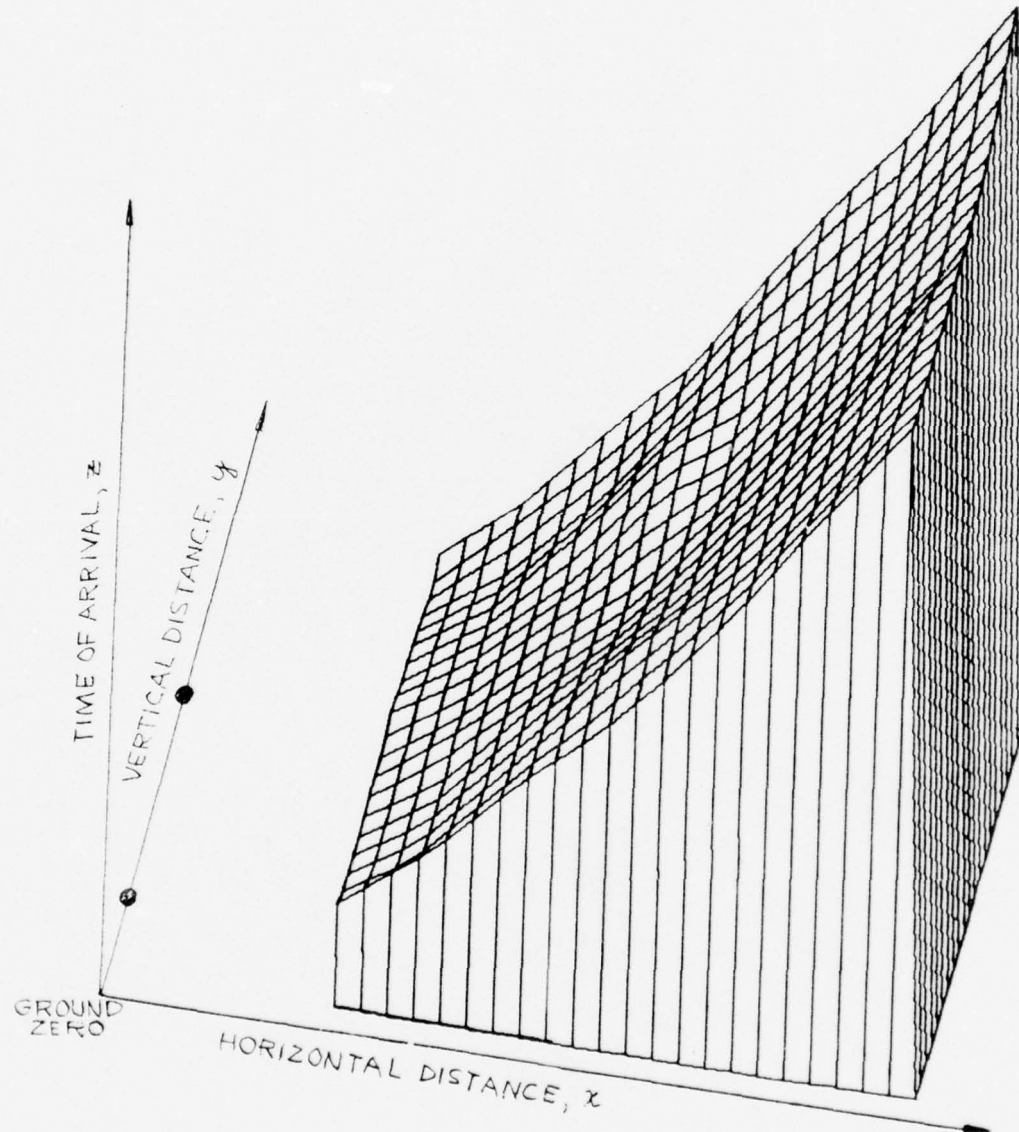


Fig. 14 Time-of-arrival surface, Dipole West/9

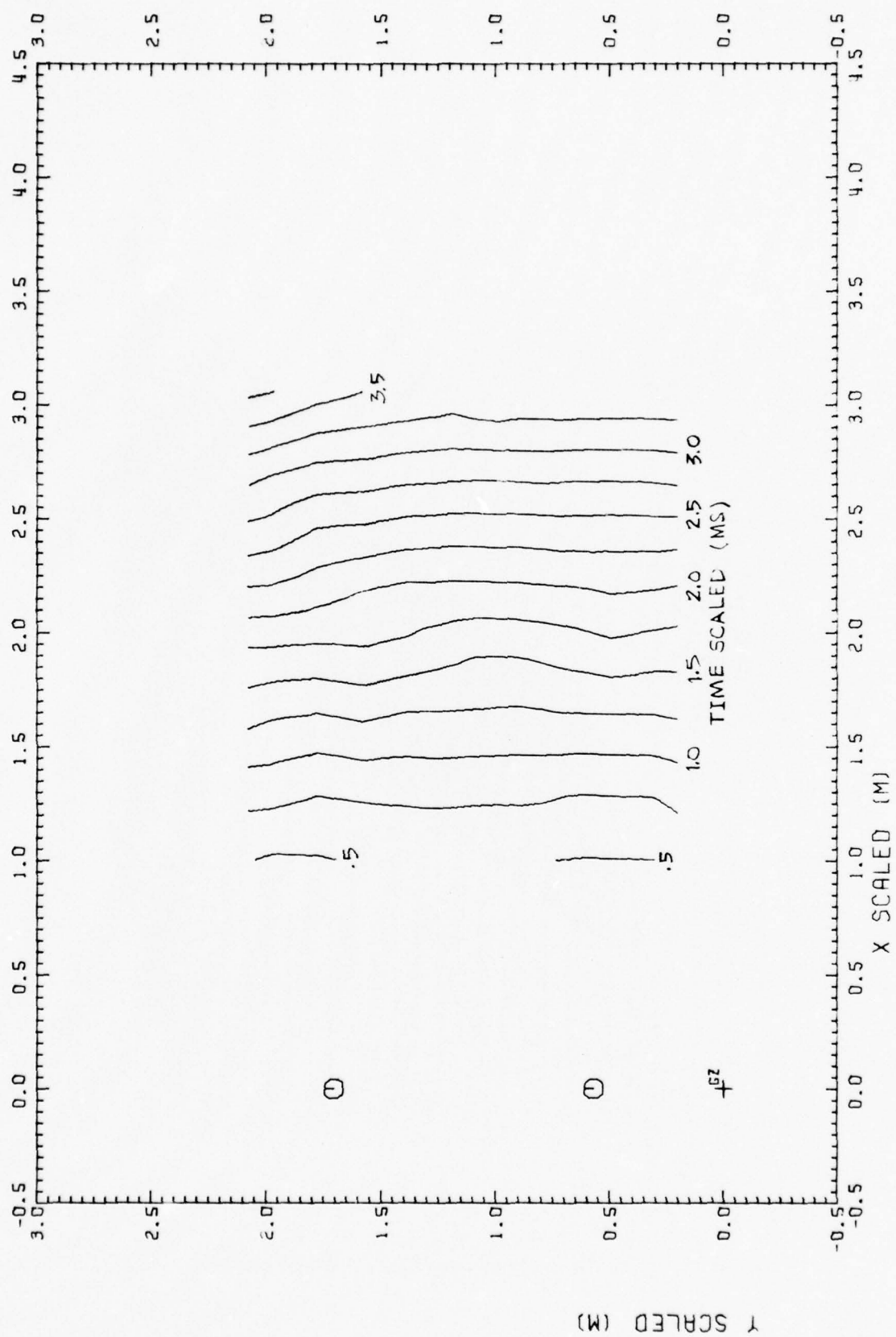


Fig. 15 SHOCK FRONT SHAPES, DIPOLE WEST/g

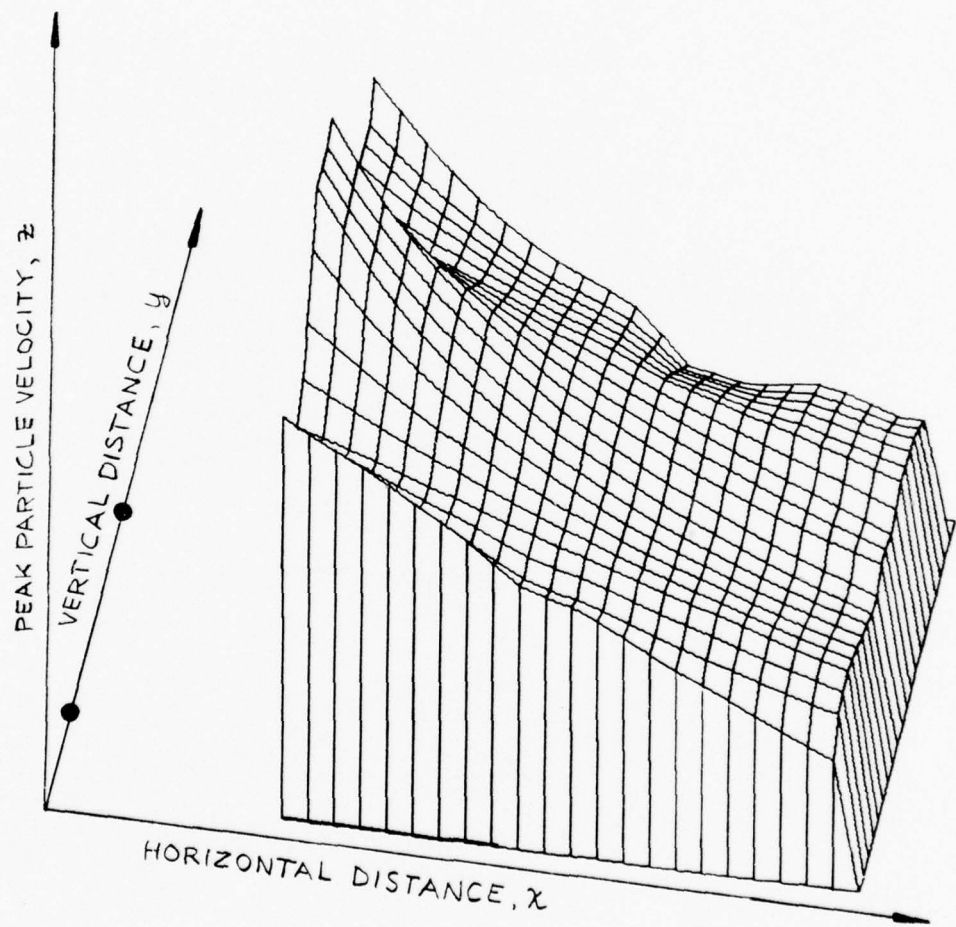


Fig. 16 A shock strength surface, Dipole West/9

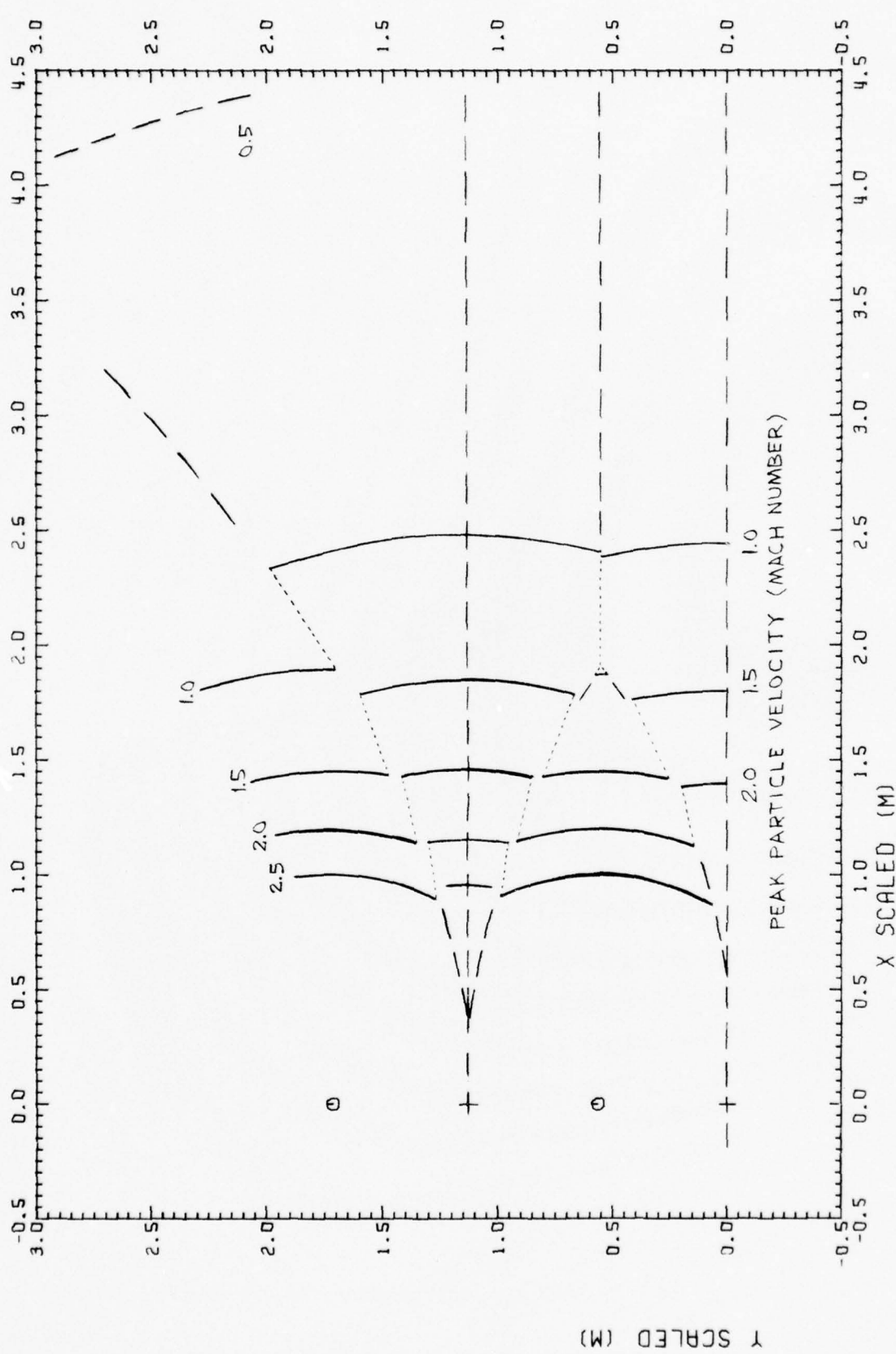


Fig. 17 SHOCK STRENGTH CONTOURS, DIPOLE WEST/9

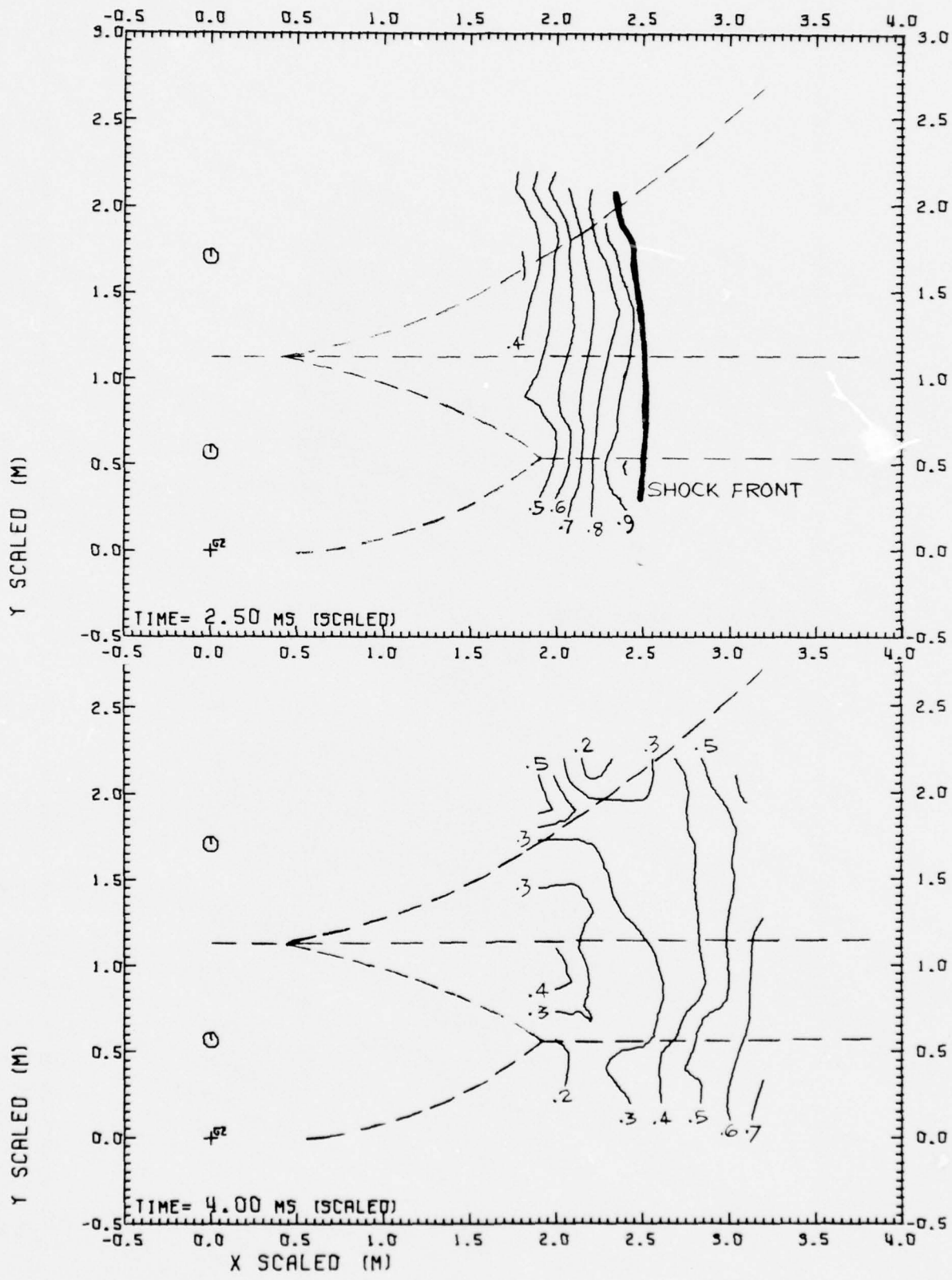


Fig. 18 DIPOLE WEST/9 PARTICLE VELOCITY

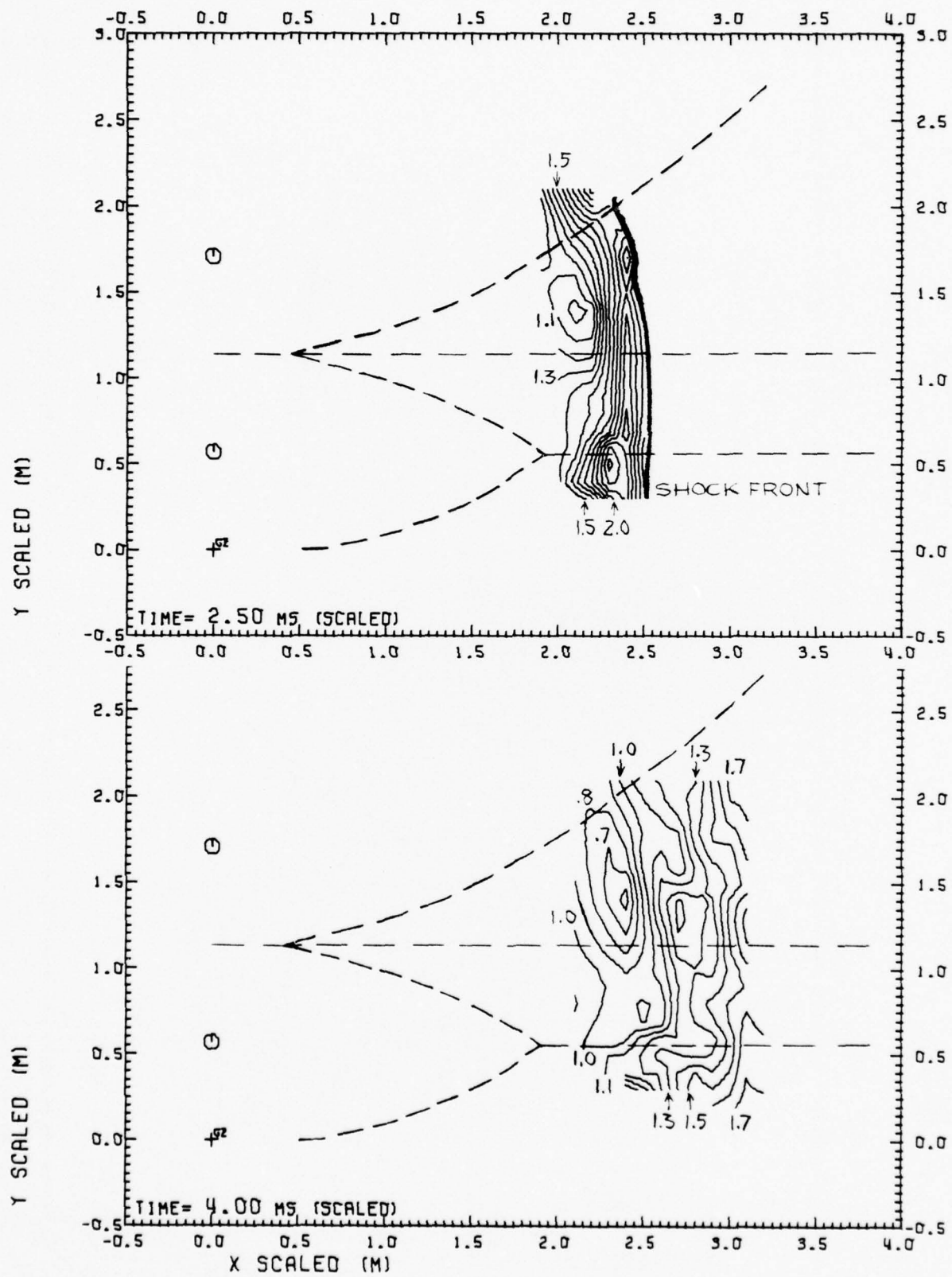


Fig. 19 DIPOLE WEST/9 DENSITY
60

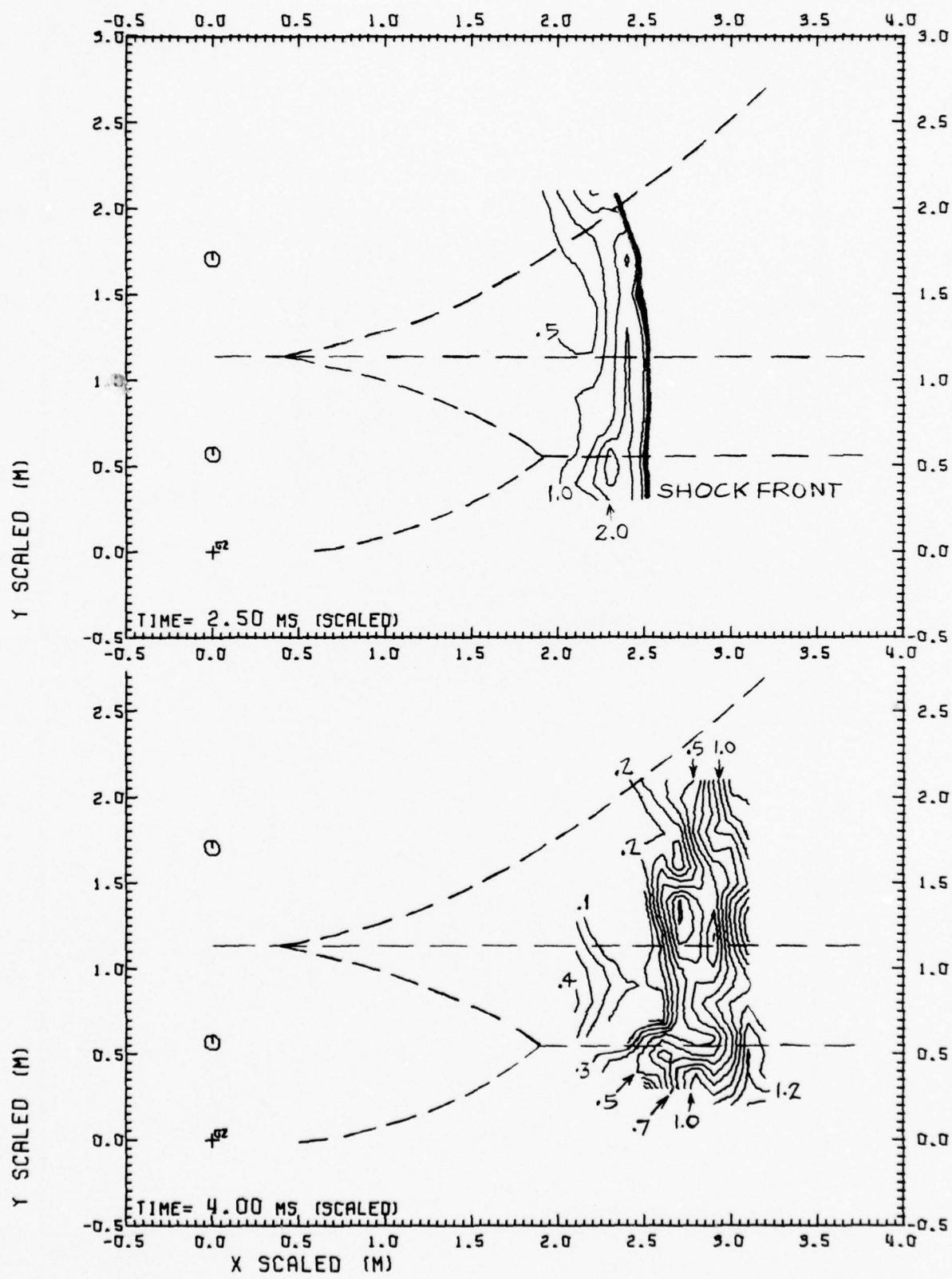


Fig. 20 DIPOLE WEST/9 HYDROSTATIC OVERPRESSURE
61

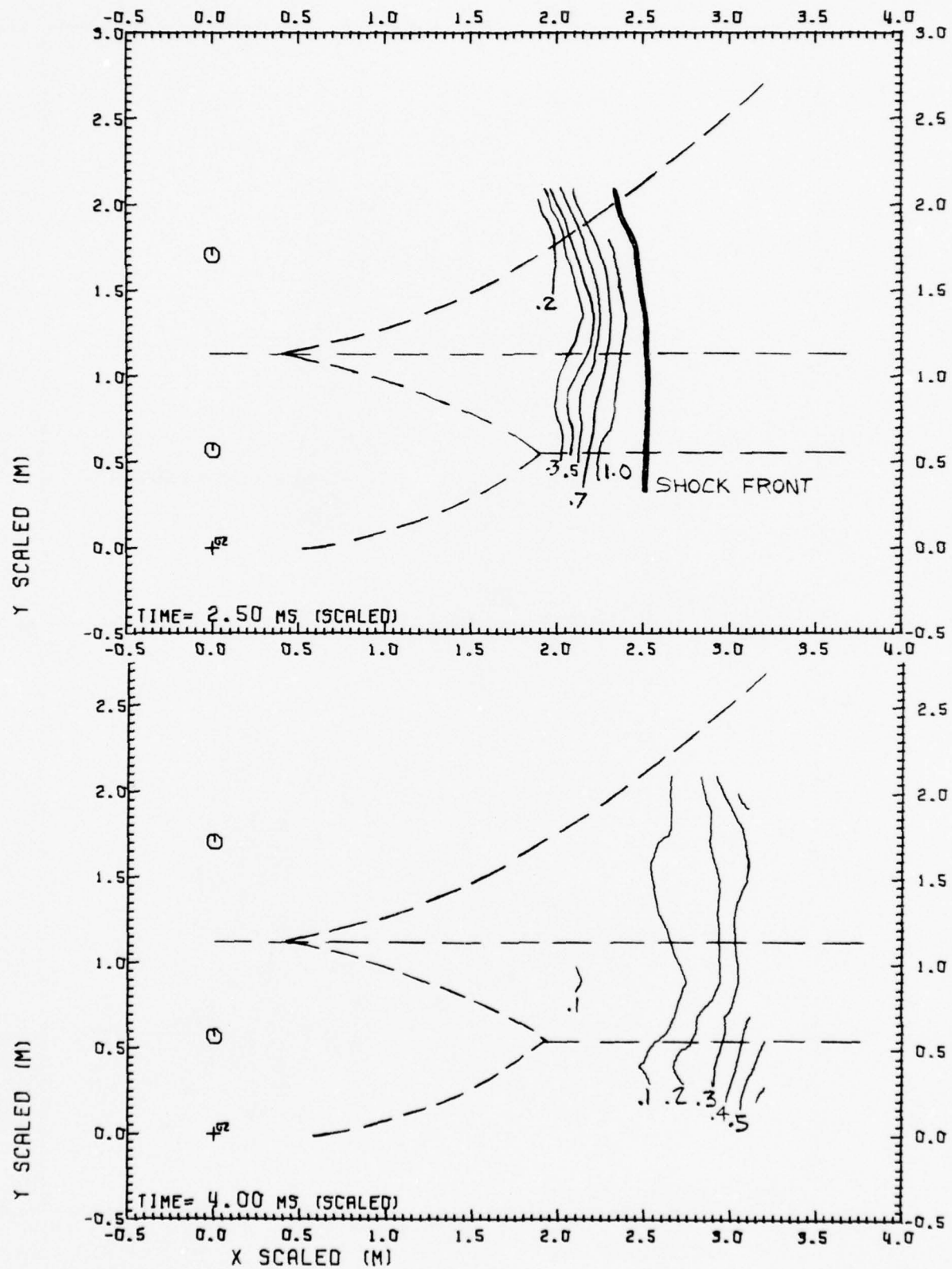


Fig. 21 DIPOLE WEST/9 DYNAMIC PRESSURE

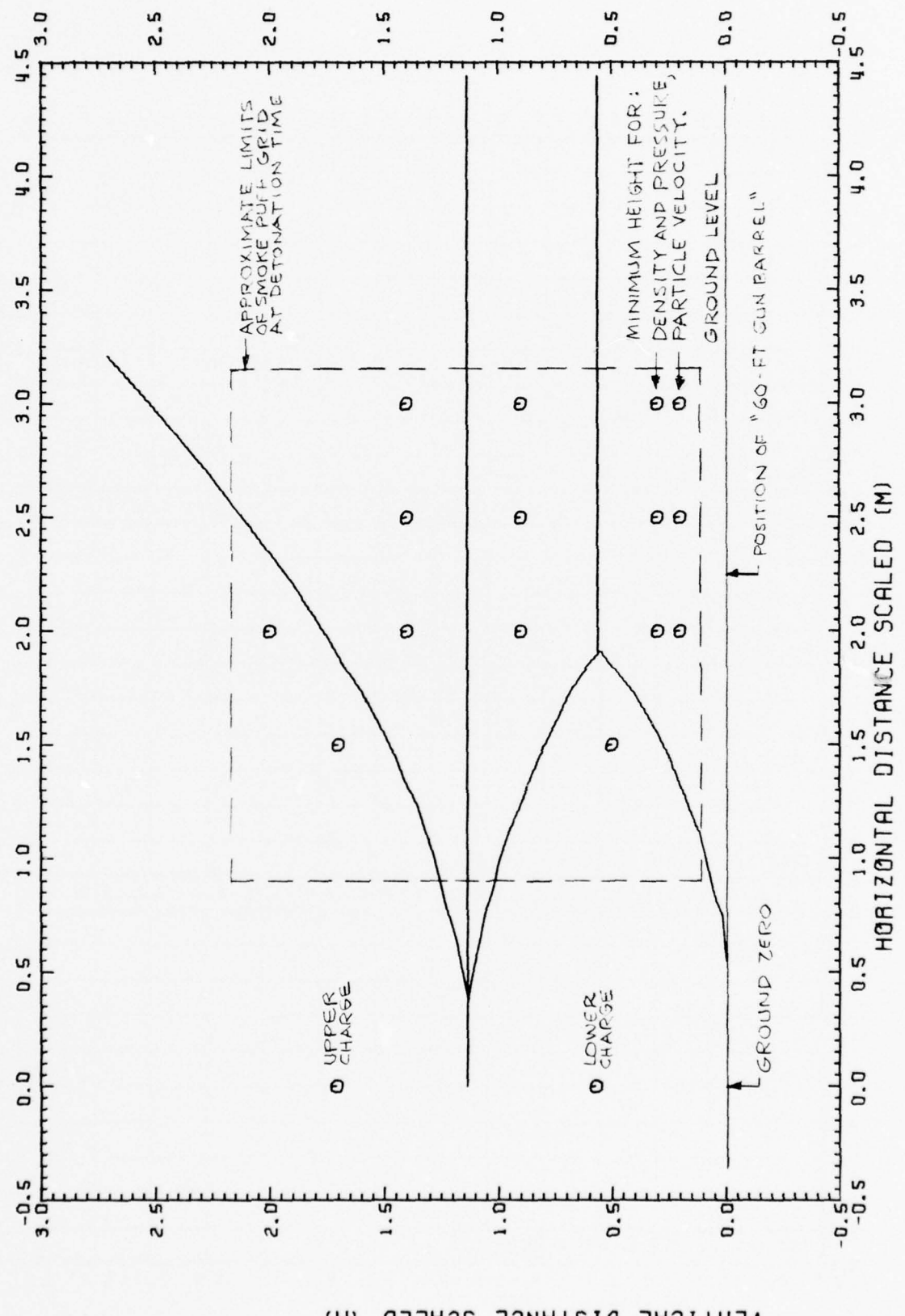


Fig. 22 TIME HISTORY STATIONS, DIPOLE WEST/9

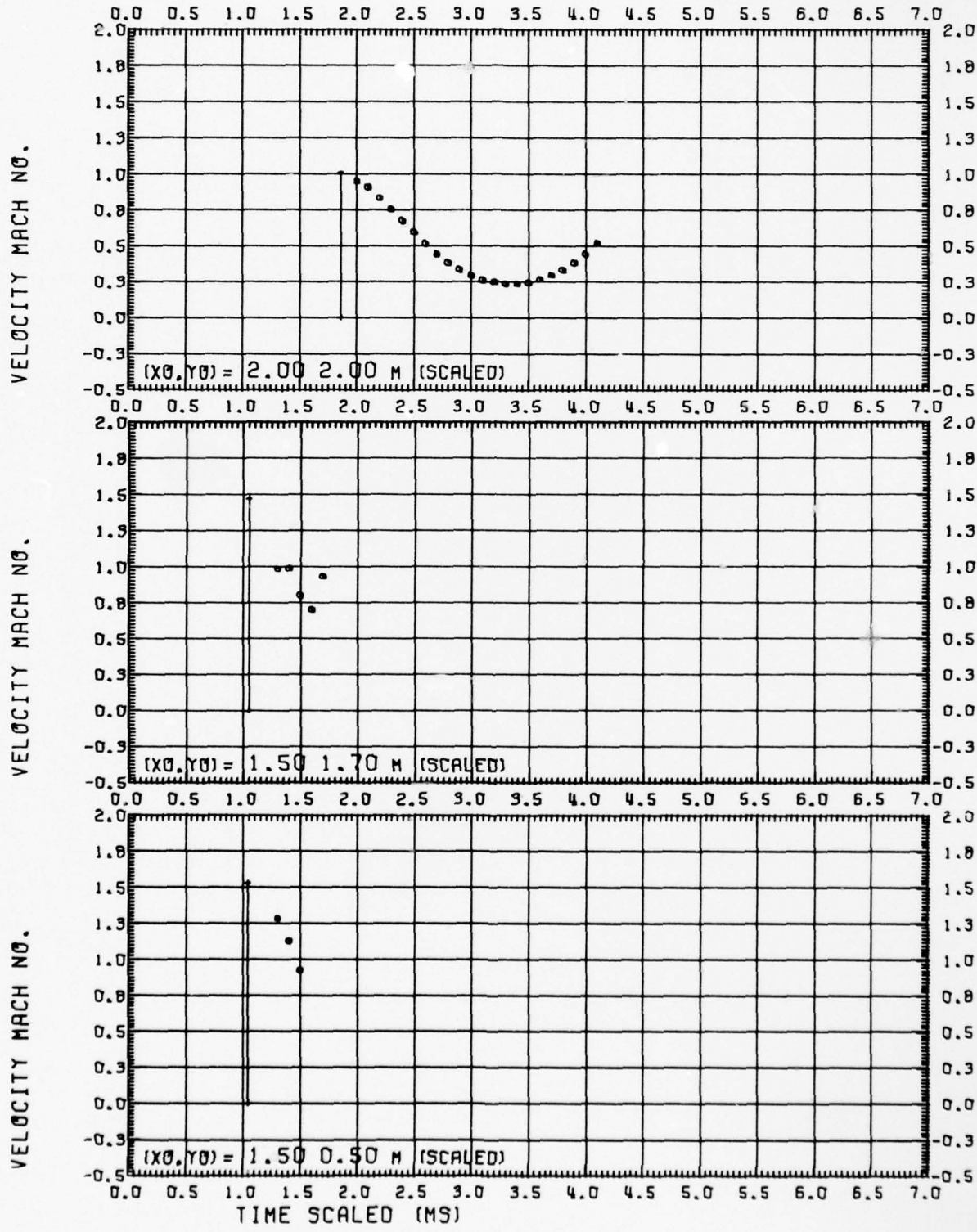


Fig. 23.1 DIPOLE WEST/9 PARTICLE VELOCITY
64

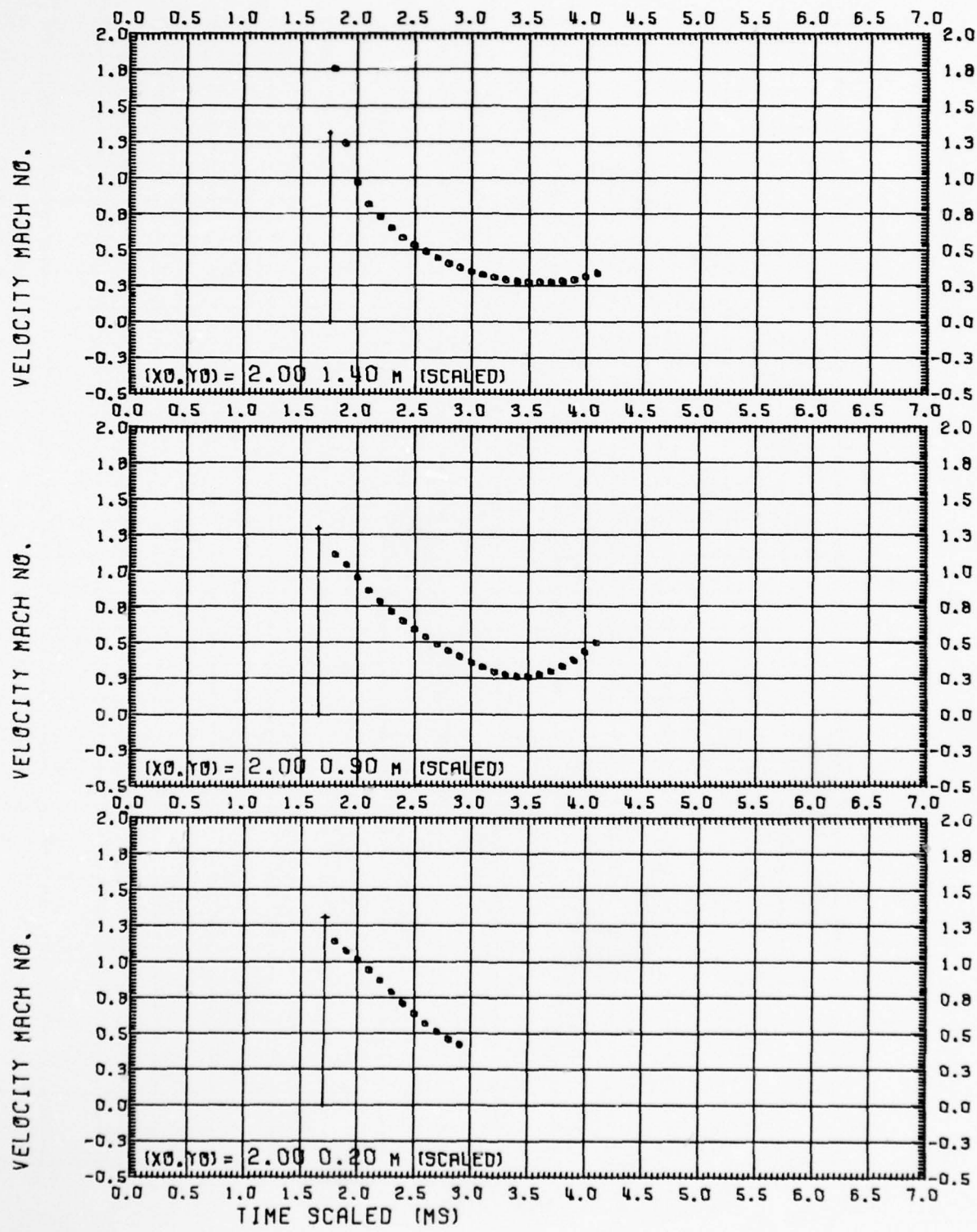


Fig. 23.2 DIPOLE WEST/9 PARTICLE VELOCITY
65

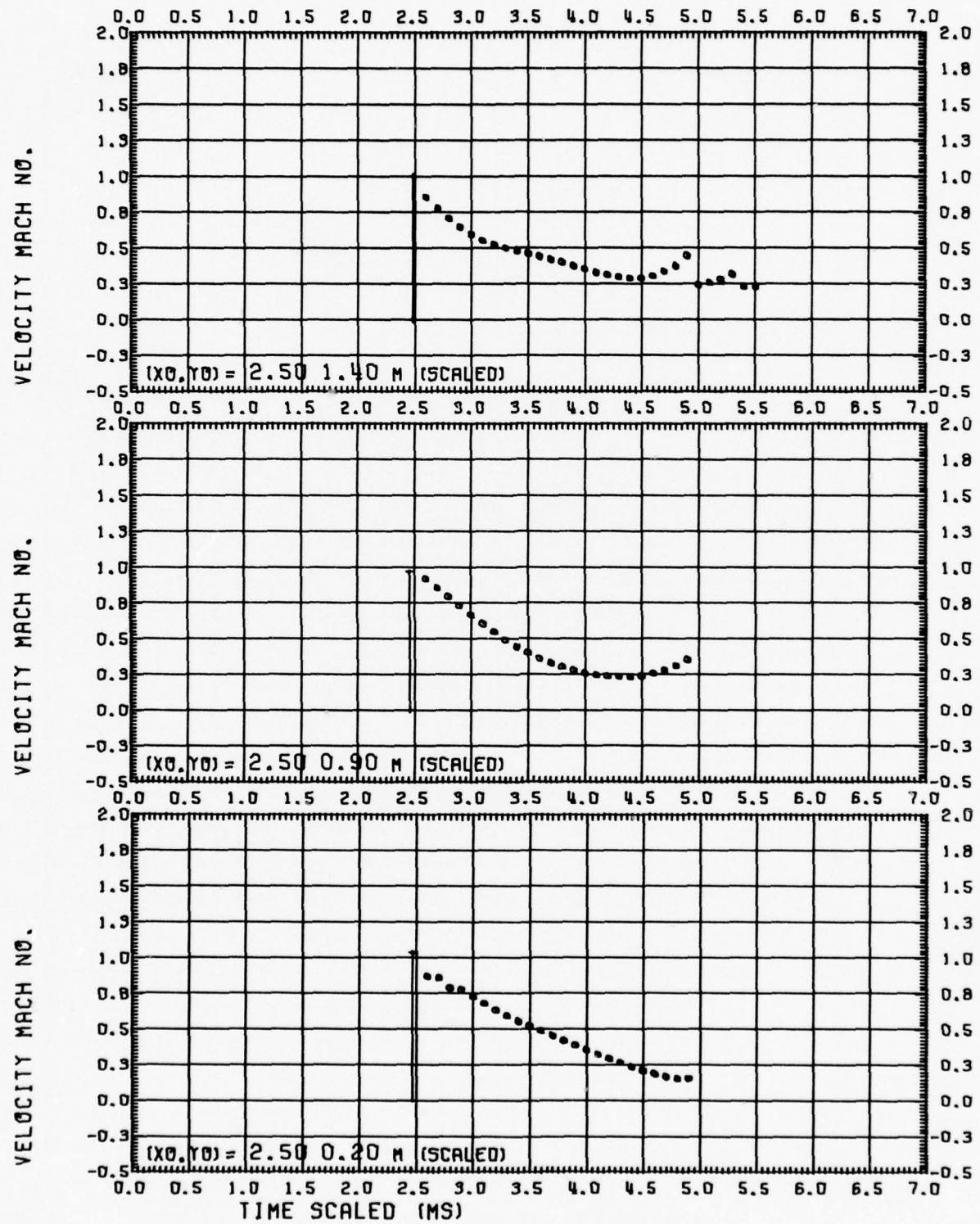


Fig. 23.3 DIPOLE WEST/9 PARTICLE VELOCITY

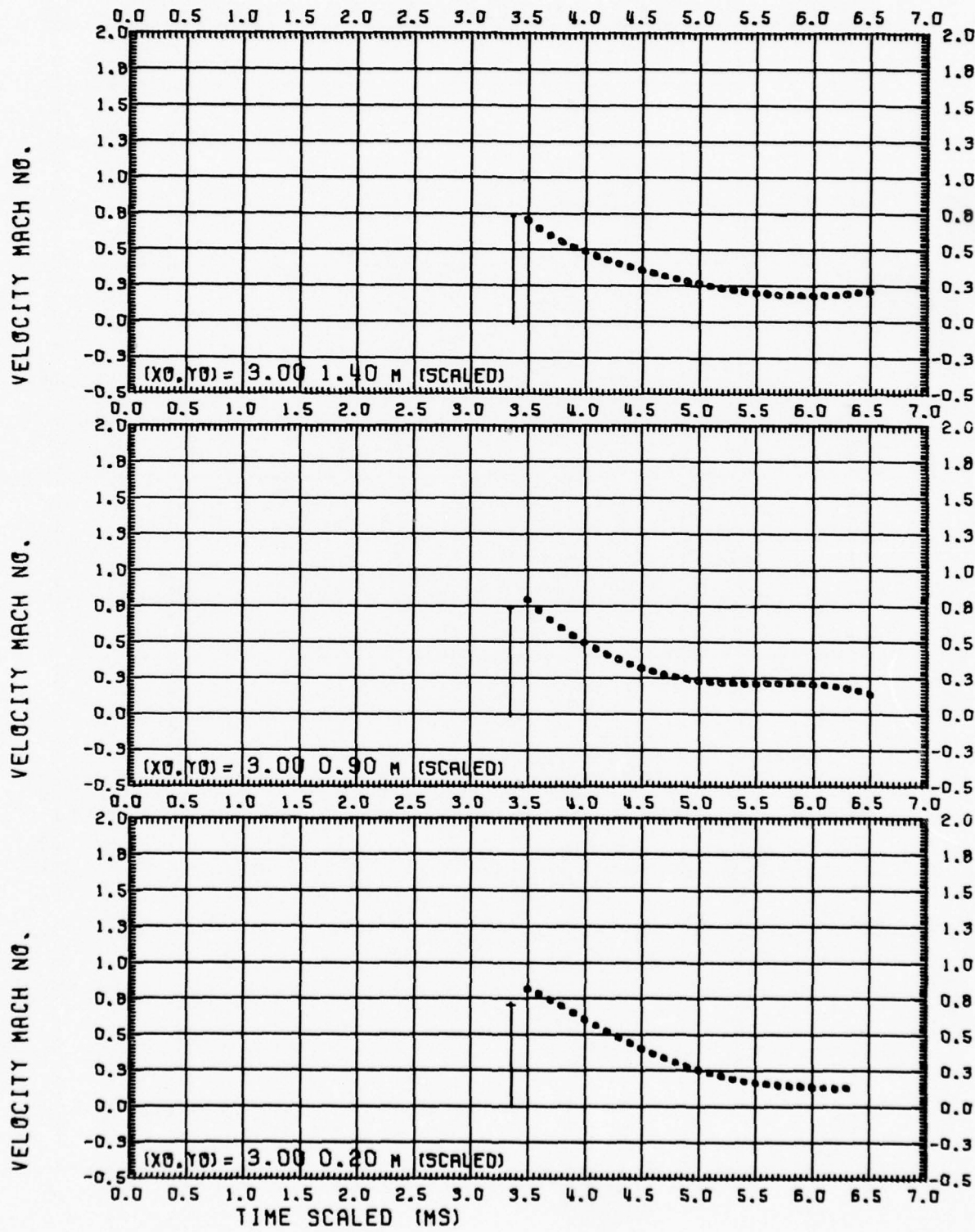


Fig. 23.4 DIPOLE WEST/9 PARTICLE VELOCITY

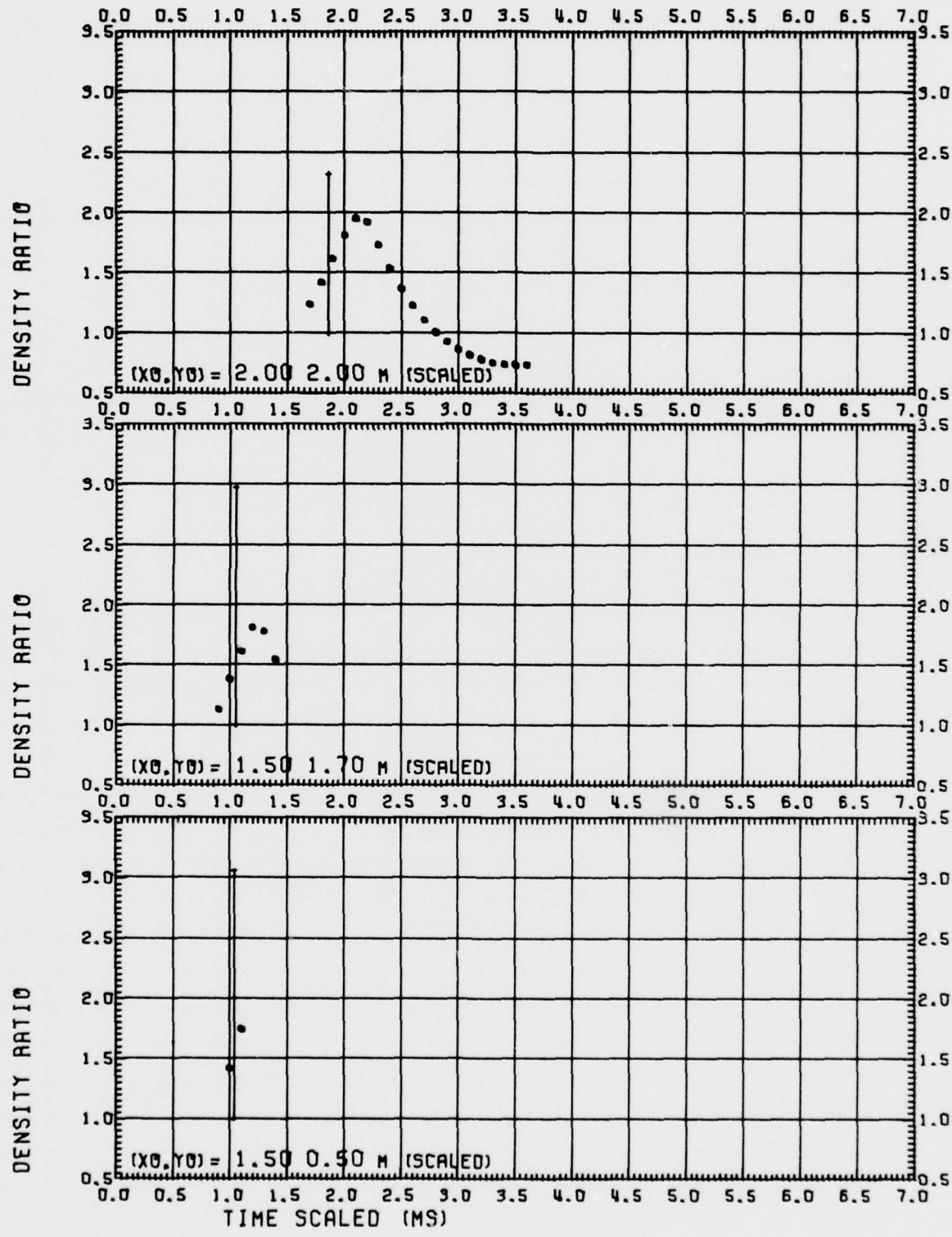


Fig. 24.1 DIPOLE WEST/9 DENSITY

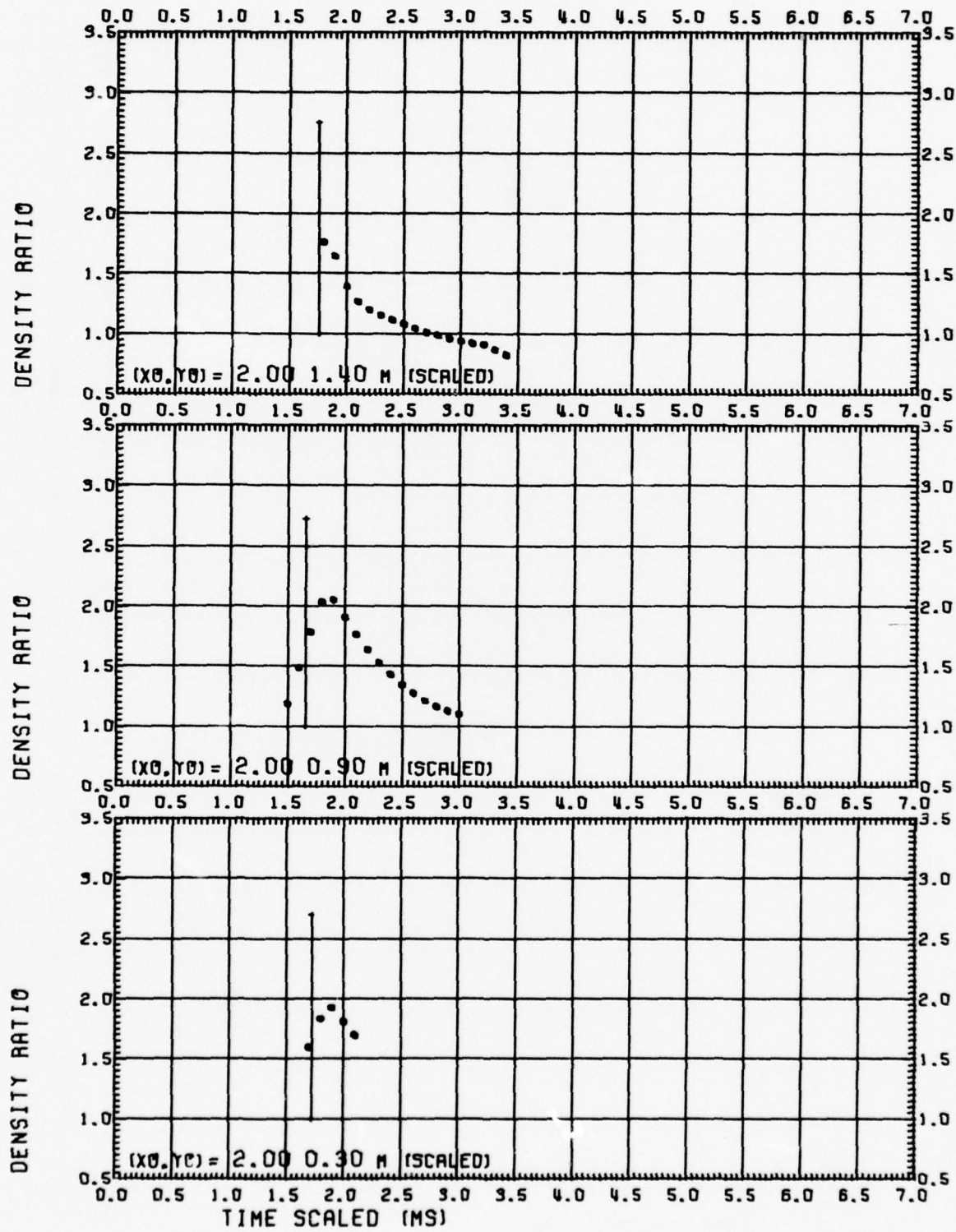


Fig. 24.2 DIPOLE WEST/9 DENSITY

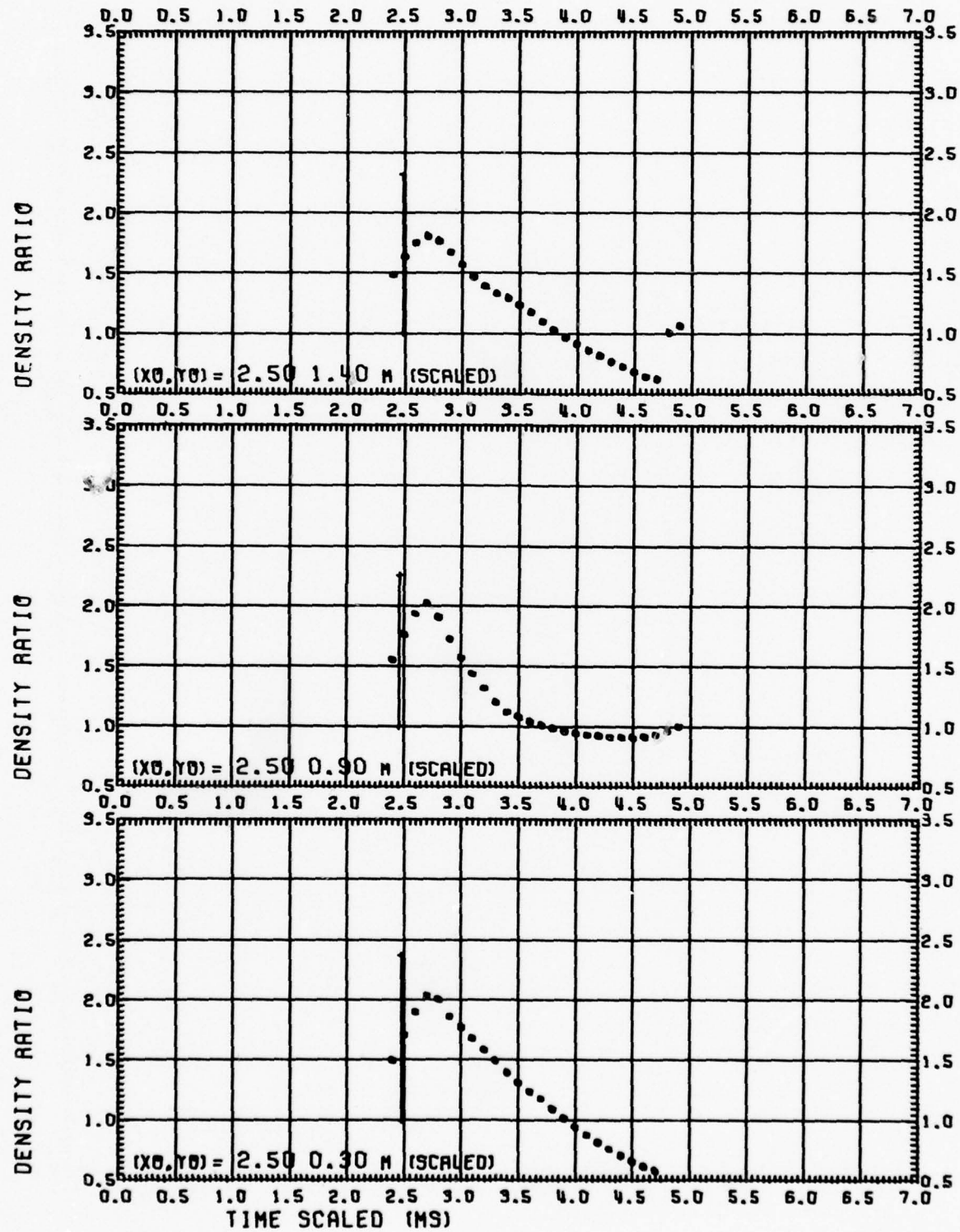


Fig. 24.3 DIPOLE WEST/9 DENSITY

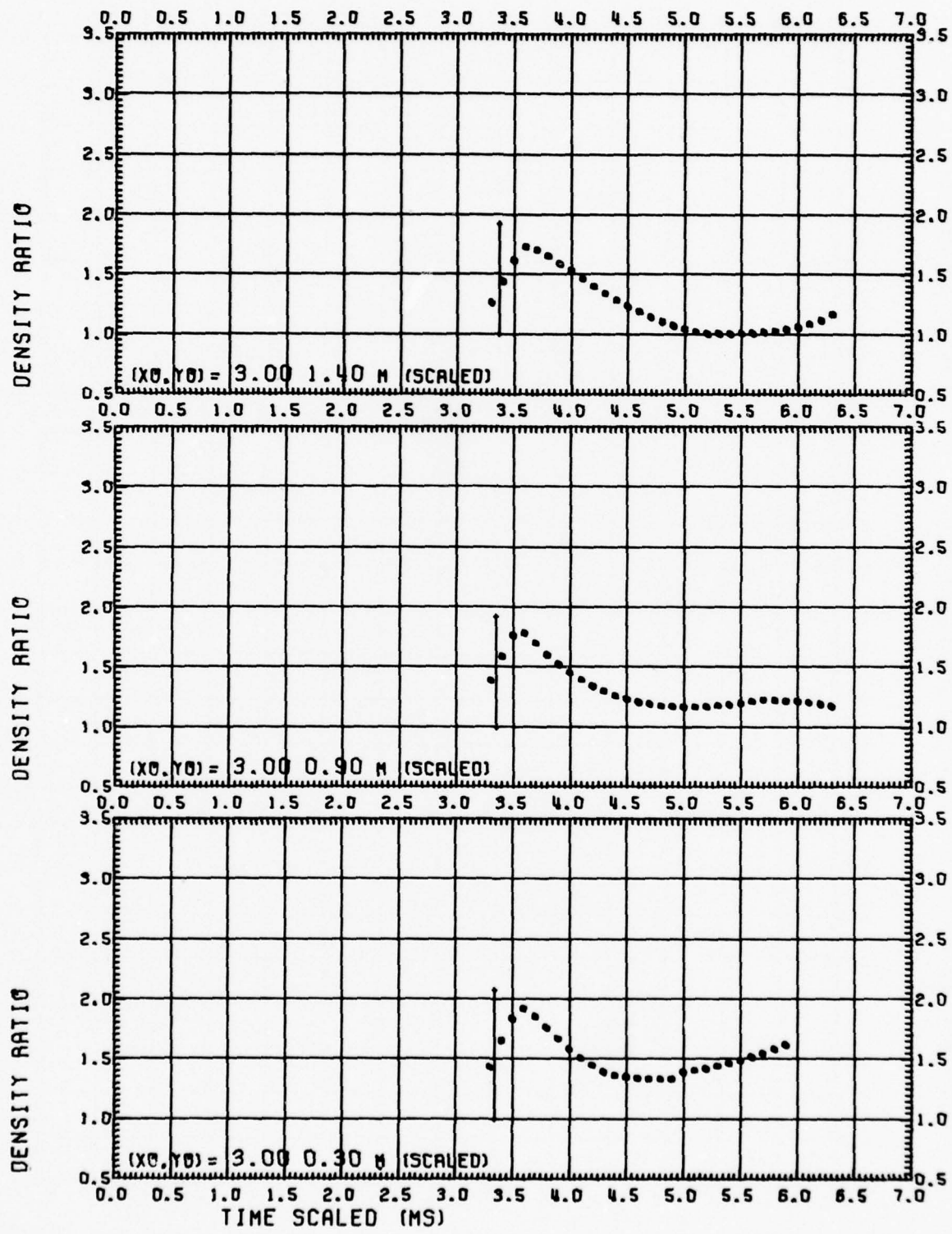


Fig. 24.4 DIPOLE WEST/9 DENSITY
71

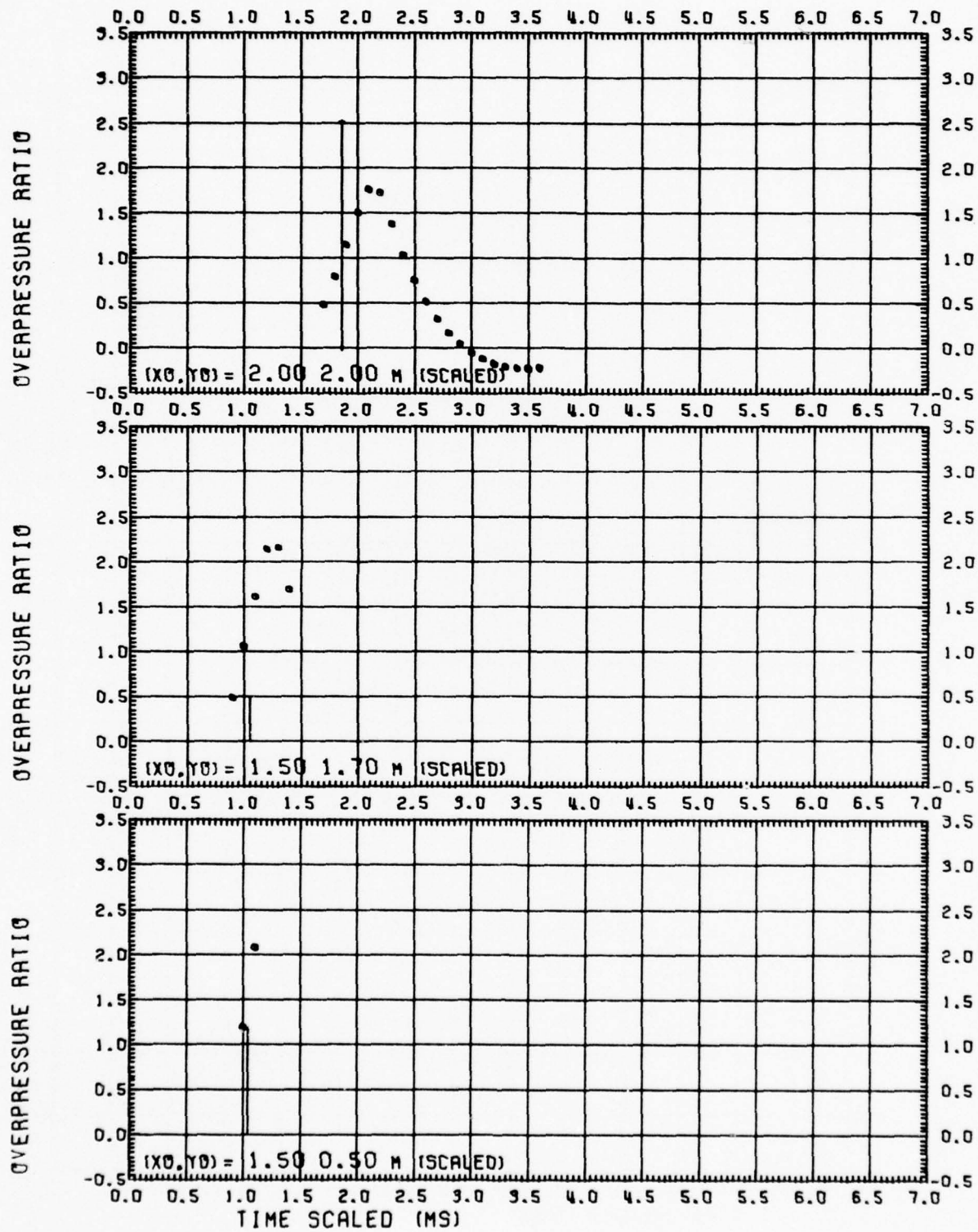


Fig. 25.1 DIPOLE WEST/9 HYDROSTATIC OVERPRESSURE
72

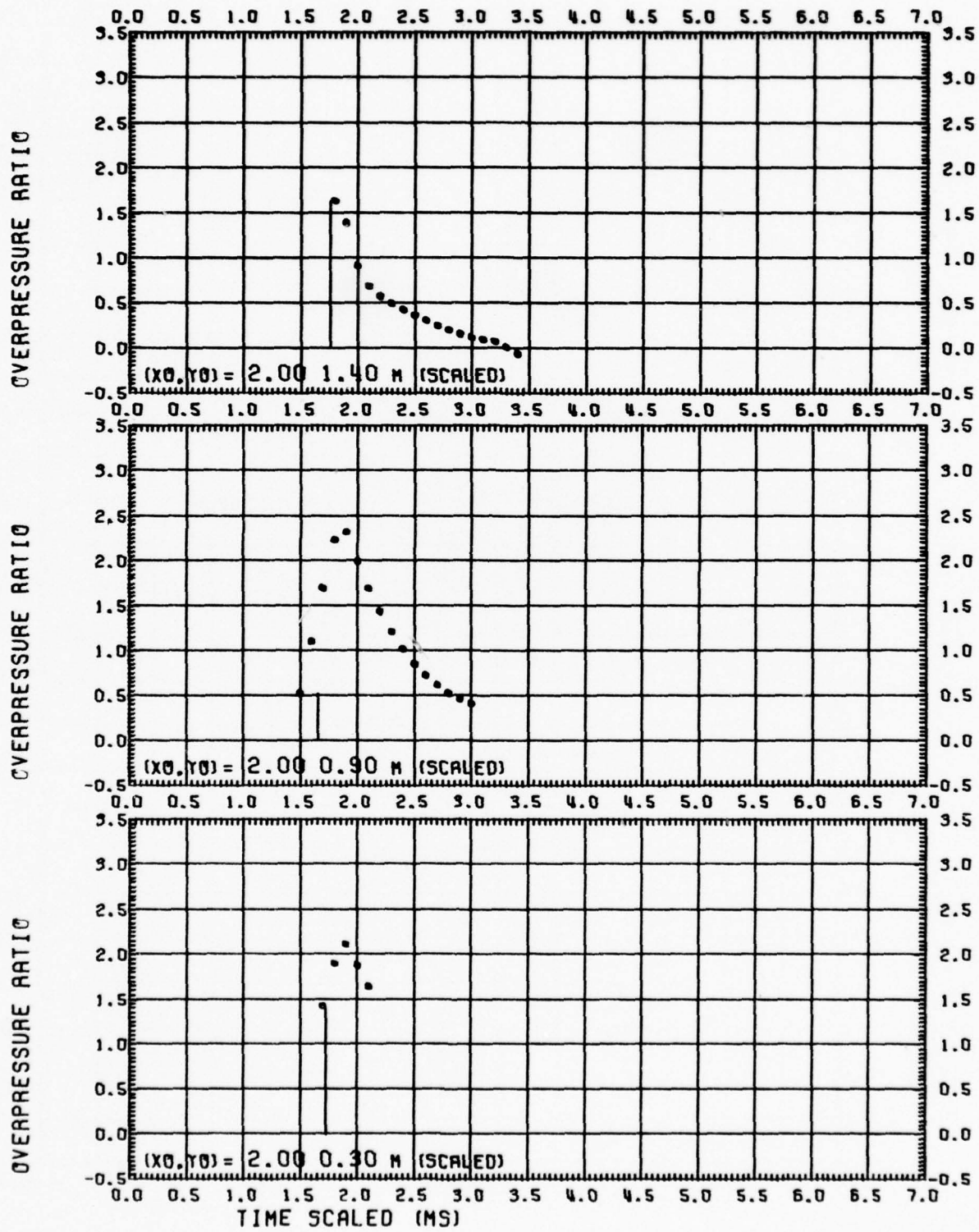


Fig. 25.2 DIPOLE WEST/9 HYDROSTATIC OVERPRESSURE
73

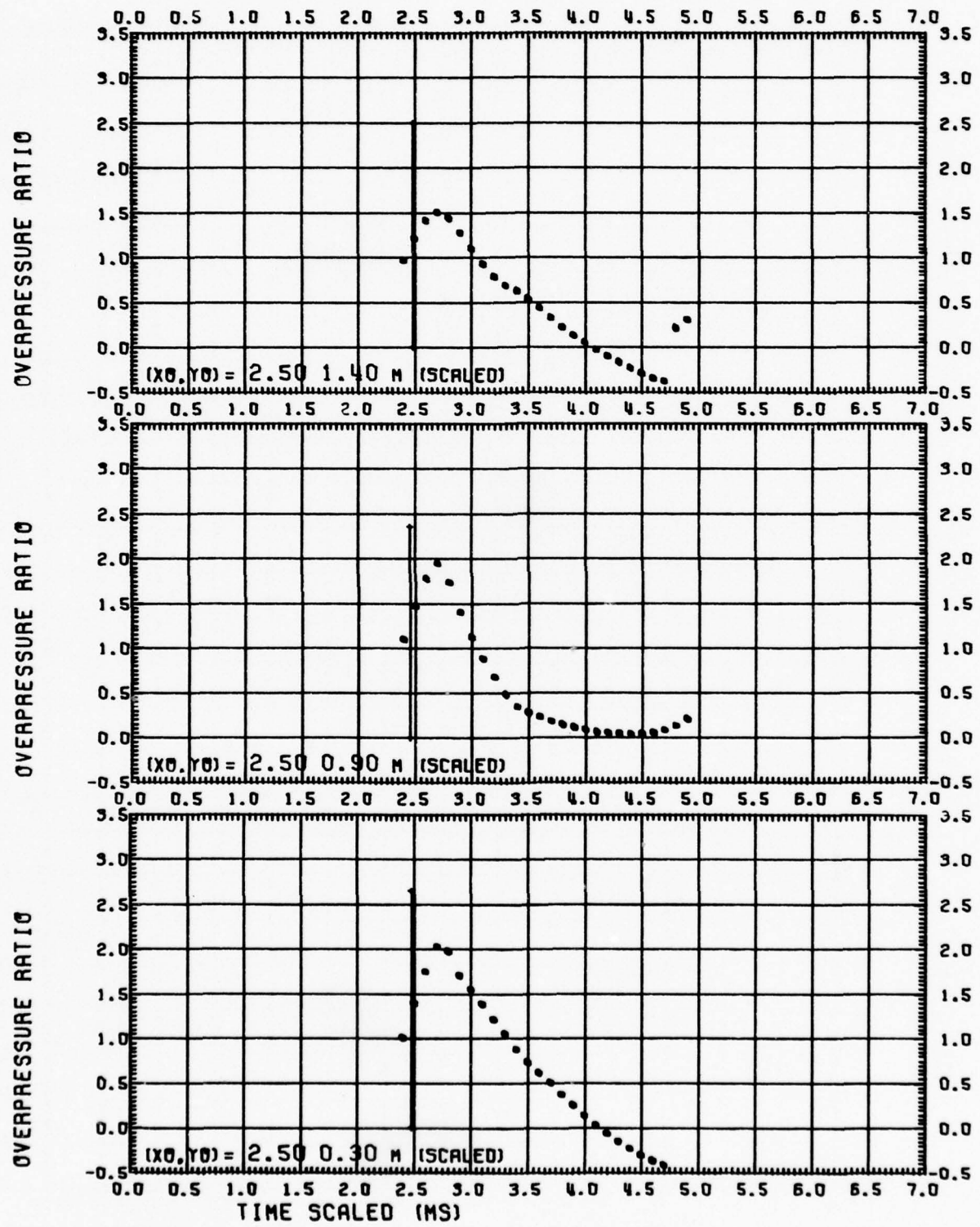


Fig. 25.3 DIPOLE WEST/9 HYDROSTATIC OVERPRESSURE
74

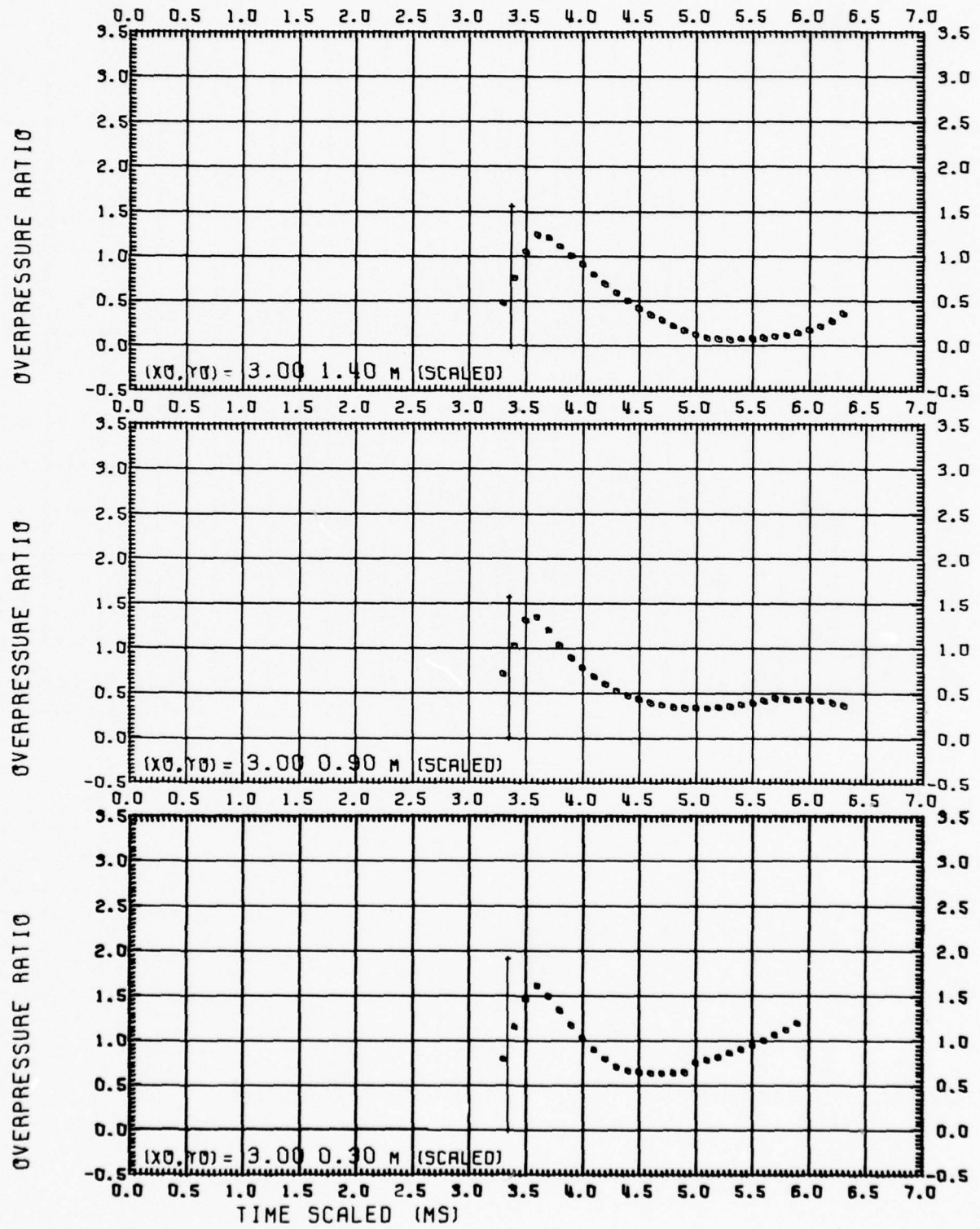
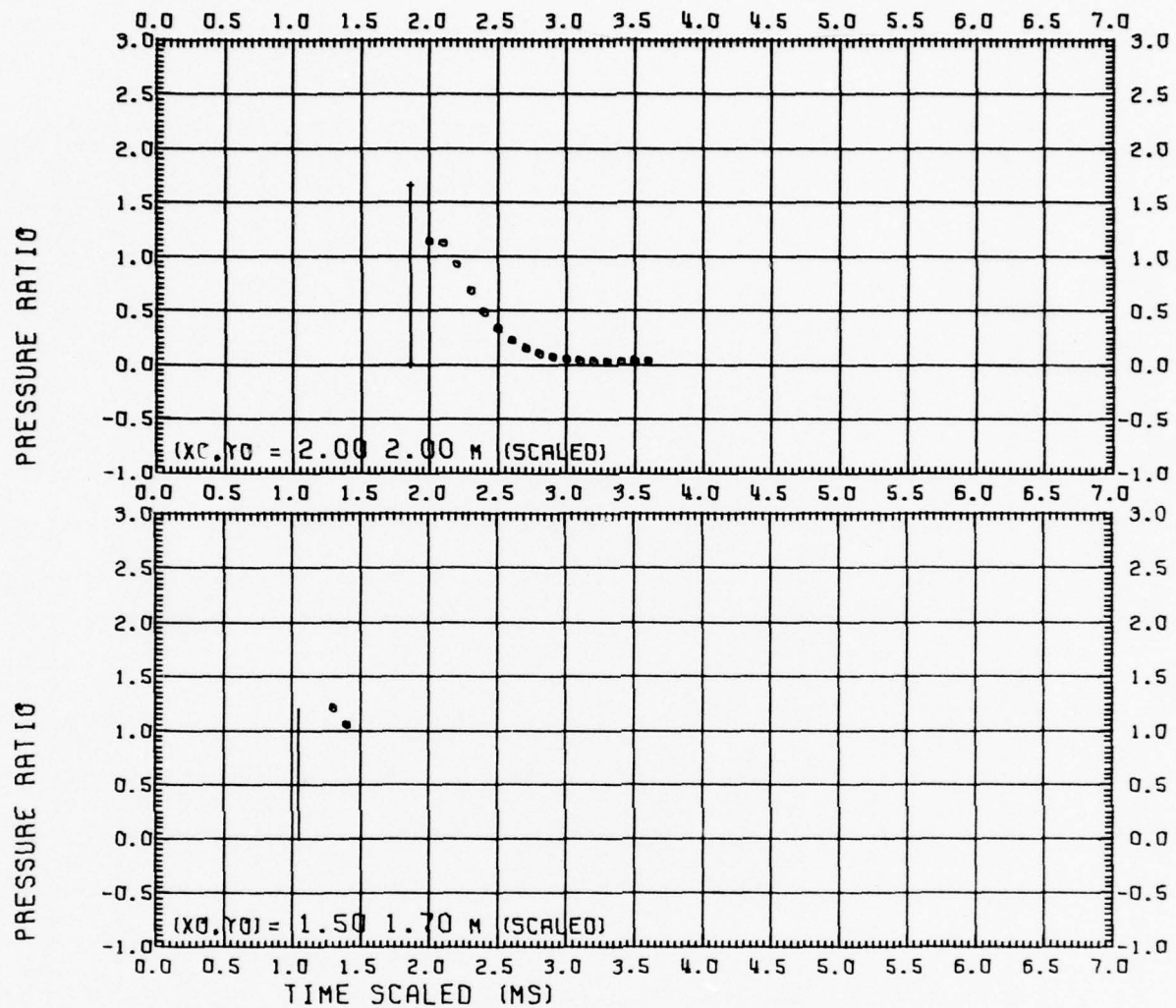


Fig. 25.4 DIPOLE WEST/9 HYDROSTATIC OVERPRESSURE



$(x_0, y_0) = 1.5, 0.5$ NO DATA

Fig. 26.1 DIPOLE WEST/9 DYNAMIC PRESSURE

$(x_0, y_0) = 2.5, 1.5$ NO DATA

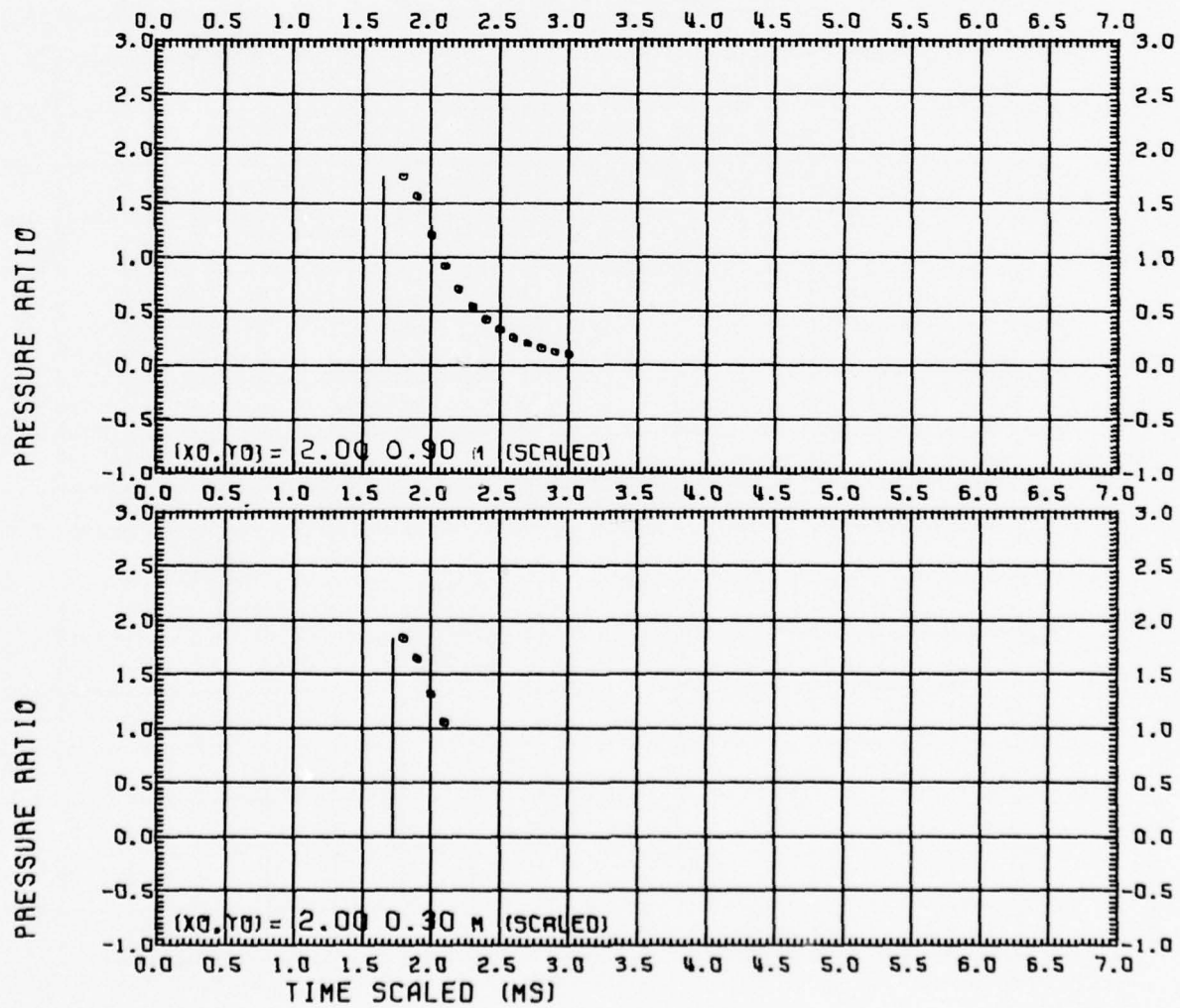


Fig. 26.2 DIPOLE WEST/9 DYNAMIC PRESSURE

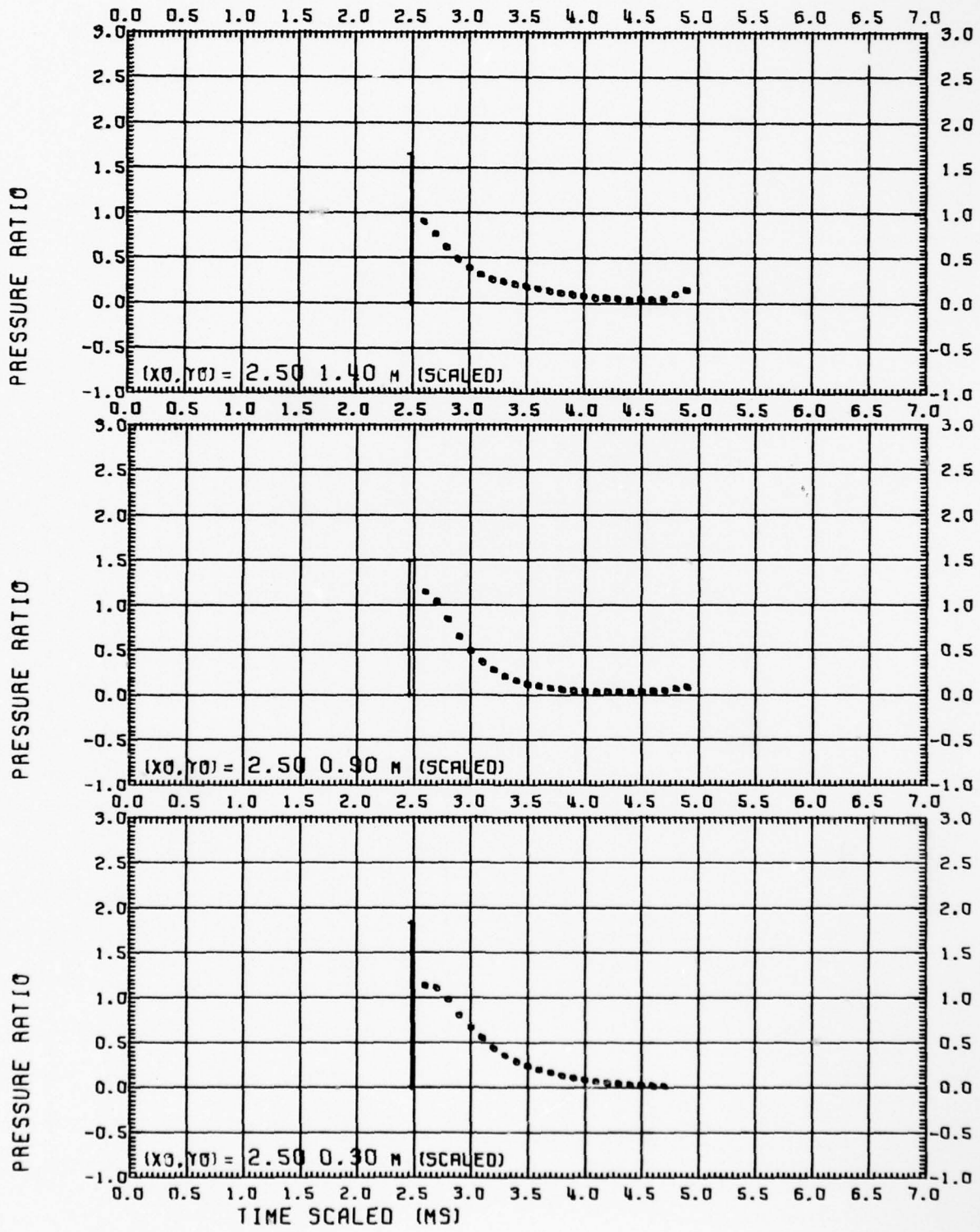
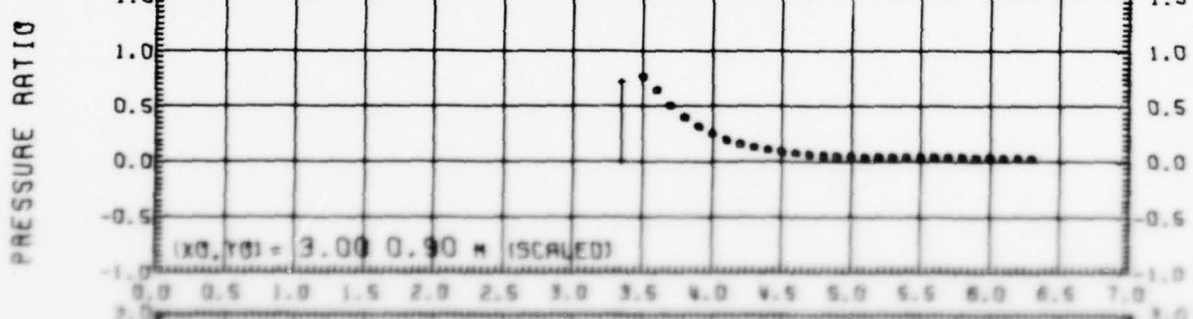
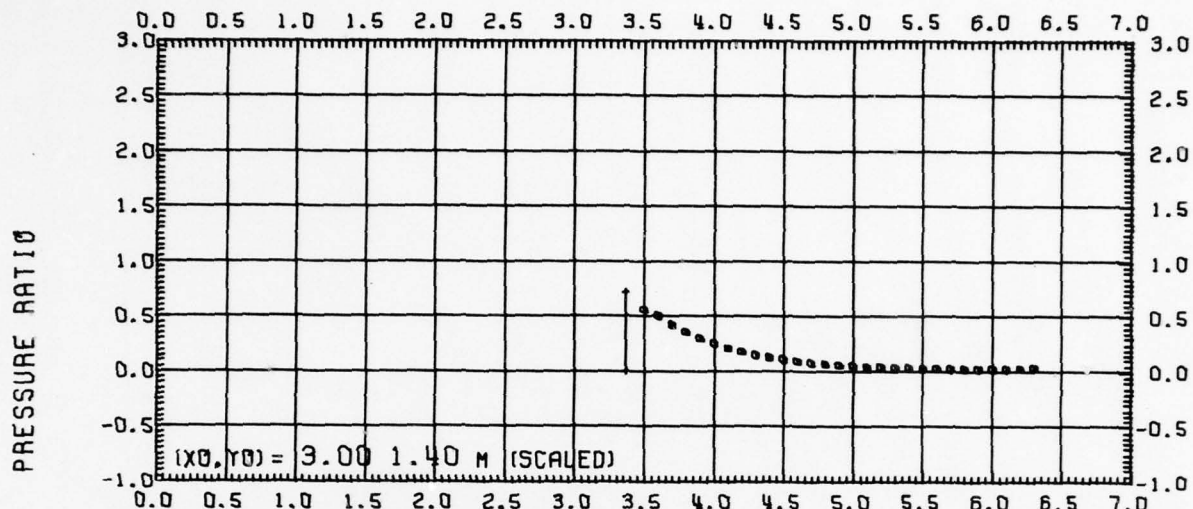
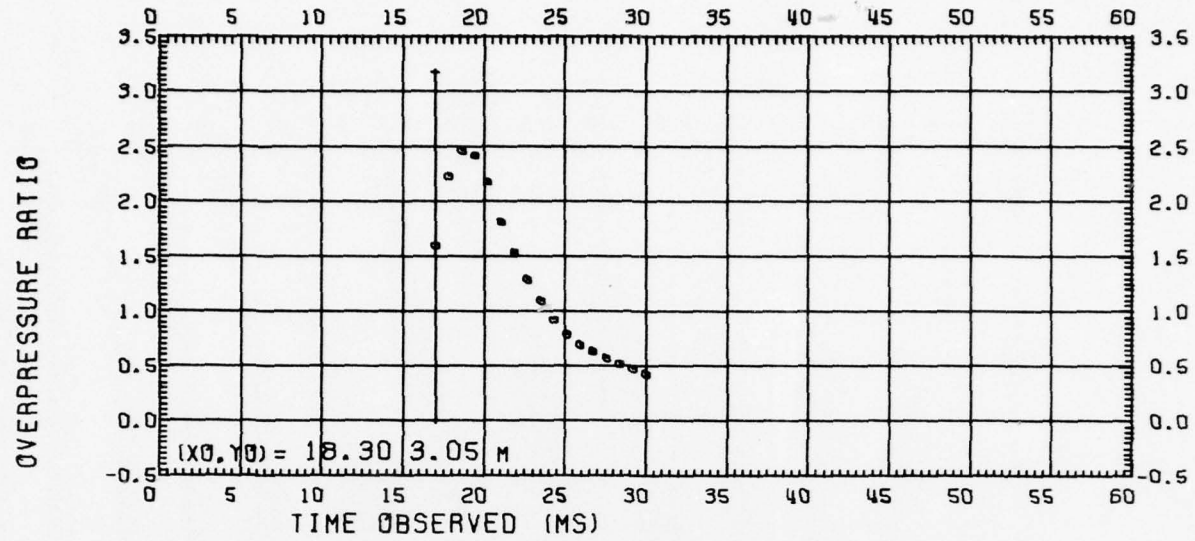
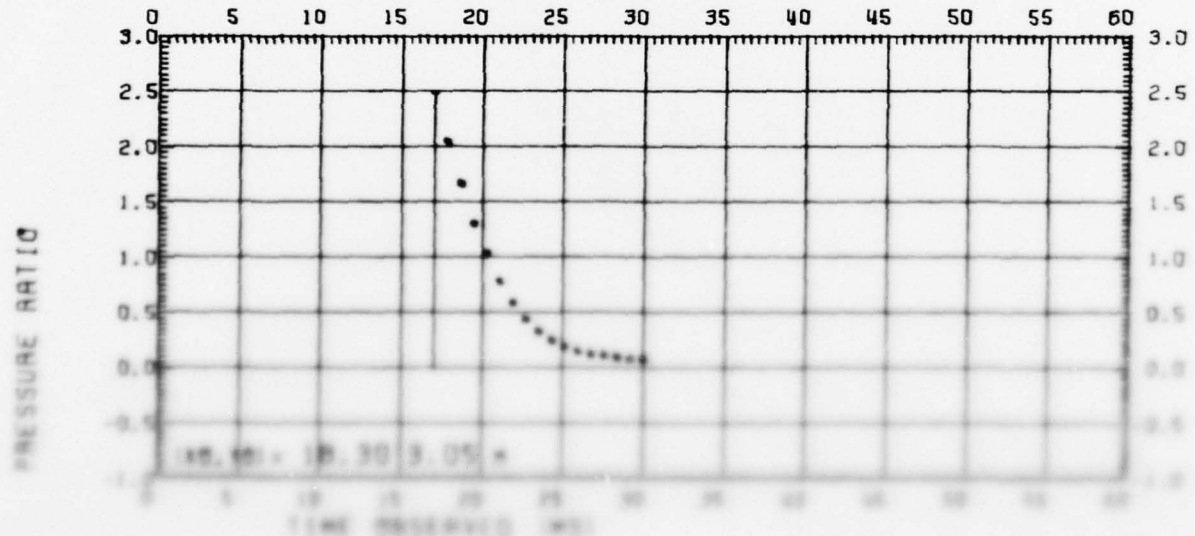


Fig. 26.3 DIPOLE WEST/9 DYNAMIC PRESSURE

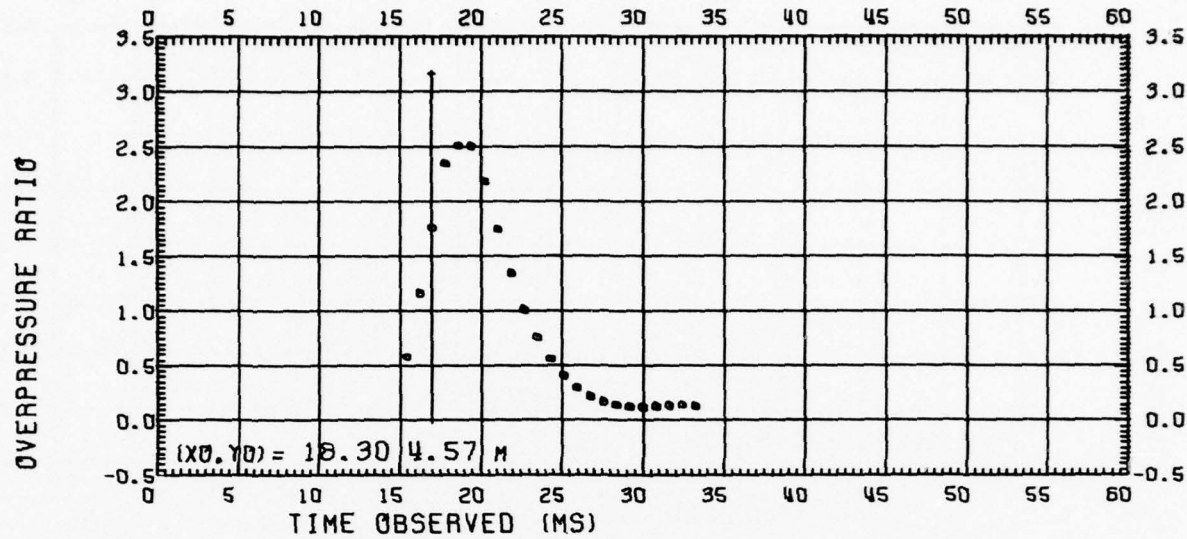




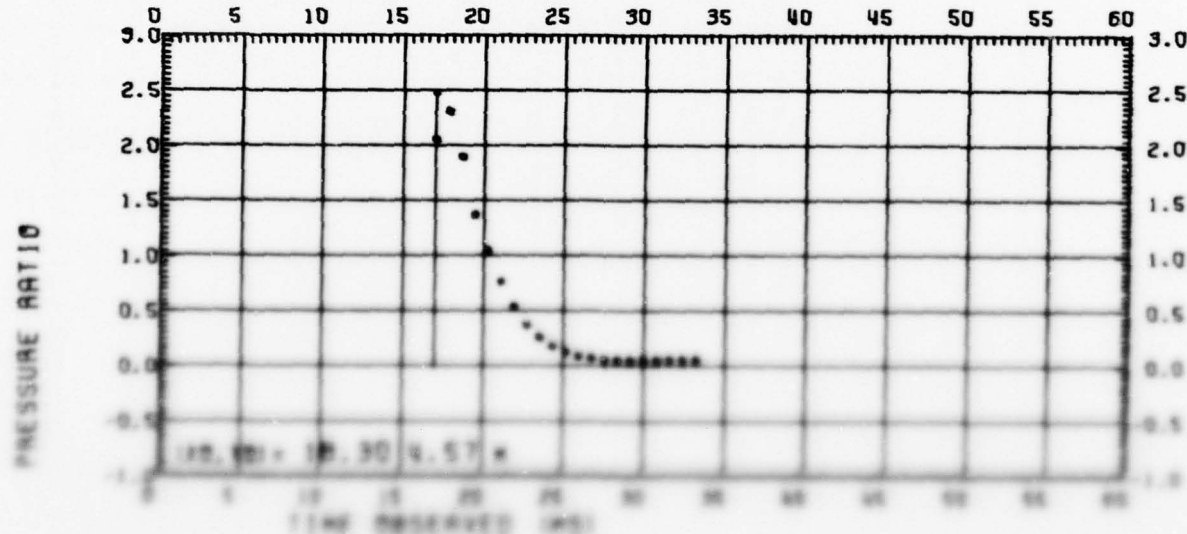
DIPOLE WEST/9 HYDROSTATIC OVERPRESSURE



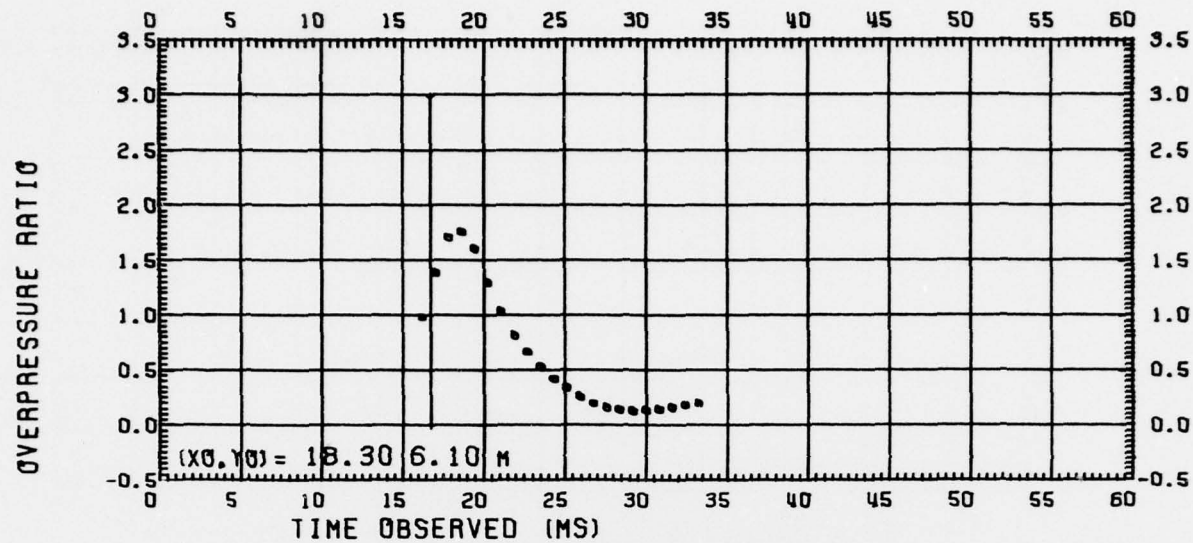
DIPOLE WEST/9 HYDROSTATIC PRESSURE



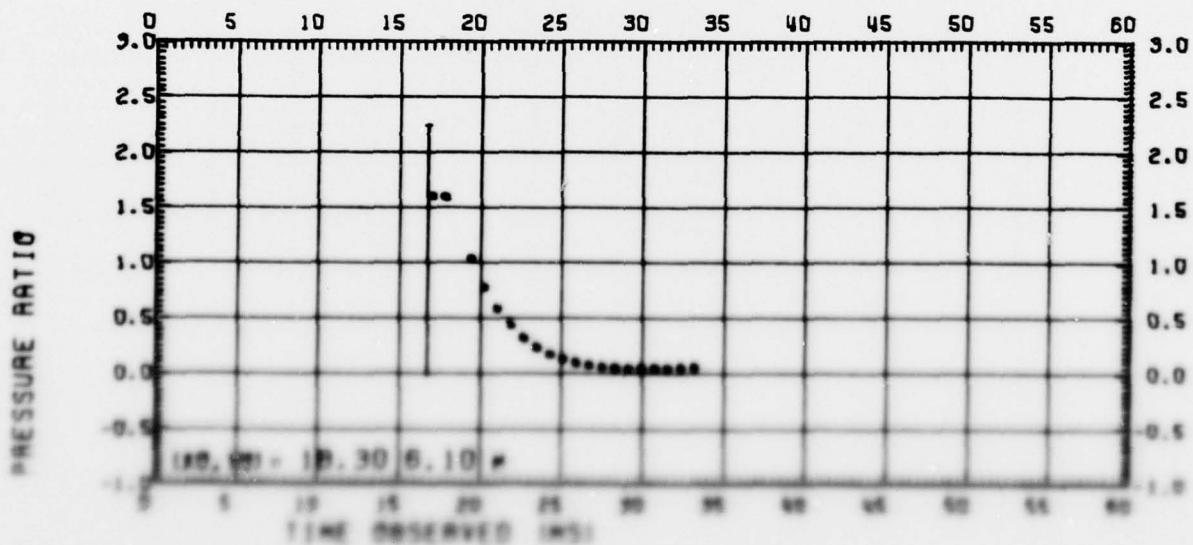
DIPOLE WEST/9 HYDROSTATIC OVERPRESSURE



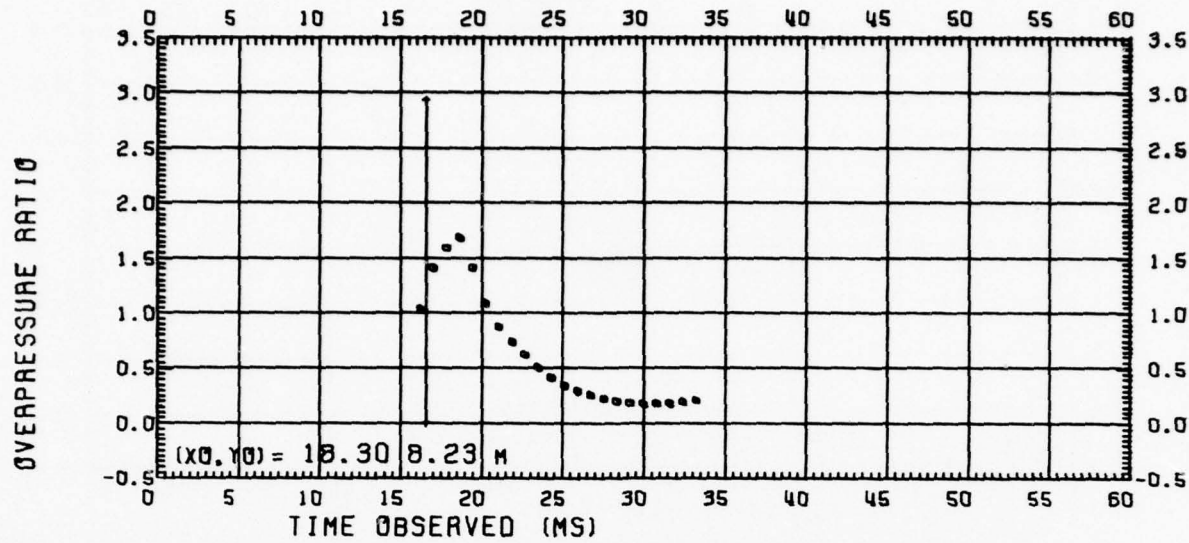
DIPOLE WEST/9 DIFFRACTED PRESSURE



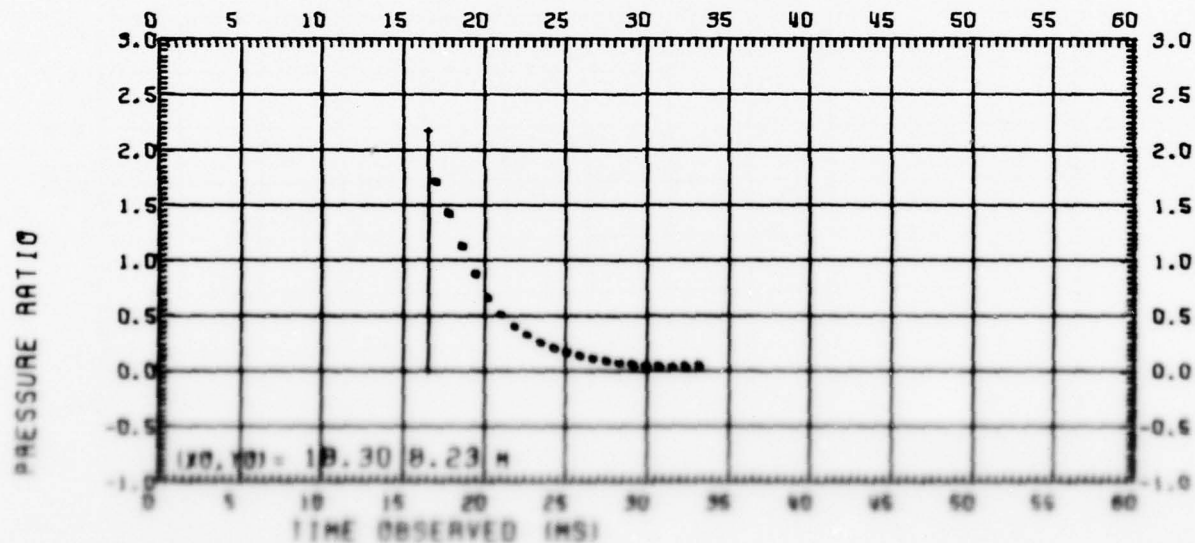
DIPOLE WEST/9 HYDROSTATIC OVERPRESSURE



DIPOLE WEST/9 DYNAMIC PRESSURE

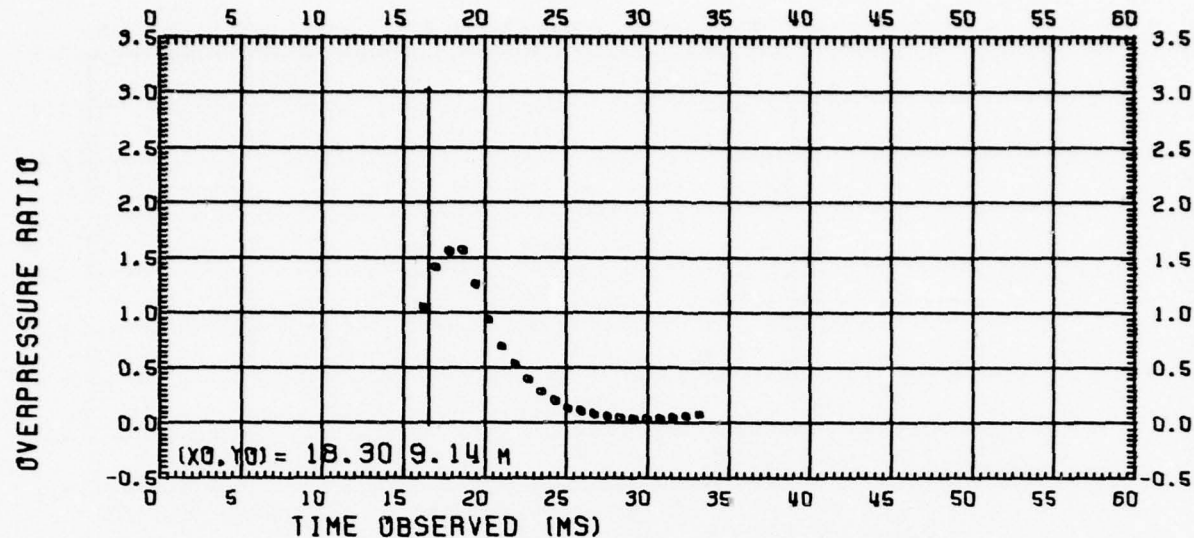


DIPOLE WEST/9 HYDROSTATIC OVERPRESSURE

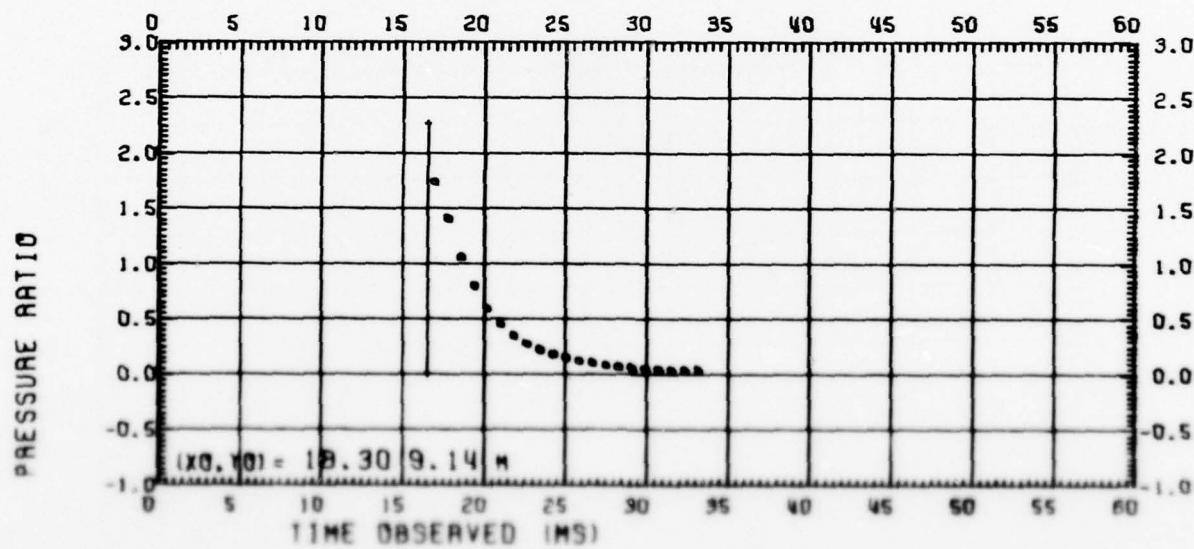


DIPOLE WEST/9 DYNAMIC PRESSURE

RECORDED RESULTS OF DIAKE MEASUREMENTS IN THE 200' DEEP BOREHOLE



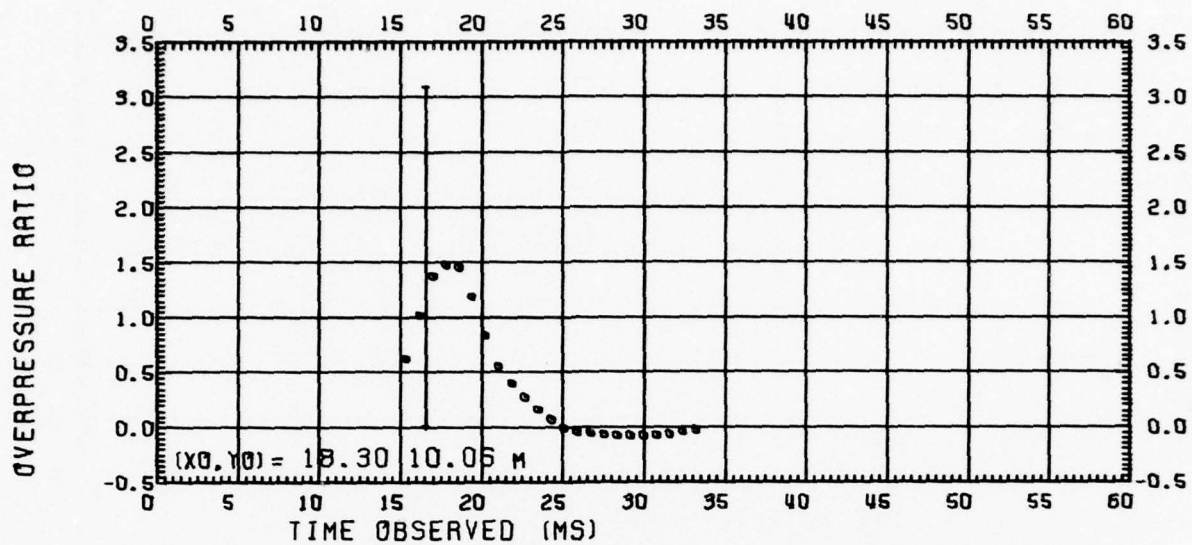
DIPOLE WEST/9 HYDROSTATIC OVERPRESSURE



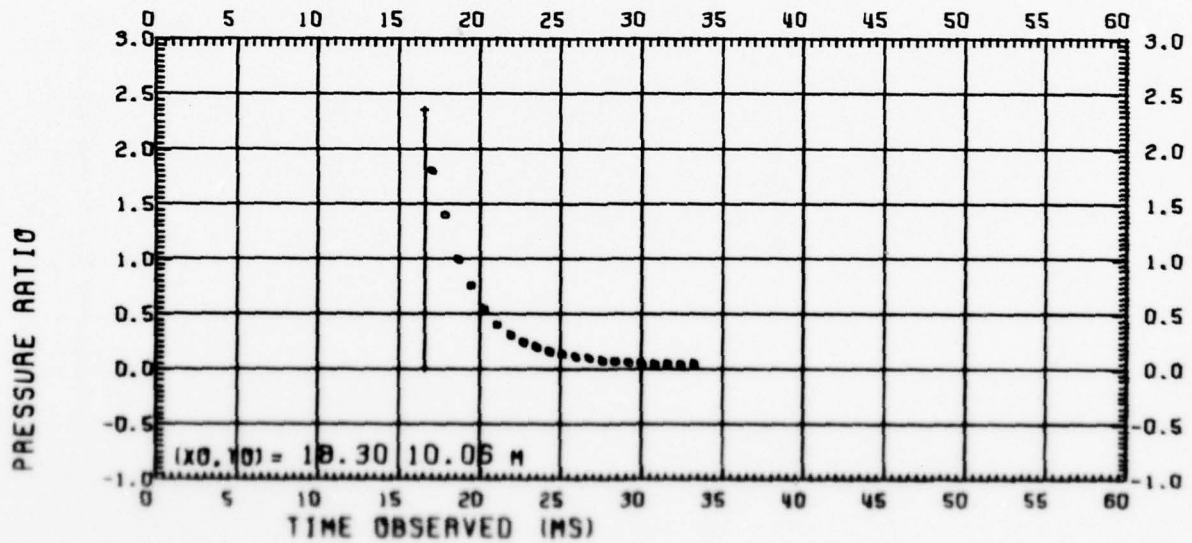
DIPOLE WEST/9 DYNAMIC PRESSURE

PRESSURE RESULTS AT DOME POSITION 180.780 ± 80 FT. 30 FT

Figure 20-3



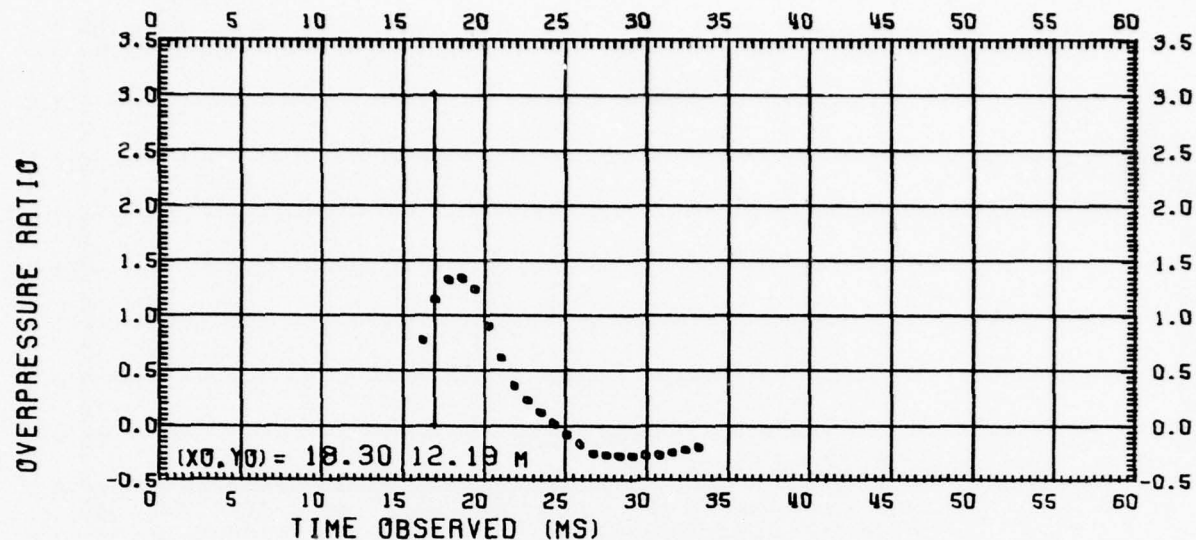
DIPOLE WEST/9 HYDROSTATIC OVERPRESSURE



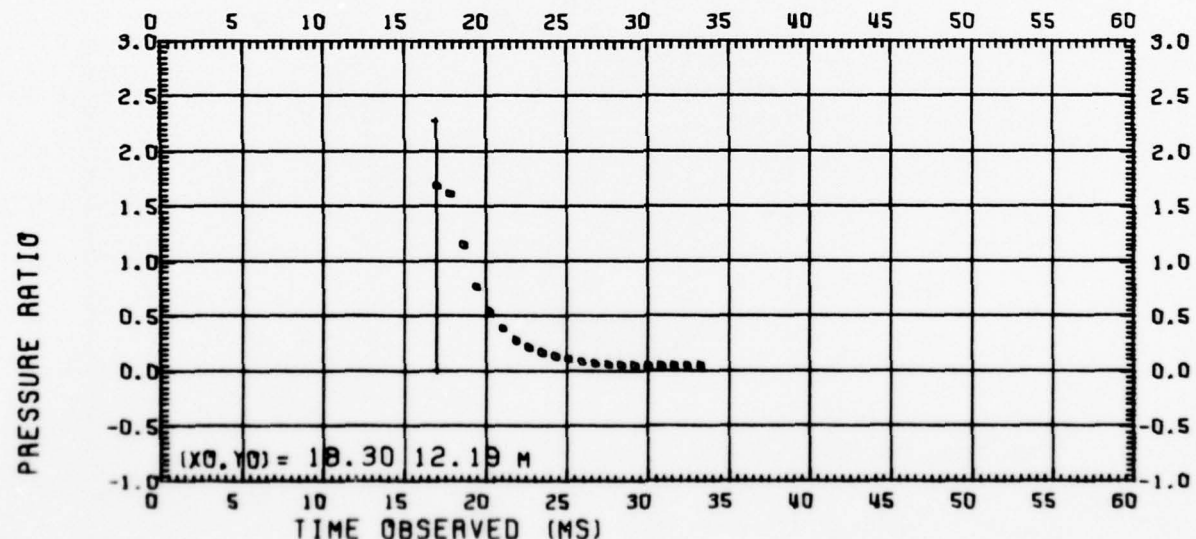
DIPOLE WEST/9 DYNAMIC PRESSURE

PRESSURE RESULTS AT GAUGE POSITION $(X_0, Y_0) = 60 \text{ FT, } 35 \text{ FT}$

Figure 27.6



DIPOLE WEST/9 HYDROSTATIC OVERPRESSURE



DIPOLE WEST/9 DYNAMIC PRESSURE

PRESSURE RESULTS AT GAUGE POSITION $(X_0, Y_0) = 60 \text{ FT. } 40 \text{ FT}$

Figure 27.7

Table 1

SURVEY DATA LIST

DIPOLE WEST/9

PT.	NAME	BEARING	DISTANCE	COORD. E	COORD. N	COORD. H
G•ZERO	0° C•C	0° 0'	2000.000	1998.000	2000.000	2316.320
G•ZERO B	167° 36' 1.6	1° 0' 0.63	2010.0227	1998.961	2216.320	
G•ZERO C	167° 36' 1.6	1° 0' 6.3	2005.0241	1998.981	2316.320	
R•CHARGE	167° 33' 4.0	1° 0' 3.2	2005.0227	1998.961	2331.526	
T•CHARGE	165° 33' 4.0	1° 0' 3.2	2005.0255	1999.000	2361.748	
MCP	180° 2.47	598.713	1998.289	1401.290	2313.750	
WF 5/295		260.2 75.8	1385.147	2341.657		
VP 1A	333° 24' 4.3	106.193	1952.648	2095.052	2348.823	
VP 1B	333° 24' 4.0	106.422	1952.533	2095.052	2383.752	
VP 2A	317° 56' 2.4	121.925	1918.429	2090.592	2348.640	
VP 2B	317° 48' 5.0	122.427	1917.926	2090.878	2382.065	
VP 3A	305° 18' 6.1	149.196	1876.448	2086.514	2348.376	
VP 3B	305° 12' 3.5	149.142	1878.275	2086.176	2382.340	
W 1	257° 20' 5.5	1965.259	1992.289	2318.150		
W 2	260° 21' 4.3	70.294	1930.578	1988.344	2318.070	
W 3	261° 29' 4.8	106.199	1895.935	1984.663	2317.550	
300 W 2	187° 38' 5.7	314.780	1979.184	1685.909	2330.730	
300 C 10	84° 7.37	320.022	1956.569	1682.941	2330.028	
1-2 C 15	83° 52' 2.0	190.864	1965.774	2020.002	2336.369	
1-2 C 15	83° 52' 2.0	201.752	2019.703	2351.376		
1-2 C 22	84° 12' 4.6	190.889	2019.792	2001.966	2336.381	
1-2 C 27	83° 53' 3.4	190.841	2019.731	2020.082	2333.354	
1-2 C 32	83° 45' 6.6	190.816	2019.689	2002.150	2346.263	
1-2 C 33	83° 43' 1.8	190.790	2012.673	2002.149	2249.316	
1-2 C 40	84° 4' 4.3	190.819	2019.717	2002.008	2356.412	
1-3 C 10	69° 25' 1.1	296.023	2027.171	2014.008	2326.517	
1-3 C 15	68° 48' 1.3	294.960	2027.874	2011.791	2336.406	
1-3 C 20	68° 23' 2.1	300.221	2027.916	2011.556	2336.462	
1-3 C 27	68° 52' 3.1	294.873	2027.860	2010.729	2343.442	
1-3 C 30	68° 54' 2.5	294.879	2027.889	2010.722	2343.473	
1-3 C 33	68° 52' 5.6	294.935	2027.951	2010.717	2344.432	
1-3 C 40	68° 36' 6	30.017	2027.950	2010.944	2356.023	

BEARING IN DEGREES, MINUTES AND SECONDS, AND DISTANCE IN FEET
 BEARING AND DISTANCE FROM G•ZERO UNLESS NOTED OTHERWISE
 NUMBER OF POINTS LISTED ABOVE IS 32

SUNDRY DATA LIST

T= 57.5 DEG F. P= 13.5 PSI. RH= 55.0 X. SVP= 12.1 MM. W= 1080.0 LBS
 SCALING TO WO= 2.02 LBS USING FACTORS S= 8.111 AND C= 1.117 FT/MSEC
 CALCULATED DISTANCE BETWEEN B•CHARGE AND G•ZERO B IS 15.206 FEET CH
 CALCULATED DISTANCE BETWEEN B•CHARGE AND T•CHARGE IS 30.222 FEET CS
 CALCULATED DISTANCE BETWEEN G•ZERO AND G•ZERO C IS 1.047 FEET
 PENTOLITE SPHERES. FIRED 22 OCT 73. SIMULTANEOUSLY

Table 2

PHOTOGRAMMETRICS

DIPOLE WEST/9 WFS/295 30.

CAMERA POSITION IS 2002.8 FEET EAST, 1385.1 FEET NORTH AND 2341.7 FEET ELEVATION
 OPTICAL AXIS IS ORIENTED -6°, 763 DEGREES EAST OF NORTH AND 0°, 555 DEGREES UPWARD
 OBJECT PLANE INCLUDES G. ZERO C AND IS 609.6 FEET FROM CAMERA ALONG OPTICAL AXIS

CALIBRATION DATA TRANSFORMED TO THE OBJECT PLANE IN FEET

PT.	NAME	COORD. X	COORD. Y	SHIFT X	SHIFT Y
B-CHARGE		69.685	-16.067	0.053	0.035
T-CHARGE		69.777	1.4195	-0.039	-0.016
VP 1A		27.505	30.032	1.516	-0.090
VP 1R		27.384	30.039	1.501	0.127
VP 2A		-0.579	0.3168	0.211	0.021
VP 2B		-0.866	30.045	-0.046	0.010
VP 3A		-34.604	0.0314	-0.497	-0.177
VP 3B		-34.864	2.9864	-0.165	-0.037
W 1		34.367	-2.90518	0.000	-0.000
W 2		-0.734	-2.90485	0.093	-0.097
W 3		-35.544	-3.00296	0.052	0.002
SC 0	W 1	24.277	-2.80118	-0.064	0.008
SC 0	W 2	-21.829	-2.79967	-0.068	-0.075
1-20.10		89.902	-2.03692	-0.528	-0.279
1-20.15		89.793	-1.5649	-0.428	-0.519
1-20.20		89.771	-1.63746	-0.353	-0.431
1-20.25		89.741	-1.3917	-0.384	-0.302
1-20.30		89.694	-0.978	-0.385	-0.297
1-20.33		89.743	2.0157	-0.454	-0.415
1-20.40		89.731	6.894	-0.413	-0.668
1-30.12		97.916	-2.0854	-1.295	-0.008
1-30.15		97.959	-1.5671	-0.744	-0.340
1-30.20		97.952	-1.1730	-0.702	-0.293
AVERAGES				-0.142	-0.179

X-AXIS IS PARALLEL TO HORIZONTAL PLANE WITH ORIGIN WHERE
 OPTICAL AXIS INTERSECTS OBJECT PLANE. SHIFTS GIVE POINT
 POSITIONS WHICH ARE CALCULATED DIRECTLY FROM SURVEY DATA

MAXIMUM CALIBRATION ERROR SCALED = 0.080 FEET

MAXIMUM CAMERA ORIENTATION ERROR = 0.011 FEET

TOTAL ERRORS IN THE OBJECT PLANE = 0.091 FEET

Table 3

FILM TIMING DATA

DIPOLE WEST/9 WFS/295 30°

STATIC ZERO = 3.90 CM
 ACTUAL ZERO = 4.37 CM
 FRAME LENGTH = 0.94625 CM

FRAME NO.	5-MSEC DISTANCE	FILM SPEED
-31	15.99 CM	3380.0 / SEC
69	16.32 CM	3449.0 / SEC
167	16.67 CM	3523.0 / SEC
269	16.96 CM	3585.0 / SEC
AVERAGES	16.48 CM	3484.0 / SEC

STATIC ZERO IS CONSTANT FOR THE CAMERA
OTHER DATA ARE OBTAINED BY MEASUREMENT

FRAME TIMES IN MILLISECONDS FOR FRAMES 1 THROUGH 200 ARE:

1	0.4	2	0.7	3	1.0	4	1.3	5	1.6	6	1.9	7	2.2	8	2.5	9	2.8	10	3.1
12	3.7	22	6.6	32	9.5	42	12.4	52	15.3	62	18.2	72	21.1	82	24.0	92	26.9	102	29.8
21	6.3	31	9.2	41	12.3	51	15.2	61	18.1	71	21.0	81	23.9	91	26.8	101	29.7	111	32.6
31	9.2	41	12.4	51	15.3	61	18.4	71	21.3	81	24.2	91	27.1	101	30.0	111	33.9	121	36.7
41	12.2	51	15.4	61	18.5	71	21.5	81	21.6	91	24.4	101	27.3	111	30.1	121	33.0	131	35.9
51	15.1	61	18.4	71	21.4	81	21.5	91	21.6	101	24.3	111	27.2	121	30.0	131	32.9	141	34.8
61	18.0	71	21.3	81	21.4	91	21.5	101	21.6	111	24.2	121	27.1	131	30.0	141	32.9	151	34.8
71	21.0	81	21.2	91	21.5	101	21.6	111	21.7	121	24.1	131	27.0	141	30.0	151	32.9	161	34.8
81	23.9	91	26.8	101	29.7	111	32.6	121	35.5	131	38.4	141	41.3	151	44.2	161	47.1	171	50.0
91	26.8	101	29.7	111	32.6	121	35.5	131	38.4	141	41.3	151	44.2	161	47.1	171	50.0	181	52.9
101	29.7	111	32.6	121	35.5	131	38.4	141	41.3	151	44.2	161	47.1	171	50.0	181	52.9	191	55.8
111	32.6	121	35.5	131	38.4	141	41.3	151	44.2	161	47.1	171	50.0	181	52.9	191	55.8	201	57.7

DETONATION ZERO TIMING MARK MISSING FROM FILM. VALUE OF ACTUAL ZERO USED ABOVE IS STATIC ZERO VALUE PLUS ONE-HALF FRAME LENGTH

Table 4

TIMES OF ARRIVAL DIPOLe WEST/9 WFS/295

SMOKE PUFF GRID 1209 /A770404

AMBIENT TEMPERATURE $T = 14.17$ DEGREES CELSIUS
 AMBIENT PRESSURE $P = 03.12$ KILOBARS
 RELATIVE HUMIDITY $RH = 55.0$ PER CENT
 BAROUM PRESSURE $V_P = 0.89$ KILOCALCS
 AMBIENT SPEED OF SOUND $C = 343.469$ METERS/SECOND
 CHARGE WEIGHT $W = 486.9$ KILOGRAMS
 CHARGE HEIGHT $H = 4.63$ METERS
 SEPARATION $+2$ MTS = 8.61 METERS
 SACHS SCALING FACTOR $S = 8.1111$
 SACHS SCALING WEIGHT $W_0 = 1.0$ KILOGRAMS

INITIAL PUFF POSITIONS, TIMES OF ARRIVAL, AND PEAK PARTICLE VELOCITIES DERIVED BY TRAJECTORY FITTING										
PUFF NUMBER	X-OBS METERS	Y-OBS METERS	Z-OBS METERS	X-SCAL METERS	Y-SCAL METERS	Z-SCAL METERS	U=DX/DT MSEC	V=DY/DT MSEC	W=DZ/DT MSEC	R-SCALE METERS
1	0.443	4.258	0.978	0.515	0.941	0.941	0.525	0.367	0.966	1.0682
2	1.749	4.378	0.971	1.071	0.943	0.947	0.518	0.618	0.957	1.0624
3	1.574	4.369	0.973	1.071	0.945	0.947	0.527	0.629	0.945	1.0622
4	1.506	4.369	0.978	1.071	0.945	0.947	0.523	0.629	0.945	1.0622
5	1.640	4.827	0.967	1.058	0.942	0.949	0.503	0.514	0.975	1.0622
6	1.538	1.129	0.962	1.058	0.942	0.949	0.736	1.051	0.78	1.0622
7	1.9795	3.671	0.964	0.910	0.964	0.928	0.452	0.736	0.78	1.0622
8	3.345	3.571	0.968	1.038	0.968	0.984	0.489	0.894	0.86	1.0622
9	8.422	3.571	0.973	0.985	0.973	0.988	0.453	0.894	0.86	1.0622
10	6.946	3.382	0.978	0.985	0.978	0.992	0.453	0.894	0.86	1.0622
11	7.623	3.78	0.978	0.985	0.978	0.992	0.453	0.894	0.86	1.0622
12	7.415	3.78	0.978	0.985	0.978	0.992	0.453	0.894	0.86	1.0622
13	6.954	3.78	0.978	0.985	0.978	0.992	0.453	0.894	0.86	1.0622
14	7.402	4.254	0.895	1.031	0.946	0.950	0.453	0.627	1.0217	1.0622
15	4.073	0.882	0.895	1.031	0.946	0.950	0.453	0.627	1.0217	1.0622
16	4.072	1.428	0.895	1.031	0.946	0.950	0.453	0.627	1.0217	1.0622
17	4.072	1.428	0.895	1.031	0.946	0.950	0.453	0.627	1.0217	1.0622
18	4.072	1.428	0.895	1.031	0.946	0.950	0.453	0.627	1.0217	1.0622
19	4.072	1.428	0.895	1.031	0.946	0.950	0.453	0.627	1.0217	1.0622
20	4.072	1.428	0.895	1.031	0.946	0.950	0.453	0.627	1.0217	1.0622
21	4.072	1.428	0.895	1.031	0.946	0.950	0.453	0.627	1.0217	1.0622
22	4.072	1.428	0.895	1.031	0.946	0.950	0.453	0.627	1.0217	1.0622
23	4.072	1.428	0.895	1.031	0.946	0.950	0.453	0.627	1.0217	1.0622
24	4.072	1.428	0.895	1.031	0.946	0.950	0.453	0.627	1.0217	1.0622
25	4.072	1.428	0.895	1.031	0.946	0.950	0.453	0.627	1.0217	1.0622
26	4.072	1.428	0.895	1.031	0.946	0.950	0.453	0.627	1.0217	1.0622
27	4.072	1.428	0.895	1.031	0.946	0.950	0.453	0.627	1.0217	1.0622
28	4.072	1.428	0.895	1.031	0.946	0.950	0.453	0.627	1.0217	1.0622
29	4.072	1.428	0.895	1.031	0.946	0.950	0.453	0.627	1.0217	1.0622
30	4.072	1.428	0.895	1.031	0.946	0.950	0.453	0.627	1.0217	1.0622
31	4.072	1.428	0.895	1.031	0.946	0.950	0.453	0.627	1.0217	1.0622
32	4.072	1.428	0.895	1.031	0.946	0.950	0.453	0.627	1.0217	1.0622
33	4.072	1.428	0.895	1.031	0.946	0.950	0.453	0.627	1.0217	1.0622
34	4.072	1.428	0.895	1.031	0.946	0.950	0.453	0.627	1.0217	1.0622
35	4.072	1.428	0.895	1.031	0.946	0.950	0.453	0.627	1.0217	1.0622
36	4.072	1.428	0.895	1.031	0.946	0.950	0.453	0.627	1.0217	1.0622
37	4.072	1.428	0.895	1.031	0.946	0.950	0.453	0.627	1.0217	1.0622
38	4.072	1.428	0.895	1.031	0.946	0.950	0.453	0.627	1.0217	1.0622
39	4.072	1.428	0.895	1.031	0.946	0.950	0.453	0.627	1.0217	1.0622
40	4.072	1.428	0.895	1.031	0.946	0.950	0.453	0.627	1.0217	1.0622
41	4.072	1.428	0.895	1.031	0.946	0.950	0.453	0.627	1.0217	1.0622
42	4.072	1.428	0.895	1.031	0.946	0.950	0.453	0.627	1.0217	1.0622
43	4.072	1.428	0.895	1.031	0.946	0.950	0.453	0.627	1.0217	1.0622
44	4.072	1.428	0.895	1.031	0.946	0.950	0.453	0.627	1.0217	1.0622
45	4.072	1.428	0.895	1.031	0.946	0.950	0.453	0.627	1.0217	1.0622
46	4.072	1.428	0.895	1.031	0.946	0.950	0.453	0.627	1.0217	1.0622
47	4.072	1.428	0.895	1.031	0.946	0.950	0.453	0.627	1.0217	1.0622
48	4.072	1.428	0.895	1.031	0.946	0.950	0.453	0.627	1.0217	1.0622
49	4.072	1.428	0.895	1.031	0.946	0.950	0.453	0.627	1.0217	1.0622
50	4.072	1.428	0.895	1.031	0.946	0.950	0.453	0.627	1.0217	1.0622
51	4.072	1.428	0.895	1.031	0.946	0.950	0.453	0.627	1.0217	1.0622
52	4.072	1.428	0.895	1.031	0.946	0.950	0.453	0.627	1.0217	1.0622
53	4.072	1.428	0.895	1.031	0.946	0.950	0.453	0.627	1.0217	1.0622
54	4.072	1.428	0.895	1.031	0.946	0.950	0.453	0.627	1.0217	1.0622
55	4.072	1.428	0.895	1.031	0.946	0.950	0.453	0.627	1.0217	1.0622
56	4.072	1.428	0.895	1.031	0.946	0.950	0.453	0.627	1.0217	1.0622
57	4.072	1.428	0.895	1.031	0.946	0.950	0.453	0.627	1.0217	1.0622
58	4.072	1.428	0.895	1.031	0.946	0.950	0.453	0.627	1.0217	1.0622
59	4.072	1.428	0.895	1.031	0.946	0.950	0.453	0.627	1.0217	1.0622
60	4.072	1.428	0.895	1.031	0.946	0.950	0.453	0.627	1.0217	1.0622
61	4.072	1.428	0.895	1.031	0.946	0.950	0.453	0.627	1.0217	1.0622
62	4.072	1.428	0.895	1.031	0.946	0.950	0.453	0.627	1.0217	1.0622
63	4.072	1.428	0.895	1.031	0.946	0.950	0.453	0.627	1.0217	1.0622
64	4.072	1.428	0.895	1.031	0.946	0.950	0.453	0.627	1.0217	1.0622

Table 5.1

SHOCK FRONT DATA		DIPOLE WEST/9		WFS/295		SMOKE PUFF GRID 1209		PRIMARY FRONT FROM LOWER CHARGE	
<i>Ambient Temperature T = 14.17 DEGREES CELSIUS</i>									
Ambient Pressure P = 93.02 KILOPASCALS									
Absolute Humidity RH = 55.0 PER CENT									
Ambient Pressure Vp = 1.49 KILOPASCALS									
Velocity of Sound C = 340.469 METERS/SECOND									
Change in Light w = 4.859 KILOGRAMS									
Change Height H = 4.63 METERS									
Orientation #2 Hs = 4.61 METERS									
Scaling Scaling Factor S = 8.1111									
Scaling to Charge weight w0 = 1.0 KILOGRAMS									
<i>SHOCK FRONT DATA COMPUTED FROM PARTICLE TRAJECTORY TIMES OF ARRIVAL</i>									
T-obs	R-fit	Difference	T-scal	R-scal	Shock	Pressure	Pressure	Particle	Density
MSEC	METERS	METERS	MSEC	METERS	VELOCITY	RATIO	KPA	VELOCITY	RATIO
3.378	7.738	7.726	0.012	0.917	0.953	3.927	16.642	1547.816	3.042
3.378	7.744	7.726	-0.018	0.917	0.953	3.927	16.642	1547.816	3.042
3.378	7.560	7.726	0.166	0.417	0.953	3.927	16.642	1547.816	3.042
3.378	8.252	7.726	-0.166	0.417	0.953	3.927	16.642	1547.816	3.042
3.378	8.252	8.125	-0.147	0.453	0.953	3.927	16.642	1547.816	3.042
3.378	1.545	1.440	-0.147	0.453	0.953	3.927	16.642	1547.816	3.042
3.378	1.545	1.255	-0.022	0.706	0.706	1.616	1359.570	2.838	4.381
3.378	1.255	1.255	-0.022	0.706	0.706	1.616	1359.570	2.838	4.381
3.378	1.0514	1.0523	0.009	0.742	0.742	2.636	6.940	6455.574	1.881
3.378	1.0514	1.071	0.019	0.742	0.742	2.636	6.940	6455.574	1.881
3.378	1.3392	1.3386	-0.006	0.778	0.778	2.537	6.343	5894.590	1.786
3.378	1.3392	1.3396	-0.013	1.247	1.247	2.446	6.13	6404.49	1.698
3.378	1.3392	1.3396	-0.013	1.650	1.650	1.700	2.03	204.953	0.926
3.378	1.3392	1.3396	-0.013	1.650	1.650	1.700	2.03	204.953	0.926

T IS TIME OF RADIAL POSITION. R IS RADIAL PUFF POSITION. RADIUS VALUES ARE FITTED USING $R = IT + B + C \cdot \log(1+T)$.
 SHOCK AND PARTICLE VELOCITIES ARE EXPRESSED IN MACH NUMBER. RELATIVE TO THE AMBIENT SOUND SPEED C ABOVE.
 OBSERVED IS PEAK OVERPRESSURE RATIO (P-MAX-P)/P. AND PEAK OVERPRESSURE (P-MAX-P) IN KILOPASCALS OBSERVED.
 AMBIENT PRESSURE IS AMBIENT PRESSURE.

SCALED TIME OBSERVED TIME MULTIPLIED BY $(C/CO)/S$, WHERE CO = 340.292 METERS/SECOND
 AND SCALED DISTANCE OBSERVED DISTANCE DIVIDED BY S = CUBE ROOT OF $(w/w_0) * (P_0/P)$.

SCALING FACTOR $w_0 = 325$ KILOPASCALS. (w_0 , w_0 , AND P_0 ARE DEFINED ABOVE.)
 SCALING FACTOR $w_0 = 1.0$ IN ATMOSPHERE WHERE CO AND PO ARE AMBIENT (TO 15 DEGREES CELSIUS).
 SCALING FACTOR $P_0 = 1.0$ IN ATMOSPHERE WHERE CO AND PO ARE AMBIENT (TO 15 DEGREES CELSIUS).

AD-A053 420

GENERAL ELECTRIC CO ALBUQUERQUE N MEX TEMPO

F/G 18/3

PHOTGRAMMETRY OF THE PARTICLE TRAJECTORIES ON DIPOLE WEST SHOT--ETC(U)

DNA001-77-C-0305

OCT 77 J M DEWEY, D J McMILLIN, D TRILL

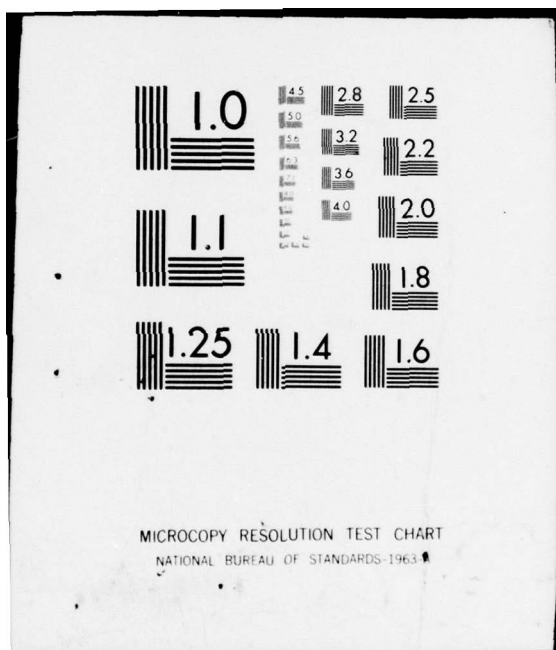
NL

UNCLASSIFIED

DNA-4326F-2

2 OF 2
AD
A053420

END
DATE
FILED
6-78
DDC



MICROCOPY RESOLUTION TEST CHART
NATIONAL BUREAU OF STANDARDS-1963

Table 5.2

SHOCK FRONT DATA DIPOLE WEST/9 WFS/295 SMOKE PUFF GRID 1209
PRIMARY FRONT FROM UPPER CHARGE

AMBIENT TEMPERATURE $T = 14.17$ DEGREES CELSIUS
AMBIENT PRESSURE $P = 93.02$ KILOPASCALS
RELATIVE HUMIDITY RH = 55.0 PER CENT
VAPOR PRESSURE VP = 2.80 KILOPASCALS
AMBIENT SPEED OF SOUND C = 340.469 METERS/SECOND
CHARGE HEIGHT $W = 4.99.9$ KILOGRAMS
CHARGE HEIGHT $H = 4.63$ METERS
SEPARATION +2 $H_S = 4.61$ METERS
SACHS SCALING FACTOR $S = 8.1111$
SCALING TO CHARGE WEIGHT $W_0 = 1.0$ KILOGRAMS

SHOCK FRONT DATA COMPUTED FROM PARTICLE TRAJECTORY TIMES OF ARRIVAL

T-OBS MSEC	R-OBS METERS	R-FIT METERS	DIFFERENCE METERS	T-SCAL MSEC	R-SCAL METERS	SHOCK VELOCITY	PRESSURE RATIO	PRESSURE KPA	PARTICLE VELOCITY	DENSITY RATIO	PUFF NUMBER	
3.0378	7.664	7.739	0.075	0.417	0.954	3.391	1.22550	1.139469	2.580	4.0182	3	
3.0671	8.159	7.739	-0.419	0.417	0.954	3.391	1.22251	1.139469	2.580	4.0182	2	
3.0964	7.912	8.071	0.111	0.453	0.955	3.243	1.11104	1.022836	2.446	4.0067	5	
4.0258	8.779	8.388	-0.391	0.476	0.469	1.634	1.92075	1.139469	2.326	3.957	4	
6.0339	10.653	10.571	-0.082	0.525	0.525	3.112	1.01135	1.92075	2.326	3.957	5	
6.0349	10.557	10.571	0.014	0.579	0.579	2.697	2.0446	9.309	6.658.882	2.219	3.854	1
6.0349	10.735	10.571	-0.164	0.713	0.713	1.303	5.811	5.404.483	1.697	3.268	17	
6.0349	11.208	11.047	-0.161	0.778	0.778	1.303	5.811	5.404.483	1.697	3.268	16	
6.0349	11.903	11.047	-0.156	0.855	0.855	1.362	5.811	5.404.483	1.697	3.268	15	
6.0349	13.423	11.047	-0.144	0.855	0.855	2.341	5.226	4.860.777	1.595	3.137	13	
10.0111	13.583	13.379	-0.204	1.247	1.247	1.649	3.326	3.326	1.595	3.137	14	
10.0443	13.573	13.573	0.000	1.283	1.283	1.962	1.0939	3.326	1.211	2.610	27	
11.0279	13.817	14.140	0.323	1.391	1.391	1.673	3.217	2.99348	1.211	2.610	27	
13.611	15.613	15.571	-0.042	1.679	1.679	1.874	2.930	2.930	2.99348	1.177	2.475	25
13.903	15.693	15.743	0.054	1.715	1.715	1.926	1.740	2.365	2.930	0.971	2.262	38
17.684	17.891	17.867	-0.024	1.757	1.757	1.941	1.726	1.726	2.309	2.14750	2.240	39
17.755	17.891	17.967	0.076	1.712	1.712	1.941	1.726	1.726	2.309	2.14750	2.240	37
21.084	20.305	19.985	-0.020	2.181	2.181	1.596	1.767	1.767	0.795	2.00088	53	
21.743	20.305	19.985	-0.020	2.682	2.682	1.487	1.487	1.487	0.679	2.00088	49	
											1.08404	

R IS TIME-OF-ARRIVAL AND R IS RADIAL PUFF POSITION. RADIAl PUFF POSITIONS ARE FITTED USING $R = f(T) = A + B * T + C * \log(1+T)$.

SHOCK AND PARTICLE VELOCITIES ARE EXPRESSED IN MACH UNITS. RELATIVE TO THE AMBIENT SOUND SPEED C ABOVE. PRESSURE IS PEAK OVERPRESSURE RATIO $(P_{MAX}-P)/P$, AND PEAK OVERPRESSURE $(P_{MAX}-P)/P$ IN KILOPASCALS OBSERVED, WHERE P IS AMBIENT PRESSURE.

DENSITY IS EXPRESSED AS A RATIO, RELATIVE TO THE AMBIENT DENSITY D.

SCALED TIME = OBSERVED TIME MULTIPLIED BY $(C/C_0)/S$, WHERE $C_0 = 340.292$ METERS/SECOND

AND SCALED DISTANCE = OBSERVED DISTANCE DIVIDED BY S^2 CUBE ROOT OF $(W/W_0)(P_0/P)$,

WHERE $P_0 = 1.01.325$ KILOPASCALS. (W, W_0, AND P ARE DEFINED ABOVE.)
SCALED EVENT STANDARD CHARGE W_0 IN ATMOSPHERE WHERE C_0 AND P_0 ARE AMBIENT (TO=15 DEGREES CELSIUS). VELOCITY, PRESSURE, AND DENSITY, EXPRESSED AS RATIOS, ARE INVARIANT UNDER SCALING.

Table 5.3

SHOCK FRONT DATA DIPOLE WEST/9 WFS/295 SMOKE PUFF GRID 1209
MACH STEM BELOW INTERACTION PLANE

AMBIENT TEMPERATURE $T = 14.17$ DEGREES CELSIUS
AMBIENT PRESSURE $P = 93.02$ KILOPASCALS
RELATIVE HUMIDITY $RH = 65.0$ PER CENT
VAPOR PRESSURE $V_P = 0.99$ KILOPASCALS
AMBIENT SPEED OF SOUND $C = 340.469$ METERS/SECOND
CHARGE WEIGHT $W = 4.849$ KILOGRAMS
CHARGE HEIGHT $H = 4.63$ METERS
SEPARATION $+2$ $H_S = 4.61$ METERS
SACHS SCALING FACTOR $S_F = 8.1111$
SCALING TO CHARGE WEIGHT $W_0 = 1.0$ KILOGRAMS

SHOCK FRONT DATA COMPUTED FROM PARTICLE TRAJECTORY TIMES OF ARRIVAL						
T- ₀	R-OBS	3-FIT	DIFFERENCE	T-SCAL	R-SCAL	SHOCK VELOCITY
MSEC	METERS	METERS	METERS	MSEC	METERS	METERS
3.071	7.656	7.581	-0.075	0.453	0.935	3.898
6.016	10.213	10.274	0.061	0.742	1.0267	2.974
9.019	13.568	13.644	0.076	1.0211	1.0682	2.0328
12.019	12.373	13.644	0.271	1.0211	1.0682	2.0328
12.424	15.526	15.424	-0.102	1.0409	1.0899	2.0116
12.454	15.546	15.424	-0.122	1.0499	1.0899	2.0116
12.737	15.453	15.424	-0.033	1.0571	1.0951	2.0174
15.358	17.795	17.599	-0.196	1.0874	1.170	1.924
15.358	17.593	17.599	0.016	1.0894	1.170	1.924
15.358	17.623	17.599	-0.023	1.0994	1.170	1.924
15.645	19.798	19.74	-0.063	1.0325	2.0440	1.0785
15.645	19.698	19.74	0.060	1.0325	2.0440	1.0785
15.645	19.74	19.74	0.000	1.0325	2.0440	1.0785
19.423	22.256	22.045	-0.111	2.396	2.0484	1.0767
22.012	22.150	22.042	-0.108	2.037	2.0714	1.0882
22.012	22.909	22.713	-0.193	2.0789	2.0789	1.0682
22.012	21.889	22.023	0.142	2.0789	2.0789	1.0682
22.057	24.309	24.269	-0.040	3.288	2.0992	1.0602
22.057	23.932	24.269	0.337	3.288	2.0992	1.0602
22.057	24.142	24.269	0.229	3.288	2.0992	1.0602
22.075	25.642	25.358	-0.284	3.537	3.0537	1.0126
22.075	25.379	25.358	-0.021	3.0537	3.0537	1.0126
22.093	25.549	25.511	-0.038	3.0573	3.0573	1.0126

T IS TIME-OF-ARRIVAL AND R IS RADIAL PUFF POSITION. RADIUS VALUES ARE FITTED USING RFIT=A+B*T+C*LOG(1+T). SHOCK AND PARTICLE VELOCITIES ARE EXPRESSED IN MACH UNITS. RELATIVE TO THE AMBIENT SOUND SPEED C ABOVE. PRESSURE IS PEAK OVERPRESSURE. DENSITY IS EXPRESSED AS A RATIO. RELATIVE TO THE AMBIENT DENSITY D.

SCALED TIME= OBSERVED TIME MULTIPLIED BY $(C/CO)/S$, WHERE CO= 340.292 METERS/SECOND AND SCALED DISTANCE= OBSERVED DISTANCE DIVIDED BY S^2 CUBE ROOT OF $((W/W_0)^{1/3} (P_0/P))$. WHERE P IS AMBIENT PRESSURE. (W, W₀, AND P ARE DEFINED ABOVE.)

SCALED EVENT= STANDARD CHARGE W₀ IN ATMOSPHERE WHERE CO AND PO ARE AMBIENT ($T_0= 15$ DEGREES CELSIUS). VELOCITY, PRESSURE, AND DENSITY, EXPRESSED AS RATIOS, ARE INVARIANT UNDER SCALING.

Table 5.4

SHOCK FRONT DATA

DIPOLE WEST/9

WFS/295

SMOKE PUFF GRID 1209

RS /A77C404

AMBIENT TEMPERATURE $T = 14.17$ DEGREES CELSIUS
 AMBIENT PRESSURE $P = 93.02$ KILOPASCALS
 RELATIVE HUMIDITY RH = 55.2 PER CENT
 VAPOUR PRESSURE $V_P = 2.89$ KILOPASCALS
 AMBIENT SPEED OF SOUND $C = 340.469$ METERS/SECOND
 CHARGE WEIGHT $W = 489.9$ KILOGRAMS
 CHARGE HEIGHT $H = 4.63$ METERS
 SEPARATION Δ = 2 METERS
 SACHS SCALING FACTOR $S = 8.111$
 SACHS SCALING TO CHARGE WEIGHT $W_0 = 1.0$ KILOGRAMS

SHOCK FRONT DATA COMPUTED FROM PARTICLE TRAJECTORY TIMES OF ARRIVAL

T-OBS MSEC	R-FIT METERS	R-SCAL METERS	T-SCAL METERS	R-SCAL METERS	SHOCK VELOCITY	PRESSURE RATIO	PARTICLE VELOCITY	DENSITY RATIO	PUFF NUMBER
3.904	7.406	7.378	7.028	0.910	4.035	1.7828	1.6580	3.156	6
6.349	1.631	1.613	1.518	1.253	2.669	9.822	9.13456	2.286	18
9.615	1.349	1.380	1.481	0.778	1.650	5.582	5.19	3.218	29
12.915	1.3559	1.380	1.519	1.233	1.736	2.302	5.14	3.087	30
15.293	1.5661	1.580	1.597	1.597	1.950	0.089	9.44	1.342	41
13.923	1.5925	1.6431	1.626	1.715	1.751	2.026	3.62	2.796	42
14.194	1.6108	1.6531	1.650	1.751	1.750	2.026	3.52	2.777	43
15.358	1.7577	1.7412	1.614	1.694	2.147	1.6937	3.21	1.258	43
15.388	1.7685	1.7412	1.6272	1.694	2.147	1.6937	2.95	1.184	43
15.940	1.7947	1.793	1.966	1.937	2.147	1.937	2.98	1.184	53
16.812	1.8313	1.8352	2.039	2.074	2.263	1.906	2.85	1.151	52
18.672	1.9723	1.969	2.114	2.129	2.418	1.777	2.67	1.105	51
19.445	2.029	1.958	2.171	2.129	2.461	1.755	2.51	1.011	50
19.445	1.9946	1.958	2.121	2.096	2.461	1.755	2.427	0.988	50
19.715	2.0351	2.0131	2.21	2.121	2.422	1.755	2.427	0.988	50
21.454	2.165	2.146	2.414	2.446	2.482	1.745	2.386	0.977	50
22.012	2.1798	2.185	2.607	2.689	2.688	1.689	2.21	0.977	50
22.914	2.1985	2.198	2.603	2.825	2.708	1.649	2.005	0.876	50
22.253	2.248	2.291	2.38	2.896	2.748	1.634	1.948	0.852	50
23.484	2.2516	2.229	2.225	2.896	2.748	1.634	1.919	0.849	50
22.817	2.2817	2.21	2.205	2.906	2.788	1.625	1.865	0.849	50
23.258	2.3254	2.3243	2.3121	2.916	2.866	1.625	1.865	0.849	50
26.657	2.4244	2.4018	2.226	2.98	2.961	1.564	1.696	0.770	50
27.334	2.4348	2.4324	2.022	2.983	2.961	1.554	1.686	0.770	50
27.544	2.4507	2.4476	2.023	2.955	2.999	1.553	1.646	0.757	50
28.675	2.4952	2.4779	2.031	2.951	2.995	1.547	1.627	0.751	50
28.963	2.5379	2.5228	2.015	2.929	3.018	1.527	1.554	0.727	50
28.993	2.518	2.5228	2.015	2.929	3.018	1.522	1.536	0.721	50
29.538	2.5224	2.5228	2.021	2.944	3.017	1.522	1.536	0.717	50
29.538	2.5387	2.5256	2.021	2.944	3.017	1.513	1.533	0.710	50
31.059	2.6058	2.6115	2.057	2.986	3.147	1.513	1.533	0.710	50
31.839	2.6440	2.6796	2.256	3.927	3.222	1.495	1.441	0.688	50
32.414	2.6785	2.6985	2.250	3.998	3.327	1.478	1.383	0.668	50
					1.471	1.356	1.261	0.659	50

T IS TIME-OF-ARRIVAL AND R IS RADIAL PUFF POSITION, UNITS ARE EXPRESSED IN MACH UNITS. RELATIVE TO THE AMBIENT SOUND SPEED C ABOVE. PRESSURE IS PEAK OVERPRESSURE RATIO (P_{MAX}/P) AND PEAK OVERPRESSURE (P_{MAX}) IN KILOPASCALS. WHERE P IS AMBIENT PRESSURE.

SCALED TIME = OBSERVED TIME MULTIPLIED BY CO = 340.292 METERS/SECOND, WHERE CO = CURF ROOT OF $(W/W_0) * (P_0/P)$.

SCALED DISTANCE = OBSERVED DISTANCE DIVIDED BY CO, WHERE CO = CURF ROOT OF $(W/W_0) * (P_0/P)$.

SCALED EVENT = STANDARD CHARGE W0 IN ATMOSPHERE WHERE CO AND PO ARE AMBIENT (TO=15 DEGREES CELSIUS).

VELOCITY, PRESSURE, AND DENSITY, EXPRESSED AS RATIOS, ARE INVARIANT UNDER SCALING.

Table 5.5

SHOCK FRONT DATA DIPOLE WEST/9 WFS/295 SMOKE PUFF GRID 1209
MACH STEM AT GROUND SURFACE R3 / A770404

AMBIENT TEMPERATURE $T = 14.17$ DEGREES CELSIUS
AMBIENT PRESSURE $P_0 = 93.32$ KILOPASCALS
RELATIVE HUMIDITY $RH = 55.2$ PER CENT
VAPOUR PRESSURE $V_P = 0.89$ KILOPASCALS
AMBIENT SPEED OF SOUND $C = 340.469$ METERS/SECOND
CHARGE WEIGHT $W = 4.89$ KILOGRAMS
CHARGE HEIGHT $H = 4.63$ METERS
SEPARATION $\delta/2$ $HS = 4.61$ METERS
SACHS SCALING FACTOR $S = 8.111$
SCALING TO CHARGE WEIGHT $W_0 = 1.0$ KILOGRAMS

SHOCK FRONT DATA COMPUTED FROM PARTICLE TRAJECTORY TIMES OF ARRIVAL

T-OBS MSEC	R-OBS METERS	R-FIT METERS	DIFFERENCE METERS	T-SCAL MSEC	R-SCAL METERS	SHOCK VELOCITY	PRESSURE RATIO	PARTICLE VELOCITY	PRESSURE KPA	PUFF NUMBER
8.005	1.1•459	1.1•442	-0.016	0.995	1.041	2.047	8.0963	833.694	2.173	3.807
10.443	1.3•742	1.3•609	-0.134	1.283	1.078	2.0532	5.97068	1.781	3.371	2.4
11.662	1.4•427	1.4•819	-0.392	1.463	1.0827	2.0349	5.271	4.97439	1.603	3.148
13.029	1.5•795	1.5•727	-0.068	1.607	1.0939	2.0231	4.639	4.31486	1.486	3.6
13.229	1.5•772	1.5•727	-0.045	1.607	1.0939	2.0231	4.639	4.31486	1.485	2.993
13.611	1.6•103	1.6•164	-0.561	1.667	1.0993	2.0179	4.371	4.62524	1.485	4.7
15.258	1.7•630	1.7•418	-0.212	1.694	2.0147	2.0445	3.711	3.45101	1.296	2.922
15.649	1.7•557	1.7•619	-0.063	1.930	2.0172	2.0125	3.617	3.56448	2.73	6.0
16.431	1.8•016	1.8•016	-0.086	2.062	2.0221	1.995	3.443	3.26255	1.237	2.076
18.945	1.9•672	1.9•719	-0.022	2.022	2.0431	1.848	2.816	2.61891	0.648	5.6
19.135	1.9•872	1.9•921	-0.029	2.036	2.0454	1.834	2.758	2.56570	1.074	7.1
19.135	1.9•142	1.9•921	-0.241	2.036	2.0454	1.834	2.758	2.56570	1.074	7.2
22.012	2.1•901	2.1•988	-0.086	2.089	2.0711	2.0215	2.071	2.05121	0.927	6.2
22.012	2.2•215	2.1•988	-0.228	2.079	2.0711	2.070	2.025	2.05121	0.927	6.2
23.484	2.2•090	2.2•485	-0.406	2.086	2.0772	1.673	1.673	2.153	0.896	8.4
20.037	2.4•006	2.4•245	-0.239	3.0288	2.0989	1.598	1.070	1.64660	0.797	2.009
20.037	2.4•265	2.4•245	-0.120	3.0288	2.0989	1.586	1.070	1.64660	0.797	2.009
20.503	2.4•136	2.4•245	-0.139	3.0288	2.0989	1.596	1.070	1.64660	0.797	2.009
20.503	2.5•604	2.5•470	-0.314	3.0573	3.140	1.515	1.584	1.47329	0.737	1.922
25.638	2.5•771	2.5•470	-0.311	3.0573	3.140	1.535	1.584	1.47329	0.737	1.922
25.638	25.610	25.769	0.160	3.0644	3.177	1.524	1.542	1.430477	0.723	1.903

T IS TIME-OF-ARRIVAL AND R IS RADIAL PUFF POSITION. RADIUS VALUES ARE FITTED USING $RFT = A + RT + C * LOG(1+T)$. SHOCK AND PARTICLE VELOCITIES ARE EXPRESSED IN MACH UNITS, RELATIVE TO THE AMBIENT SOUND SPEED C ABOVE. PRESSURE IS PEAK OVERPRESSURE RATIO $(P_{MAX}-P)/P$, AND PEAK OVERPRESSURE $(P_{MAX}-P)$ IN KILOPASCALS OBSERVED. WHERE P IS AMBIENT PRESSURE. DENSITY IS EXPRESSED AS A RATIO. RELATIVE TO THE AMBIENT DENSITY D.

SCALED TIME OBSERVED TIME MULTIPLIED BY $(C/C_0)/S$, WHERE $C_0 = 340.292$ METERS/SECOND
AND SCALED DISTANCE OBSERVED DIVIDED BY S (CURE ROOT OF $(W/W_0) \cdot (P_0/P)$).
WHERE $P_0 = 1.0$ KILOPASCALS. (W, W₀ AND P ARE DEFINED ABOVE)
SCALED EVENT = STANDARD CHARGE W₀ IN ATMOSPHERE WHERE C₀ AND P₀ ARE AMBIENT (TO= 15 DEGREES CELSIUS). VELOCITY, PRESSURE, AND DENSITY, EXPRESSED AS RATIOS. ARE INVARIANT UNDER SCALING.

Table 7.1

VELOCITY FIELD		DIPOLE WEST/9		WFS/295		SMOKE PUFF GRID 1209	
PARTICLE VELOCITIES AT SCALED TIME = 1.000 MS				/A770404			
X-SCAL	Y-SCAL	U=DX/DT	V=DY/DT	PARTICLE	R-SCAL	REGN	REGN
METERS	METERS	MACH NO	MACH NO	VELOCITY	METERS	CODE	CODE
1.0107	2.0256	0.91	0.42	1.0285	1.0285	1.0411	2
1.0107	1.0787	1.068	0.05	1.0187	2	1.0364	
1.0246	1.0568	1.035	2.019	1.0359	1.0254	1.0412	2
1.0269	1.0356	1.035	-0.12	1.0352	1.0287	1.0405	5
1.0221	1.0273	1.036	0.03	1.0364	1.0223	1.0413	5
1.0208	0.895	1.041	-0.07	1.0414	1.0291	1.0422	4
1.0274	0.685	1.031	-0.07	1.0309	1.0276	1.0434	4
1.0263	2.0239	1.053	0.07	1.0529	1.0326	1.0427	4
1.0359	2.0162	1.015	0.36	1.0201	1.0433	1.0398	1
1.0380	1.098	1.035	0.28	1.0377	1.0416	1.0391	1
PARTICLE VELOCITIES AT SCALED TIME = 2.000 MS							
X-SCAL	Y-SCAL	U=DX/DT	V=DY/DT	PARTICLE	R-SCAL	REGN	REGN
METERS	METERS	MACH NO	MACH NO	VELOCITY	METERS	CODE	CODE
1.0108	2.0253	0.59	0.23	0.633	1.0716	2.0028	2
1.0600	2.0083	0.64	0.31	0.711	1.0717	2.0029	2
1.0715	1.0851	0.50	0.17	0.581	1.0721	0.0016	
1.0725	1.0607	0.49	0.06	0.493	1.0728	0.0016	
1.0609	1.039	0.46	-0.02	0.457	1.0698	2.0040	2
1.0744	0.8859	0.469	0.10	0.706	1.0767	2.0040	2
1.0747	0.6668	0.77	0.05	0.768	1.0848	2.0040	2
1.0763	0.4455	0.73	-0.05	0.729	1.0768	2.0040	2
1.0754	0.2511	0.76	-0.26	0.814	1.0772	2.0040	2
1.0539	2.0238	0.74	0.26	0.785	1.0914	2.0040	2
1.0383	2.0032	0.80	0.26	0.847	1.0911	2.0040	2
1.0902	1.0918	0.83	0.30	0.883	1.0916	2.0040	2
1.0963	1.0470	0.86	0.28	0.902	1.0991	2.0040	2
1.0981	1.0284	0.83	0.37	0.831	1.0983	2.0040	2
1.0986	0.9817	0.90	-0.06	0.904	2.0044	2.0040	2
1.0974	0.7819	0.98	-0.08	0.985	2.0025	2.0040	2
1.0919	0.6958	0.89	0.10	0.891	1.0979	2.0040	2
1.0938	0.474	0.95	-0.03	0.949	1.0996	2.0040	2
1.0574	0.349	1.02	0.05	1.017	2.0021	1.004	1
1.0983	0.136	1.01	0.02	1.005	1.0988	2.0040	2
OBSERVED DISTANCE VALUES = 8.1111 TIMES SCALED VALUES AND OBSERVED TIME VALUE = 8.1069 TIMES SCALED VALUE. VELOCITY VALUES AS SHOWN ARE INVARIANT UNDER SCALING.							

Table 7.2

VELOCITY FIELD		DIPOLE WEST/9	WFS/295	SMOKE PUFF GRID 1209	
PARTICLE VELOCITIES AT SCALED TIME = 3.000 MS					
X-SCAL METERS	Y-SCAL METERS	U=DX/DT MACH NO	V=DY/DT MACH NO	PARTICLE VELOCITY METERS	R-SCAL METERS
1.0714	2.0314	0.016	0.013	1.0817	2
1.0707	2.0145	0.019	0.010	1.0845	2
1.0828	1.0694	0.021	0.006	1.0823	2
1.0660	1.0620	0.020	0.009	1.0823	2
1.0782	1.0641	0.024	0.009	1.0823	2
1.0899	1.0925	0.028	0.011	1.0888	5
1.0940	1.0702	0.028	0.016	1.0800	5
1.0914	1.0444	0.021	0.016	1.0911	4
1.0934	1.0222	0.027	0.006	1.0932	4
2.0059	2.0304	0.024	0.008	1.0942	3
2.0057	2.0120	0.035	0.013	1.0942	3
2.0064	1.0873	0.020	0.017	1.0942	3
2.0164	1.0534	0.021	0.009	1.0942	3
2.0185	1.0290	0.044	0.013	1.0942	3
2.0234	1.0652	0.051	0.010	1.0942	3
2.0249	1.0785	0.043	0.012	1.0942	3
2.0143	1.0591	0.025	0.015	1.0942	3
2.0143	1.0457	0.021	0.008	1.0942	3
2.0210	1.0357	0.047	0.002	1.0942	3
2.0232	1.0337	0.059	0.001	1.0942	3
2.0207	2.0242	0.049	0.025	1.0942	3
2.0207	2.0576	0.058	0.018	1.0942	3
2.0242	1.0958	0.055	0.017	1.0942	3
2.0324	1.0713	0.047	0.017	1.0942	3
2.0377	1.0493	0.053	0.011	1.0942	3
2.0308	1.0208	0.055	0.008	1.0942	3
2.0304	1.0036	0.055	0.005	1.0942	3
2.0301	1.0037	0.057	0.004	1.0942	3
2.0344	1.0017	0.054	-0.003	1.0942	3
2.0369	1.0496	0.061	-0.005	1.0942	3
2.0305	1.0315	0.063	-0.006	1.0942	3
2.0375	1.0120	0.067	0.007	1.0942	3
2.0348	2.0232	0.063	0.029	1.0942	3

OBSERVED DISTANCE VALUES = $8.1111 \times$ SCALED VALUES
 AND OBSERVED TIME VALUE = $8.1069 \times$ SCALED VALUE.
 VELOCITY VALUES AS SHOWN ARE INVARIANT UNDER SCALING.

/A777404

REGN CODE	R-SCAL MFTERS	PARTICLE VELOCITY
2	2.0156	0.015
5	1.0843	0.638
5	1.0844	0.652
5	1.0846	0.653
5	1.0848	0.575
5	1.0849	0.575
5	1.0850	0.567
5	1.0851	0.639
5	1.0852	0.603
4	1.0853	0.669
4	1.0854	0.609
4	1.0855	0.677
4	1.0856	0.677
4	1.0857	0.677
4	1.0858	0.678
4	1.0859	0.654
3	1.0860	0.656
3	1.0861	0.625
3	1.0862	0.825
3	1.0863	0.715
3	1.0864	0.715
3	1.0865	0.762
2	1.0866	0.840
2	1.0867	0.705
2	1.0868	0.771
2	1.0869	0.677
5	1.0870	0.750
5	1.0871	0.750
5	1.0872	0.659
5	1.0873	0.659
5	1.0874	0.750
5	1.0875	0.640
5	1.0876	0.640
5	1.0877	0.640
5	1.0878	0.640
5	1.0879	0.640
5	1.0880	0.640
5	1.0881	0.640
5	1.0882	0.640
5	1.0883	0.640
5	1.0884	0.640
5	1.0885	0.640
5	1.0886	0.640
5	1.0887	0.640
5	1.0888	0.640
5	1.0889	0.640
5	1.0890	0.640
5	1.0891	0.640
5	1.0892	0.640
5	1.0893	0.640
5	1.0894	0.640
5	1.0895	0.640
5	1.0896	0.640
5	1.0897	0.640
5	1.0898	0.640
5	1.0899	0.640
5	1.0900	0.640
5	1.0901	0.640
5	1.0902	0.640
5	1.0903	0.640
5	1.0904	0.640
5	1.0905	0.640
5	1.0906	0.640
5	1.0907	0.640
5	1.0908	0.640
5	1.0909	0.640
5	1.0910	0.640
5	1.0911	0.640
5	1.0912	0.640
5	1.0913	0.640
5	1.0914	0.640
5	1.0915	0.640
5	1.0916	0.640
5	1.0917	0.640
5	1.0918	0.640
5	1.0919	0.640
5	1.0920	0.640
5	1.0921	0.640
5	1.0922	0.640
5	1.0923	0.640
5	1.0924	0.640
5	1.0925	0.640
5	1.0926	0.640
5	1.0927	0.640
5	1.0928	0.640
5	1.0929	0.640
5	1.0930	0.640
5	1.0931	0.640
5	1.0932	0.640
5	1.0933	0.640
5	1.0934	0.640
5	1.0935	0.640
5	1.0936	0.640
5	1.0937	0.640
5	1.0938	0.640
5	1.0939	0.640
5	1.0940	0.640
5	1.0941	0.640
5	1.0942	0.640
5	1.0943	0.640
5	1.0944	0.640
5	1.0945	0.640
5	1.0946	0.640
5	1.0947	0.640
5	1.0948	0.640
5	1.0949	0.640
5	1.0950	0.640
5	1.0951	0.640
5	1.0952	0.640
5	1.0953	0.640
5	1.0954	0.640
5	1.0955	0.640
5	1.0956	0.640
5	1.0957	0.640
5	1.0958	0.640
5	1.0959	0.640
5	1.0960	0.640
5	1.0961	0.640
5	1.0962	0.640
5	1.0963	0.640
5	1.0964	0.640
5	1.0965	0.640
5	1.0966	0.640
5	1.0967	0.640
5	1.0968	0.640
5	1.0969	0.640
5	1.0970	0.640
5	1.0971	0.640
5	1.0972	0.640
5	1.0973	0.640
5	1.0974	0.640
5	1.0975	0.640
5	1.0976	0.640
5	1.0977	0.640
5	1.0978	0.640
5	1.0979	0.640
5	1.0980	0.640
5	1.0981	0.640
5	1.0982	0.640
5	1.0983	0.640
5	1.0984	0.640
5	1.0985	0.640
5	1.0986	0.640
5	1.0987	0.640
5	1.0988	0.640
5	1.0989	0.640
5	1.0990	0.640
5	1.0991	0.640
5	1.0992	0.640
5	1.0993	0.640
5	1.0994	0.640
5	1.0995	0.640
5	1.0996	0.640
5	1.0997	0.640
5	1.0998	0.640
5	1.0999	0.640
5	1.1000	0.640

Table 7.3

OBSERVED DISTANCE VALUES = 8.1111 TIMES SCALED VALUES AND OBSERVED TIME VALUES = 8.1069 TIMES SCALED VALUE. VELOCITY VALUES AS SHOWN ARE INVARIANT UNDER SCALING.

Table 7.4

VELOCITY FIELD

DIPOLE WEST/9

SMOKE PUFF GRID 1209

PARTICLE VELOCITIES AT SCALED TIME = 5.000 MS

X-SCAL METERS	Y-SCAL METERS	Z-SCAL METERS	U=DX/DT MACH NO	V=DY/DT MACH NO	PARTICLE VELOCITY MACH NO	R-SCAL METERS	REGN CODE
2.0435	2.163	2.027	0.015	0.007	2.0167	2.6473	2
2.0534	1.970	1.877	0.023	0.013	0.0070	0.0057	1
2.0622	1.877	1.777	0.026	0.017	0.0064	0.0086	2
2.0572	1.877	1.777	0.026	0.013	0.0070	0.0086	3
2.0570	1.877	1.777	0.026	0.013	0.0070	0.0086	4
2.0573	1.877	1.777	0.025	0.014	0.0064	0.0071	5
2.0524	1.849	1.720	0.026	0.012	0.0071	0.0059	6
2.0535	1.857	1.772	0.026	0.011	0.0064	0.0071	7
2.0633	1.892	1.772	0.026	0.017	0.0071	0.0176	8
2.0547	1.819	1.714	0.026	0.014	0.0073	0.0179	9
2.0593	2.314	1.714	0.015	0.015	0.0073	0.0155	10
2.0593	2.145	1.966	0.015	0.015	0.0073	0.0155	11
2.073	1.772	1.966	0.023	0.014	0.0064	0.0174	12
2.073	1.772	1.772	0.024	0.014	0.0064	0.0174	13
2.0734	1.714	1.772	0.026	0.012	0.0064	0.0174	14
2.0752	1.728	1.772	0.026	0.012	0.0064	0.0174	15
2.0762	1.782	1.772	0.016	0.012	0.0064	0.0174	16
2.0733	1.714	1.714	0.023	0.024	0.0064	0.0175	17
2.0871	0.476	0.476	0.024	0.024	0.0064	0.0175	18
2.0871	0.759	0.759	0.024	0.024	0.0064	0.0175	19
2.0891	0.461	0.461	0.033	0.033	0.0064	0.0176	20
2.0891	0.349	0.349	0.021	0.019	0.0064	0.0176	21
2.0758	0.784	0.738	0.021	0.019	0.0064	0.0176	22
2.0831	1.012	0.831	0.021	0.012	0.0064	0.0176	23
2.0871	1.044	0.771	0.023	0.012	0.0064	0.0176	24
2.0891	1.071	0.771	0.024	0.013	0.0064	0.0176	25
2.0904	1.049	0.886	0.024	0.016	0.0064	0.0176	26
2.0881	1.028	0.886	0.021	0.016	0.0064	0.0176	27
2.0911	1.071	0.871	0.019	0.003	0.0064	0.0176	28
2.0911	1.071	0.851	0.019	0.005	0.0064	0.0176	29
2.0911	1.071	0.851	0.019	0.005	0.0064	0.0176	30
2.0911	1.071	0.851	0.019	0.005	0.0064	0.0176	31
2.0911	1.071	0.851	0.019	0.005	0.0064	0.0176	32
2.0911	1.071	0.851	0.019	0.005	0.0064	0.0176	33
2.0911	1.071	0.851	0.019	0.005	0.0064	0.0176	34
2.0911	1.071	0.851	0.019	0.005	0.0064	0.0176	35
2.0911	1.071	0.851	0.019	0.005	0.0064	0.0176	36
2.0911	1.071	0.851	0.019	0.005	0.0064	0.0176	37
2.0911	1.071	0.851	0.019	0.005	0.0064	0.0176	38
2.0911	1.071	0.851	0.019	0.005	0.0064	0.0176	39
2.0911	1.071	0.851	0.019	0.005	0.0064	0.0176	40
2.0911	1.071	0.851	0.019	0.005	0.0064	0.0176	41
2.0911	1.071	0.851	0.019	0.005	0.0064	0.0176	42
2.0911	1.071	0.851	0.019	0.005	0.0064	0.0176	43
2.0911	1.071	0.851	0.019	0.005	0.0064	0.0176	44
2.0911	1.071	0.851	0.019	0.005	0.0064	0.0176	45
2.0911	1.071	0.851	0.019	0.005	0.0064	0.0176	46
2.0911	1.071	0.851	0.019	0.005	0.0064	0.0176	47
2.0911	1.071	0.851	0.019	0.005	0.0064	0.0176	48
2.0911	1.071	0.851	0.019	0.005	0.0064	0.0176	49
2.0911	1.071	0.851	0.019	0.005	0.0064	0.0176	50

OBSERVED DISTANCE VALUES = 8.1111 TIMES SCALED VALUES
AND OBSERVED TIME VALUES = 9.1009 TIMES SCALED VALUES.
VELOCITY VALUES AS SHOWN ARE INVARIANT UNDER SCALING.

Table 7.5

VELOCITY FIELD

DIPOLE WEST/9

WFS/295

SMOKE PUFF GRID 1209

PARTICLE VELOCITIES AT SCALED TIME= 6.030

MS

X-SCAL METERS	Y-SCAL METERS	Z-SCAL METERS	U=DX/DT MACH NO	V=DY/DT MACH NO	W=DZ/DT MACH NO	PARTICLE NO	R-SCAL METERS	REGN CODE
2.0661	2.0186	0.27	0.016	0.316	0.859	5	0.896	5
2.0738	2.0458	0.26	0.011	0.279	2.891	5	0.739	4
2.0789	1.8203	0.24	0.009	0.261	2.867	5	0.522	3
2.0773	1.6327	0.26	0.006	0.266	2.812	5	0.225	3
2.0816	2.0292	0.27	0.010	0.285	2.820	5	0.196	3
2.0843	1.0140	0.25	0.010	0.275	2.843	5	0.166	3
2.0534	0.9927	0.18	0.002	0.180	2.644	4	0.231	5
2.0645	0.6050	0.19	-0.001	0.188	2.897	4	0.19	5
2.0683	0.4668	0.23	-0.001	0.228	2.220	3	0.220	5
2.0614	0.3622	0.13	0.015	0.135	2.817	5	0.192	6
2.0902	2.0173	0.22	0.015	0.215	2.265	5	0.06	6
2.0945	1.987	0.22	0.013	0.259	2.259	5	0.07	6
2.0991	1.0743	0.18	0.005	0.190	2.022	5	0.215	6
2.0943	1.5118	0.17	0.003	0.169	2.994	5	0.247	4
2.0979	1.3206	0.18	0.027	0.193	2.948	5	0.727	4
2.0961	1.694	0.22	0.010	0.241	2.979	4	0.475	3
2.0961	0.8884	0.19	0.017	0.207	2.972	4	0.251	3
2.0953	0.6767	0.19	0.012	0.212	2.948	4	0.258	3
2.0950	1.4550	0.19	0.012	0.188	3.106	5	0.583	5
2.0937	0.336	0.12	0.025	0.134	3.024	5	0.276	5
2.0945	0.124	0.13	0.002	0.136	3.048	5	0.215	5
2.0937	0.323	0.19	0.011	0.225	3.260	5	0.06	5
2.0927	2.044	0.23	0.013	0.257	3.256	5	0.252	5
2.0919	1.940	0.19	0.014	0.239	3.220	5	0.915	4
2.0912	1.0710	0.19	0.006	0.252	3.190	5	0.677	4
2.0915	1.504	0.16	0.004	0.169	3.179	5	0.557	4
2.0915	1.304	0.18	0.007	0.191	3.189	5	0.496	4
2.0916	1.693	0.20	0.010	0.222	3.166	5	0.04	5

OBSERVED DISTANCE VALUES = 8.1111 TIMES SCALED VALUES
 AND OBSERVED TIME VALUE = 8.1069 TIMES SCALED VALUES.
 VELOCITY VALUES AS SHOWN ARE INVARIANT UNDER SCALING.

/A770404

R-SCAL METERS		PARTICLE NO		PARTICLE NO		PARTICLE NO		PARTICLE NO	
3.0178	0.896	2.021	0.10	2.024	0.10	2.022	0.10	2.023	0.10
3.0269	0.739	2.021	0.10	2.022	0.10	2.023	0.10	2.024	0.10
3.0284	0.84	2.022	0.10	2.023	0.10	2.024	0.10	2.025	0.10
3.0269	0.69	2.023	0.10	2.024	0.10	2.025	0.10	2.026	0.10
3.0269	0.69	2.024	0.10	2.025	0.10	2.026	0.10	2.027	0.10
3.0256	0.56	2.025	0.10	2.026	0.10	2.027	0.10	2.028	0.10
3.0256	0.56	2.026	0.10	2.027	0.10	2.028	0.10	2.029	0.10
3.0256	0.56	2.027	0.10	2.028	0.10	2.029	0.10	2.030	0.10
3.0256	0.56	2.028	0.10	2.029	0.10	2.030	0.10	2.031	0.10
3.0256	0.56	2.029	0.10	2.030	0.10	2.031	0.10	2.032	0.10

Table 7.6

VELOCITY FIELD DIPOLE WEST/9 WFS/295

SMOKE PUFF GRID 1209

PARTICLE VELOCITIES AT SCALED TIME = 7.000 MS									
X-SCAL METERS	Y-SCAL METERS	Z-SCAL MACH NO	U=DX/DT MACH	V=DY/DT MACH	W=DZ/DT MACH	PARTICLE NO	PARTICLE NO	PARTICLE NO	R-SCAL METERS
REGN CODE	REGN CODE	REGN CODE	REGN CODE	REGN CODE	REGN CODE	REGN CODE	REGN CODE	REGN CODE	REGN CODE
2.0507	2.0216	0.11	0.037	0.011	0.001	130	157	157	0.000
2.0498	2.0117	0.119	-0.021	0.018	0.001	154	154	154	0.000
3.0-2.9	1.0767	0.22	0.022	0.022	0.002	273	259	259	0.000
3.0-3.2	1.0546	0.23	0.023	0.021	0.002	307	359	359	0.000
3.0-3.4	1.0114	0.24	-0.024	0.027	0.004	328	328	328	0.000
2.9994	0.9887	-0.25	-0.013	0.013	0.001	137	115	115	0.000
2.9941	0.9796	-0.29	0.013	0.011	0.001	296	156	156	0.000
2.991	0.9449	0.15	-0.001	0.0149	0.001	223	159	159	0.000
2.9537	0.351	0.15	0.006	0.006	0.001	176	157	157	0.000
3.0-0.85	0.4132	0.17	0.005	0.005	0.001	082	088	088	0.000
3.0-1.05	4.0181	0.18	0.004	0.004	0.001	296	312	312	0.000
3.0-1.88	1.0978	0.22	0.028	0.024	0.004	234	207	207	0.000
3.0-1.98	1.0716	0.22	0.022	0.017	0.002	207	253	253	0.000
3.0-2.31	1.0533	0.37	0.037	0.021	0.001	416	256	256	0.000
3.0-2.58	1.0335	0.31	0.021	0.021	0.001	264	326	326	0.000
3.0-2.30	1.0120	0.19	-0.022	0.019	0.001	190	216	216	0.000
3.0-2.31	0.9924	0.19	-0.013	0.013	0.001	152	216	216	0.000
3.0-3.36	0.9757	0.24	-0.022	0.022	0.002	239	239	239	0.000
3.0-3.38	0.9528	0.11	0.033	0.033	0.003	358	444	444	0.000
3.0-3.44	0.9259	0.16	-0.034	0.034	0.004	159	379	379	0.000
3.0-2.71	0.108	0.04	-0.001	0.043	0.001	160	334	334	0.000
3.0-3.29	2.0312	0.24	0.009	0.009	0.001	256	273	273	0.000

OBSERVED DISTANCE VALUES = $8 \cdot 10^{11}$ TIMES SCALED VALUES
 AND OBSERVED TIME VALUE = $8 \cdot 10^9$ TIMES SCALED VALUE.
 VELOCITY VALUES AS SHOWN ARE INVARIANT UNDER SCALING.

Table 8.1

DENSITY FIELD DIPOLE WEST/9 WFS/295

AVERAGE DENSITIES AT SCALED TIME= 1.000 MS

X-SCAL METERS	Y-SCAL METERS	DENSITY RATIO	R-SCAL METERS	REGN CODE	X-SCAL METERS	Y-SCAL METERS	DENSITY RATIO	R-SCAL METERS	REGN CODE
1.033	1.0076	1.796	1.333	2	1.0524	1.085	1.0264	1.0534	2
1.032	1.0491	1.955	1.341	2	1.0524	1.316	1.0416	1.0561	1
1.031	1.0663	1.791	1.343	4	1.0552	1.134	1.0552	1.0561	5
1.033	0.776	2.267	1.343	4	1.0531	0.931	1.0661	1.0545	4
1.051	2.0079	1.203	1.558	2	1.0523	0.761	1.0394	1.0535	1

AVERAGE DENSITIES AT SCALED TIME= 2.000 MS

X-SCAL METERS	Y-SCAL METERS	DENSITY RATIO	R-SCAL METERS	REGN CODE	X-SCAL METERS	Y-SCAL METERS	DENSITY RATIO	R-SCAL METERS	REGN CODE
1.075	1.0151	1.264	1.812	2	2.031	0.236	0.415	2.0466	3
1.079	1.0949	1.314	1.806	2	2.081	0.236	0.464	2.0302	3
1.063	1.0751	1.729	1.893	4	2.068	0.668	1.0419	2.0113	4
1.085	1.0559	1.867	1.853	1	2.091	0.678	1.0578	2.0134	5
1.085	1.0379	1.758	1.889	3	2.074	1.074	1.0578	2.0102	3
1.085	1.0551	2.016	1.966	2	2.036	1.528	1.0797	2.0113	2
1.092	1.0402	2.071	1.962	2	2.054	1.533	1.0938	2.0179	4
1.095	1.0431	1.932	1.949	5	2.032	1.53	1.0938	2.0179	4
2.037	1.0355	1.326	1.564	2	2.053	1.040	2.0153	2.0131	5
2.043	1.0112	1.929	1.960	4	2.043	1.48	0.946	2.0153	4
2.039	0.039	0.929	1.960	2	2.052	0.52	2.0156	2.0156	3
2.015	0.727	1.955	1.957	4	2.033	0.94	2.0168	2.0195	2
1.099	0.570	2.079	2.076	4	2.025	1.25	0.575	2.0508	3

AVERAGE DENSITIES AT SCALED TIME= 3.000 MS

X-SCAL METERS	Y-SCAL METERS	DENSITY RATIO	R-SCAL METERS	REGN CODE	X-SCAL METERS	Y-SCAL METERS	DENSITY RATIO	R-SCAL METERS	REGN CODE
1.050	1.0221	0.918	1.969	2	2.043	0.430	1.046	2.0350	5
1.054	1.0111	0.778	1.964	2	2.053	0.778	1.094	2.0353	4
2.020	0.798	1.119	2.156	4	2.050	0.731	1.0207	2.0444	4
2.018	0.568	1.004	2.098	4	2.033	0.547	1.0918	2.0449	4
2.037	0.3662	1.052	2.169	3	2.043	0.391	1.0730	2.0463	3
2.013	2.0186	1.043	2.169	2	2.052	0.121	1.0122	2.0463	3
2.010	1.0952	1.085	2.178	2	2.049	1.0948	1.0855	2.0482	2
2.027	1.0430	0.711	2.287	5	2.057	1.575	1.0547	2.0502	5
2.028	1.0153	0.926	2.284	5	2.038	1.548	1.0329	2.0521	5
2.029	0.913	1.226	2.322	4	2.051	1.239	1.0886	2.0559	5
2.020	0.727	1.119	2.302	4	2.056	1.137	1.0886	2.0559	5
2.022	0.556	1.066	2.299	4	2.058	0.944	1.0798	2.0575	4
2.024	0.412	1.047	2.18	3	2.051	0.943	1.0917	2.0592	4
2.030	0.235	1.064	2.312	3	2.050	0.547	1.0671	2.0637	3
2.031	0.153	1.792	2.343	2	2.057	1.557	1.0853	2.0681	4
2.032	1.0961	1.326	2.471	5	2.069	0.926	1.0592	2.0777	5
2.037	1.0791	1.19	2.459	5	2.043	0.904	1.0966	2.0752	5
2.041	1.0589	1.326	2.452	5	2.064	1.041	1.0718	2.0727	5
2.042	1.0428	1.413	2.437	5	2.069	1.523	1.0934	2.0707	5

X AND Y LOCATE THE CENTER OF A PLANE QUADRILATERAL WHICH IS A CELL OF 4 NEIGHBOURING SMOKE PUFFS.
 DENSITY IS AVERAGED OVER THE AREA OF THE CELL AND IS EXPRESSED AS A RATIO TO THE AMBIENT DENSITY.
 OBSERVED DISTANCE VALUE = 8.1111 TIMES SCALED VALUES
 AND OBSERVED TIME VALUE = 8.1069 TIMES SCALED VALUE.
 DENSITY VALUES AS SHOWN ARE INVARIANT UNDER SCALING.

Table 6.2

DENSITY FIELD DIPOLE WEST/9 WFS/295

/A77C404.

AVERAGE DENSITIES AT SCALED TIME = 4.000 MS					
X-SCAL METERS	Y-SCAL METERS	DENSITY RATIO	REGN CODE	X-SCAL METERS	Y-SCAL METERS
2.0312	2.034	0.813	2.137	2.0616	2.0193
2.112	2.082	1.116	2.137	2.059	2.027
2.056	2.065	1.064	2.165	2.055	2.082
2.124	2.039	1.064	2.165	2.072	2.082
2.07	2.074	2.074	2.165	2.0715	2.078
2.039	2.043	2.043	2.18	2.0739	2.075
2.046	2.0185	2.0185	2.18	2.0742	2.066
2.0371	2.026	2.026	2.16	2.0745	2.074
2.321	2.0588	2.0673	2.385	2.0798	2.054
2.044	2.0445	1.261	2.451	2.0805	2.0170
2.0446	2.0446	0.692	2.451	2.0843	1.0971
2.0444	2.0209	1.253	2.476	2.0659	1.0765
2.0474	2.0510	1.057	2.619	2.0873	1.0552
2.0514	1.0829	1.031	2.67	2.0892	1.254
2.0532	1.0635	1.199	2.601	2.0891	1.162
2.0564	1.0382	1.215	2.597	2.0967	1.0563
2.0584	1.0173	1.022	2.589	2.0921	0.970
2.0583	0.9753	0.990	2.589	2.0950	0.574
2.0509	0.9732	0.810	2.601	2.0950	0.347
2.0503	0.9547	1.404	2.660	2.0927	0.970
2.0014	0.410	1.236	2.046	2.0960	2.132
AVERAGE DENSITIES AT SCALED TIME = 5.000 MS					
X-SCAL METERS	Y-SCAL METERS	DENSITY RATIO	REGN CODE	X-SCAL METERS	Y-SCAL METERS
2.0537	2.039	1.017	2.699	2.0912	2.0215
2.0540	1.0871	0.981	2.699	2.0945	2.0171
2.0045	1.0679	1.071	2.699	2.0945	1.0814
2.0067	0.983	0.928	2.672	2.0928	1.0659
2.0052	0.572	2.072	2.651	2.094	1.0393
2.0745	0.572	2.0738	2.764	2.099	1.0182
2.0716	0.447	1.024	2.752	2.099	0.990
2.0092	2.0232	1.001	2.935	2.0944	0.791
2.0742	2.0448	1.019	2.125	2.0988	0.945
2.0794	1.0850	1.025	2.879	2.0938	0.950
2.0004	1.0621	0.859	2.841	2.0856	0.964
2.0089	1.0422	1.276	2.821	2.0826	0.936
2.0089	1.0187	1.034	2.829	2.0829	0.916
2.0052	0.952	1.0245	2.834	2.0829	0.977
2.0084	0.752	1.156	2.872	2.0872	1.063
2.0026	0.576	0.924	2.931	2.0924	1.0192
2.0011	0.587	1.613	2.937	2.0937	1.0361
2.0014	0.387	1.613	2.937	2.094	1.0166

X AND Y LOCATE THE CENTER OF A PLANE QUADRILATERAL WHICH IS A CELL OF 4 NEIGHBOURING SMOKE PUFFS. DENSITY IS AVERAGED OVER THE AREA OF THE CELL AND IS EXPRESSED AS A RATIO TO THE AMBIENT DENSITY.

OBSERVED DISTANCE VALUES = 8.1111 TIMES SCALED VALUES
AND OBSERVED TIME VALUE = 8.1069 TIMES SCALED VALUE.
DENSITY VALUES AS SHOWN ARE INVARIANT UNDER SCALING.

Table 8.3

DENSITY FIELD DIPOLE WEST/9 WFS/295

SMOKE PUFF GRID 1219

/A77C4C4

AVERAGE DENSITIES AT SCALED TIME = 6.000 MS		X-SCAL METERS		Y-SCAL METERS		REGN CODE		X-SCAL METERS		Y-SCAL METERS		REGN CODE		X-SCAL METERS		Y-SCAL METERS		REGN CODE		X-SCAL METERS		Y-SCAL METERS		REGN CODE	
2.816	2.093	1.014	2.973	5	5	5	5	3.068	1.024	3.068	1.024	5	5	3.069	1.024	3.069	1.024	5	5	3.069	1.024	3.069	1.024	5	5
2.866	1.857	0.916	0.982	5	5	5	5	3.071	1.024	3.071	1.024	4	4	3.074	1.024	3.074	1.024	4	4	3.074	1.024	3.074	1.024	4	4
2.874	1.846	0.914	0.982	5	5	5	5	3.072	1.024	3.072	1.024	4	4	3.075	1.024	3.075	1.024	4	4	3.075	1.024	3.075	1.024	4	4
2.874	1.841	0.914	0.982	5	5	5	5	3.073	1.024	3.073	1.024	4	4	3.076	1.024	3.076	1.024	4	4	3.076	1.024	3.076	1.024	4	4
2.893	1.208	1.042	1.442	5	5	5	5	3.074	1.024	3.074	1.024	4	4	3.077	1.024	3.077	1.024	4	4	3.077	1.024	3.077	1.024	4	4
2.903	1.008	1.036	1.364	4	4	4	4	3.075	1.024	3.075	1.024	4	4	3.078	1.024	3.078	1.024	4	4	3.078	1.024	3.078	1.024	4	4
2.927	0.787	0.787	0.943	4	4	4	4	3.076	1.024	3.076	1.024	4	4	3.079	1.024	3.079	1.024	4	4	3.079	1.024	3.079	1.024	4	4
2.914	0.599	0.825	0.962	4	4	4	4	3.077	1.024	3.077	1.024	4	4	3.080	1.024	3.080	1.024	4	4	3.080	1.024	3.080	1.024	4	4
2.914	0.495	0.442	0.734	3	3	3	3	3.078	1.024	3.078	1.024	3	3	3.081	1.024	3.081	1.024	3	3	3.081	1.024	3.081	1.024	3	3
2.918	0.38	0.346	0.456	3	3	3	3	3.079	1.024	3.079	1.024	3	3	3.082	1.024	3.082	1.024	3	3	3.082	1.024	3.082	1.024	3	3
2.953	0.63	0.017	0.205	3	3	3	3	3.080	1.024	3.080	1.024	3	3	3.083	1.024	3.083	1.024	3	3	3.083	1.024	3.083	1.024	3	3
2.963	1.040	0.961	0.974	5	5	5	5	3.081	1.024	3.081	1.024	5	5	3.084	1.024	3.084	1.024	5	5	3.084	1.024	3.084	1.024	5	5
2.963	1.040	0.961	0.974	5	5	5	5	3.082	1.024	3.082	1.024	5	5	3.085	1.024	3.085	1.024	5	5	3.085	1.024	3.085	1.024	5	5
AVERAGE DENSITIES AT SCALED TIME = 7.000 MS		X-SCAL METERS		Y-SCAL METERS		REGN CODE		X-SCAL METERS		Y-SCAL METERS		REGN CODE		X-SCAL METERS		Y-SCAL METERS		REGN CODE		X-SCAL METERS		Y-SCAL METERS		REGN CODE	
3.093	1.099	1.016	1.149	5	5	5	5	3.083	1.024	3.083	1.024	5	5	3.085	1.024	3.085	1.024	5	5	3.085	1.024	3.085	1.024	5	5
3.104	1.094	1.036	1.205	5	5	5	5	3.084	1.024	3.084	1.024	5	5	3.086	1.024	3.086	1.024	5	5	3.086	1.024	3.086	1.024	5	5
3.123	1.643	1.017	0.908	5	5	5	5	3.085	1.024	3.085	1.024	5	5	3.087	1.024	3.087	1.024	5	5	3.087	1.024	3.087	1.024	5	5
3.145	1.004	1.004	1.213	4	4	4	4	3.086	1.024	3.086	1.024	4	4	3.089	1.024	3.089	1.024	4	4	3.089	1.024	3.089	1.024	4	4
3.145	1.041	0.840	1.486	3	3	3	3	3.087	1.024	3.087	1.024	3	3	3.090	1.024	3.090	1.024	3	3	3.090	1.024	3.090	1.024	3	3
3.145	0.037	0.754	0.754	4	4	4	4	3.088	1.024	3.088	1.024	4	4	3.091	1.024	3.091	1.024	4	4	3.091	1.024	3.091	1.024	4	4
3.145	0.391	0.947	0.947	3	3	3	3	3.089	1.024	3.089	1.024	3	3	3.092	1.024	3.092	1.024	3	3	3.092	1.024	3.092	1.024	3	3
3.175	0.220	0.914	0.914	3	3	3	3	3.090	1.024	3.090	1.024	3	3	3.093	1.024	3.093	1.024	3	3	3.093	1.024	3.093	1.024	3	3
3.262	2.056	1.234	3.094	5	5	5	5	3.091	1.024	3.091	1.024	5	5	3.094	1.024	3.094	1.024	5	5	3.094	1.024	3.094	1.024	5	5

X AND Y LOCATE THE CENTER OF A PLANE QUADRILATERAL WHICH IS AVERAGED OVER THE AREA OF THE CELL AND IS EXPRESSED AS A RATIO TO THE AMBIENT DENSITY.

OBSERVED DISTANCE VALUES = 8.1111 TIMES SCALED VALUES
AND OBSERVED TIME VALUE = 9.1069 TIMES SCALED VALUE.
DENSITY VALUES AS SHOWN ARE INVARIANT UNDER SCALING.

K AND L LOCATE THE CENTER OF A PLANE QUADRILATERAL WHICH IS A CELL OF 4 NEIGHBOURING SMOKE PUFFS.

DENSITY RATIO = 1.0000

Table 9.1

PRESSURE FIELD DIPOLE WEST/9 WFS/295 SMOKE PUFF GRID 1209 /A770404

AVERAGE HYDROSTATIC OVERPRESSURES AT SCALED TIME = 1.000 MS				AVERAGE HYDROSTATIC OVERPRESSURES AT SCALED TIME = 2.000 MS				AVERAGE HYDROSTATIC OVERPRESSURES AT SCALED TIME = 3.000 MS			
X-SCAL METERS	Y-SCAL PRESSURE METERS	R-SCAL REGN CODE	X-SCAL METERS	Y-SCAL PRESSURE METERS	R-SCAL REGN CODE	X-SCAL METERS	Y-SCAL PRESSURE METERS	R-SCAL REGN CODE	X-SCAL METERS	Y-SCAL PRESSURE METERS	R-SCAL REGN CODE
1.032	2.0416	1.0333	1.0524	1.0534	1.0534	1.0523	1.0544	1.0522	1.0517	1.0517	1.0517
1.076	2.0461	2.0779	1.1331	1.1343	1.1343	1.1341	1.1341	1.1341	1.1355	1.1355	1.1355
1.322	1.0481	1.0631	3.0216	1.0343	1.0343	1.0552	1.0552	1.0552	1.0576	1.0576	1.0576
1.331	0.9631	0.9776	4.0493	1.0346	1.0346	1.0531	1.0531	1.0531	1.0555	1.0555	1.0555
1.334	0.9776	2.079	0.524	1.0558	2	1.0523	0.761	1.0523	1.0535	1.0535	1.0535
1.533	2.079	0.524	0.524	0.969	1	0.969	0.969	0.969	0.886	0.886	0.886
<hr/>											
REGN CODE											
3	2	2	3	3	3	2	2	3	2	2	3
5	5	5	5	5	5	5	5	5	5	5	5

X AND Y LOCATE THE CENTER OF A PLANE QUADRILATERAL WHICH IS A CELL OF 4 NEIGHBOURING SMOKE PUFFS. OVERPRESSURE IS AVERAGED OVER THE AREA OF THE CELL AND IS EXPRESSED AS A RATIO TO THE AMBIENT PRESSURE.

OBSERVED DISTANCE VALUES = 8.0111 TIMES SCALED VALUES
OBSERVED TIME VALUE = 9.0109 TIMES SCALED VALUE.
PRESSURE VALUES AS SHOWN ARE INVARIANT UNDER SCALING.

Table 9.2

PRESSURE FIELD DIPPLE WEST/9 WFS/295

AVERAGE HYDROSTATIC OVERPRESSURES AT SCALED TIME = 4, C.O.C. MS

X-SCAL METERS	Y-SCAL METERS	PRESSURE R-SCAL METERS	REGN CODE	X-SCAL METERS	Y-SCAL METERS	PRESSURE R-SCAL METERS	REGN CODE
2.0 4.31	2.0 6.34	-0.117	2.0 5.57	2.0 6.16	2.0 1.93	0.6353	2.0 9.91
2.0 1.12	2.0 8.24	0.441	2.0 1.36	2.0 0.59	2.0 0.17	0.441	2.0 0.17
2.0 0.98	2.0 6.25	0.319	2.0 1.65	2.0 1.65	2.0 1.8	0.583	2.0 7.97
2.0 1.24	2.0 3.91	0.253	2.0 1.60	2.0 7.9	2.0 1.0	0.583	2.0 9.9
2.0 4.07	2.0 0.74	-0.154	2.0 2.86	2.0 7.15	2.0 1.4	0.725	2.0 7.76
2.0 3.99	1.0 4.43	-0.050	2.0 4.18	2.0 7.39	2.0 1.6	0.916	2.0 7.25
2.0 4.48	1.0 1.85	-0.264	2.0 4.49	2.0 7.42	2.0 0.9	0.557	2.0 7.47
2.0 4.06	0.9 2.6	0.131	2.0 4.16	2.0 7.45	2.0 0.7	0.617	2.0 7.73
2.0 3.71	0.9 7.35	0.621	2.0 4.16	2.0 7.98	2.0 0.5	0.554	2.0 8.92
2.0 3.61	0.5 5.98	-0.073	2.0 3.85	2.0 7.85	2.0 0.4	0.351	2.0 8.95
2.0 4.14	0.6 4.45	0.667	2.0 4.51	2.0 8.61	2.0 0.3	0.363	2.0 8.61
2.0 4.46	0.2 4.68	-0.251	2.0 4.61	2.0 8.43	2.0 0.2	0.284	2.0 8.69
2.0 4.24	2.0 2.09	0.447	2.0 4.76	2.0 8.58	2.0 0.1	0.961	2.0 9.25
2.0 4.74	2.0 0.10	0.203	2.0 6.19	2.0 8.73	2.0 0.0	0.537	2.0 9.62
2.0 3.14	1.0 8.29	0.154	2.0 6.27	2.0 8.92	2.0 0.0	0.444	2.0 8.92
2.0 5.53	1.0 6.35	0.457	2.0 6.01	2.0 8.91	2.0 0.0	0.319	2.0 8.91
2.0 5.81	1.0 3.92	0.496	2.0 5.91	2.0 8.97	2.0 0.0	0.547	2.0 9.03
2.0 5.86	1.0 1.73	0.481	2.0 5.80	2.0 9.21	2.0 0.0	0.939	2.0 9.39
2.0 5.83	0.6 9.65	0.150	2.0 5.89	2.0 9.50	2.0 0.0	0.574	2.0 9.46
2.0 5.69	0.6 7.32	-0.150	2.0 6.01	2.0 9.53	2.0 0.0	0.547	2.0 9.53
2.0 0.3	0.6 5.47	0.854	2.0 6.00	2.0 9.27	2.0 0.0	0.179	2.0 9.70
2.0 6.14	0.6 4.10	0.578	2.0 6.46	2.0 9.60	2.0 0.0	0.132	2.0 9.60

AVERAGE HYDROSTATIC OVERPRESSURES AT SCALED TIME = 5.001 MS

X-SCAL METERS	Y-SCAL METERS	PRESSURE R-SCAL METERS	REGN CODE	X-SCAL METERS	Y-SCAL METERS	PRESSURE R-SCAL METERS	REGN CODE
2.0 5.37	2.0 0.39	0.096	2.0 5.91	2.0 9.02	2.0 2.15	0.651	2.0 1.95
2.0 5.56	1.0 6.71	0.247	2.0 6.99	2.0 9.45	2.0 1.87	0.316	2.0 0.73
2.0 0.07	0.6 9.83	0.333	2.0 6.72	2.0 9.83	2.0 1.59	0.163	2.0 0.17
2.0 0.52	0.6 7.52	-0.278	2.0 6.81	2.0 9.94	2.0 1.42	-0.013	2.0 0.04
2.0 7.65	0.6 5.72	0.554	2.0 7.64	2.0 9.99	2.0 1.16	0.0181	2.0 0.00
2.0 7.10	0.6 4.47	0.229	2.0 7.52	2.0 9.01	2.0 0.96	0.28	2.0 0.06
2.0 6.92	2.0 2.32	0.245	2.0 7.95	2.0 8.04	2.0 0.79	0.648	2.0 0.64
2.0 7.42	2.0 0.48	0.252	2.0 8.88	2.0 8.91	2.0 0.59	0.093	2.0 1.45
2.0 7.54	2.0 0.50	0.129	2.0 8.79	2.0 8.94	2.0 0.36	0.325	2.0 1.19
2.0 8.04	1.0 6.21	-0.145	2.0 8.41	2.0 8.64	2.0 0.19	0.419	2.0 0.70
2.0 8.19	1.0 4.32	0.547	2.0 8.21	2.0 8.96	2.0 1.79	0.030	2.0 2.57
2.0 8.29	1.0 1.97	0.647	2.0 8.29	2.0 9.77	2.0 1.16	0.0380	2.0 2.27
2.0 8.29	0.9 9.82	0.892	2.0 8.34	2.0 1.44	2.0 0.76	0.402	2.0 2.05
2.0 6.46	0.7 7.92	0.345	2.0 8.72	2.0 1.64	2.0 1.56	0.335	2.0 1.92
2.0 5.28	0.5 5.76	-0.010	2.0 9.81	2.0 1.91	2.0 1.36	0.568	2.0 1.99
2.0 9.11	0.4 3.87	1.185	2.0 9.37	2.0 1.94	2.0 1.66	0.367	2.0 1.94

X AND Y LOCATE THE CENTER OF A PLANE QUADRILATERAL WHICH IS A CELL OF 4 NEIGHBORING SMOKE PUFFS.
 OVERPRESSURE IS AVERAGED OVER THE AREA OF THE CELL AND IS EXPRESSED AS A RATIO TO THE AMBIENT PRESSURE,
 OBSERVED DISTANCE VALUES = 8.1111 TIMES SCALED VALUES
 OBSERVED TIME VALUE = 8.1069 TIMES SCALED VALUE.
 PRESSURE VALUES AS SHOWN ARE INVARIANT UNDER SCALING.

Table 9.3

PRESSURE FIELD DIPOLE WEST/9 WFS/295

/A77C404

AVERAGE HYDROSTATIC OVERPRESSURES AT SCALED TIME =

6.000 MS

X-SCAL METERS	Y-SCAL METERS	R-SCAL METERS	REGN CODE	X-SCAL METERS	Y-SCAL METERS	R-SCAL METERS	REGN CODE	X-SCAL METERS	Y-SCAL METERS	R-SCAL METERS	REGN CODE
4.0 3.10	2.0 1.93	2.0 2.29	5 2.973	3.0 0.68	1.0 2.4	-0.0 1.35	6 3.169	0.0 825	0.0 248	0.0 345	4
2.0 2.00	1.0 0.87	1.0 0.66	3 0.663	2.0 0.76	0.0 96.9	0.0 0.74	3 0.361	0.0 611	0.0 317	0.0 402	4
2.0 0.87	1.0 0.46	-0.0 1.12	2 0.914	3.0 1.25	0.0 82.5	0.0 0.659	3 0.362	0.0 378	0.0 177	0.0 393	3
2.0 0.74	1.0 0.19	0.0 0.49	2 0.887	3.0 1.25	0.0 62.2	-0.0 1.49	4 0.341	2.0 1.68	0.0 230	0.0 496	5
2.0 0.69	1.0 0.18	0.0 0.81	2 0.859	3.0 1.32	0.0 37.7	0.0 0.363	3 0.347	1.0 985	0.0 276	0.0 462	5
2.0 0.63	1.0 0.08	0.0 0.71	2 0.906	4 0.134	0.0 21.1	0.0 0.61	1 0.141	3 0.384	1.0 772	0.0 566	3 0.443
2.0 0.57	1.0 0.78	0.0 3.45	2 0.944	4 0.218	0.0 21.1	0.0 0.61	3 0.342	3 0.452	1.0 57.2	0.0 186	5 0.429
2.0 0.51	0.0 5.99	-0.0 1.15	3 0.962	4 0.195	2 0.021	0.0 0.432	2 0.421	1 0.367	0.0 215	0.0 215	5 0.428
2.0 0.42	0.0 4.02	1 0.41	7 3.009	3 0.224	1 0.802	0.0 1.32	3 0.291	1 0.166	0.0 295	0.0 446	5 0.446
2.0 0.32	0.0 2.63	0.0 2.86	3 0.156	5 0.243	1 0.595	0.0 0.47	5 0.347	1 0.469	0.0 616	0.0 651	4 0.471
3.0 0.63	1.0 0.84	0.0 3.86	3 0.156	5 0.243	1 0.385	0.0 0.349	3 0.275	3 0.488	0.0 818	0.0 667	3 0.544
3.0 0.53	1.0 0.07	0.0 0.02	5 0.190	5 0.269	1 0.185	0.0 0.267	5 0.269	3 0.515	0.0 590	0.0 167	3 0.548
3.0 0.43	1.0 0.47	0.0 0.09	3 0.074	5 0.277	0.0 997	0.0 0.211	3 0.521	0.0 377	0.0 351	0.0 664	3 0.541

AVERAGE HYDROSTATIC OVERPRESSURES AT SCALED TIME =

7.000 MS

X-SCAL METERS	Y-SCAL METERS	R-SCAL METERS	REGN CODE	X-SCAL METERS	Y-SCAL METERS	R-SCAL METERS	REGN CODE	X-SCAL METERS	Y-SCAL METERS	R-SCAL METERS	REGN CODE
3.0 0.82	2.0 0.99	2.0 1.49	5 3.229	5 3.191	1.0 83.0	0.0 1.14	5 3.360	2.0 421	2.0 0.2	0.0 167	5 0.532
3.0 1.04	2.0 0.75	0.0 2.14	5 3.191	5 3.117	1.0 62.1	0.0 1.31	5 3.344	5 3.442	1.0 796	0.0 581	5 0.54
3.0 1.22	1.0 0.63	-0.0 2.72	5 3.160	5 3.338	1 0.413	0.0 42.4	5 3.349	5 4.641	1 0.564	0.0 226	5 0.491
3.0 1.45	1.0 0.04	0.0 1.35	5 3.128	4 3.319	1 0.216	0.0 24.6	5 3.346	5 4.642	1 0.395	0.0 374	5 0.492
3.0 1.64	1.0 0.84	0.0 84.7	4 3.195	4 3.340	1 0.021	-0.0 0.01	4 3.319	4 3.514	1 0.202	0.0 111	5 0.515
3.0 2.45	0.0 0.37	-0.0 2.77	3 3.283	4 3.395	0.0 85.0	0.0 1.2	4 3.407	4 3.542	1 0.52	-0.0 0.52	3 0.543
3.0 2.32	0.0 3.61	0.0 2.01	3 3.254	3 3.423	0.0 62.8	0.0 1.51	4 3.461	4 3.560	0.0 838	0.0 1.56	4 0.572
3.0 1.75	0.0 2.20	-0.0 0.50	3 3.183	3 3.422	0.0 39.6	0.0 0.31	3 3.444	3 3.575	0.0 606	-0.0 1.87	3 0.610
3.0 2.02	2.0 0.56	0.0 3.99	3 3.389	5 3.411	2.0 2.9	0.0 1.21	5 3.575	3 3.593	0.0 388	-0.0 171	3 0.614

X AND Y LOCATE THE CENTER OF A PLANE QUADRILATERAL WHICH IS A CELL OF 4 NEIGHBOURING SMOKE PUFFS. OVERPRESSURE IS AVERAGED OVER THE AREA OF THE CELL AND IS EXPRESSED AS A RATIO TO THE AMBIENT PRESSURE.

OBSERVED DISTANCE VALUES = 8.0111 TIMES SCALING VALUES
 OBSERVED TIME VALUE = 8.01069 TIMES SCALING VALUES
 PRESSURE VALUES AS SHOWN ARE INVARIANT UNDER SCALING.

DISTRIBUTION LIST

DEPARTMENT OF DEFENSE

Director
 Defense Advanced Rsch. Proj. Agency
 ATTN: Strategic Tech. Office

Defense Communication Engineer Center
 ATTN: Code 720, John Worthington

Director
 Defense Communications Agency
 ATTN: NMSSC, Code 510

Defense Documentation Center
 Cameron Station
 12 cy ATTN: TC

Director
 Defense Intelligence Agency
 ATTN: DI-7D
 ATTN: DT-1C, Nuc. Eng. Branch
 ATTN: DT-2, Wpns. & Sys. Div.

Director
 Defense Nuclear Agency
 ATTN: SPSS
 ATTN: STSP
 ATTN: SPAS
 ATTN: DDST
 ATTN: TISI, Archives
 3 cy ATTN: TTIL, Tech. Library

Under Secretary of Def. for Rsch. & Engrg.
 ATTN: S&SS (OS)

Commander, Field Command
 Defense Nuclear Agency
 ATTN: FCTMD
 ATTN: FCPR
 ATTN: FCTMOF
 ATTN: FCTMOT

Director
 Joint Strat. Tgt. Planning Staff, JCS
 ATTN: JPTP
 ATTN: JLTW-2
 ATTN: JPTM

Chief
 Livermore Division, Field Command, DNA
 Lawrence Livermore Laboratory
 ATTN: FCPRL

DEPARTMENT OF THE ARMY

Director
 BMD Advanced Tech. Ctr.
 Huntsville Office
 ATTN: CRDABH-S, William C. Loomis
 ATTN: Marcus Whitfield
 ATTN: ATC-T, Melvin T. Capps

Commander
 BMD System Command
 ATTN: BDMSSC-TEB, R. Simpson
 ATTN: BDMSC-TEN, Noah J. Hurst

DEPARTMENT OF THE ARMY (Continued)

Program Manager
 BMD Program Office
 ATTN: DACS-BMZ-D, Julian Davidson
 ATTN: DACS-BMZ
 ATTN: DACS-BMT, Clifford E. McLain
 ATTN: DACS-BMT, John Shea

Dep. Chief of Staff for Rsch. Dev. & Acq.
 ATTN: NCB Division

Deputy Chief of Staff for Ops. & Plans
 ATTN: Dir. of Nuc. Plans & Policy

Commander
 Harry Diamond Laboratories
 ATTN: DELHD-NP, Francis N. Wimenitz
 ATTN: DRXDO-RBH, James H. Gwaltney
 ATTN: DELHD-NP, Louis J. Belliveau
 ATTN: DRXDO-TF, Robert B. Oswald, Jr.

Commander
 Picatinny Arsenal
 ATTN: Al Loeb
 ATTN: Louis Ayrami, SARPA-FR-E
 ATTN: Henry Opat, SMUPA-MD
 ATTN: Donald Miller, SARPA-ND-C-T

Director
 TRASANA
 ATTN: R. E. Dekinder, Jr.

Director
 U.S. Army Ballistic Research Labs.
 ATTN: DRXBR-X, Julius J. Meszaros
 ATTN: Robert E. Eichelberger
 3 cy ATTN: DRDAR-BLE, J. H. Keefer

Commander
 U.S. Army Missile Command
 ATTN: Troy Smith
 ATTN: DRS-RKP, W. B. Thomas
 ATTN: DRSMI-RRR, Bud Gibson
 ATTN: DRSMI-XS, Chief Scientist
 ATTN: DRCPM-PE-EA, Wallace O. Wagner

Commander
 U.S. Army Nuclear Agency
 ATTN: MONA-WE

Chief
 U.S. Army Research Office
 ATTN: Technical Library

DEPARTMENT OF THE NAVY

Chief of Naval Operations
 ATTN: OP 981
 ATTN: OP 62
 ATTN: Robert A. Blaise
 ATTN: Code 604C3, Robert Piacesi

Chief of Naval Research
 ATTN: Code 464, Thomas P. Quinn

DEPARTMENT OF THE NAVY (Continued)

Director
 Naval Research Laboratory
 ATTN: Gerald Cooperstein, Code 7770
 ATTN: Mario A. Persechino, Code 5180
 ATTN: Code 2600, Tech. Lib.

Commander
 Naval Sea Systems Command
 ATTN: Code 0351
 ATTN: ORD-0333A

Officer-In-Charge
 Naval Surface Weapons Center
 ATTN: Code 322, Victor C. Dawson
 ATTN: Code WA07, W. Carson Lyons
 ATTN: Code WA501, Navy Nuc. Prgms. Off.
 ATTN: Code WR10, Joseph Petes

Commanding Officer
 Naval Weapons Evaluation Facility
 ATTN: Lawrence R. Oliver
 ATTN: Peter Hughes

Director
 Strategic Systems Project Office
 ATTN: NSP-273
 ATTN: NSP-272

DEPARTMENT OF THE AIR FORCE

Commandant
 AF Flight Dynamics Laboratory, AFSC
 ATTN: FXG

AF Materials Laboratory, AFSC
 ATTN: LTM
 ATTN: T. Nicholas
 ATTN: MAS

AF Rocket Propulsion Laboratory, AFSC
 ATTN: RTSN, G. A. Beale

AF Weapons Laboratory, AFSC
 ATTN: Al Sharp
 ATTN: DYS,
 ATTN: SAB
 ATTN: SUL
 ATTN: DYV
 ATTN: DYT

Headquarters
 Air Force Systems Command
 ATTN: SOSS
 ATTN: XRT0

Commander
 ASD
 4 cy ATTN: EWFS, D. Ward

Commander
 Foreign Technology Division, AFSC
 ATTN: TDPTN
 ATTN: TDFBD, J. D. Pumphrey

Hq. USAF/RD
 ATTN: RDQSM
 ATTN: RDQ
 ATTN: RD

DEPARTMENT OF THE AIR FORCE (Continued)

Hq. USAF/XO
 ATTN: XOSS

SAMSO/DY
 ATTN: DYS

SAMSO/MN
 ATTN: MNNH
 ATTN: MNMR

SAMSO/RS
 ATTN: RSSE
 ATTN: RSS

Commander in Chief
 Strategic Air Command
 ATTN: XOBM
 ATTN: XPQM

DEPARTMENT OF ENERGY

Division of Military Application
 ATTN: Doc. Con. for Res. & Dev. Branch

University of California
 Lawrence Livermore Laboratory
 ATTN: Joseph E. Keller, Jr., L-125
 ATTN: G. Stahle, L-24
 ATTN: C. Joseph Taylor, L-92
 ATTN: Joseph B. Knox, L-216
 ATTN: Larry W. Woodruff, L-96

Los Alamos Scientific Laboratory
 ATTN: Doc. Con for R. S. Thurston
 ATTN: Doc. Con. for Richard A. Gentry
 ATTN: Doc. Con. for J. W. Taylor
 ATTN: Doc. Con. for John McQueen
 ATTN: Doc. Con. for T. Talley

Sandia Laboratories
 Livermore Laboratory
 ATTN: Doc. Con. for C. S. Hoyle
 ATTN: Doc. Con. for 8131, H. F. Norris, Jr.
 ATTN: Doc. Con. for T. Gold

Sandia Laboratories
 ATTN: Doc. Con. for Thomas B. Cook
 ATTN: Doc. Con. for Albert Chabai
 ATTN: Doc. Con. for M. L. Merritt

DEPARTMENT OF DEFENSE CONTRACTORS

Acurex Corporation
 ATTN: J. Huntington
 ATTN: J. Courtney
 ATTN: C. Nardo

Aerospace Corporation
 ATTN: W. Mann
 ATTN: R. Allen
 ATTN: Richard Crolius, A2-Rm1027
 ATTN: Robert L. Strickler
 ATTN: R. Mortensen

Analytic Services, Inc.
 ATTN: Jack Selig

ARO, Incorporated
 ATTN: John C. Adams

DEPARTMENT OF DEFENSE CONTRACTORS (Continued)

Avco Research & Systems Group
ATTN: John Gilmore, J400
ATTN: George Weber, J230
ATTN: John F. Stevens, J100
ATTN: William G. Reinecke, K 100
ATTN: Doc. Control
ATTN: George J. Davis
ATTN: William Broding
ATTN: J. Patrick

Battelle Memorial Institute
ATTN: Merwyn R. Vanderlind
ATTN: Richard Castle

The Boeing Company
ATTN: William Crist
ATTN: Brian Lempriere
ATTN: Ed York
ATTN: Robert Holmes
ATTN: Robert Dyrdaal

Boeing Wichita Company
ATTN: T. Swaney

Brown Engineering Company, Inc.
ATTN: Ronald Patrick

California Research & Technology, Inc.
ATTN: Ken Kreyenhagen

Calspan Corporation
ATTN: M. S. Holden
ATTN: Romeo A. Deliberis
ATTN: M. G. Dunn

University of Dayton
ATTN: Hallock F. Swift
ATTN: D. Gerdiman

University of Denver
Denver Research Institute
3 cy ATTN: John Wisotski

Effects Technology, Inc.
ATTN: Robert Wengler

Ford Aerospace & Communications Operations
ATTN: P. Spangler

GARD, Incorporated
ATTN: Marion J. Balcerzak

General Dynamics Corp.
Fort Worth Division
ATTN: R. Shemensky

General Electric Company
Space Division
ATTN: B. M. Maguire
ATTN: G. Harrison
ATTN: A. Martellucci
ATTN: C. Kyriess
ATTN: Daniel Edelman
ATTN: Phillip Cline

General Electric Company
TEMPO-Center for Advanced Studies
3 cy ATTN: DASIAC
ATTN: A. P. R. Lambert (Canada)

DEPARTMENT OF DEFENSE CONTRACTORS (Continued)

GE-TEMPO
ATTN: L. W. Kennedy

General Research Corporation
ATTN: T. Stathacopoulos

Institute for Defense Analyses
ATTN: IDA Librarian
ATTN: Joel Bengston

ION Physics Corporation
ATTN: Robert D. Evans

Kaman AviDyne
Division of Kaman Sciences Corp.
ATTN: Ray Reutinick
ATTN: Norman P. Hobbs
ATTN: F. S. Criscione

Kaman Sciences Corporation
ATTN: R. Keefe
ATTN: Donald C. Sachs
ATTN: Thomas Meagher
ATTN: Frank H. Shelton
ATTN: John Keith

Lockheed Missiles & Space Co., Inc.
ATTN: R. Walz, Dept. 81-14

Lockheed Missiles & Space Co.
ATTN: T. R. Fortune

Lockheed Missiles & Space Co., Inc.
ATTN: F. G. Borgardt

Martin Marietta Aerospace
Orlando Division
ATTN: Gene Aiello
ATTN: James M. Potts, MP-61
ATTN: Laird Kinnaird
ATTN: William A. Gray, MP-61

McDonnell Douglas Corporation
ATTN: J. F. Garibotti
ATTN: L. Cohen
ATTN: R. J. Reck

Northrop Corporation
ATTN: Don Hicks

Pacific-Sierra Research Corp.
ATTN: Gary Lang

Physics International Company
ATTN: Doc. Con. for James Shea

Prototype Development Associates, Inc.
ATTN: John Slaughter
ATTN: John McDonald

R&D Associates
ATTN: Harold L. Brode
ATTN: Jerry Carpenter
ATTN: F. A. Field
ATTN: Cyrus P. Knowles

Science Applications, Inc.
ATTN: Carl Swain
ATTN: Lyle Dunbar

DEPARTMENT OF DEFENSE CONTRACTORS (Continued)

Science Applications, Inc.

ATTN: John Warner
ATTN: G. Ray
ATTN: R. Fisher
ATTN: Dwane Hove

Science Applications, Inc.

ATTN: William R. Seebaugh
ATTN: William M. Layson
ATTN: John Cockayne

Stanford Research Institute

ATTN: George R. Abrahamson
ATTN: Herbert E. Lindberg
ATTN: Donald Curran
ATTN: Philip J. Dolan

Stanford Research Institute

ATTN: Harold Carey

Systems, Science and Software, Inc.

ATTN: G. A. Gurtman
ATTN: Russell E. Duff

DEPARTMENT OF DEFENSE CONTRACTORS (Continued)

TRW Defense & Space Sys. Group

ATTN: W. W. Wood
ATTN: D. H. Baer, RI-2136
ATTN: R. K. Plebuch, RI-2078
ATTN: Peter Brandt, EI-2006
ATTN: Peter K. Dai, RI/2170
ATTN: Jorg Arenguren

TRW Defense & Space Sys. Group

San Bernardino Operations

ATTN: L. Berger
ATTN: V. Blankenship
ATTN: William Polich

University of Victoria

Department of Physics
100 cy ATTN: Prof. John Dewey
ATTN: D. J. McMillin
ATTN: D. Trill

Defence Research Establishment, Suffield

3 cy ATTN: R. M. Heggie